Copyright Warning & Restrictions

The copyright law of the United States (Title 17, United States Code) governs the making of photocopies or other reproductions of copyrighted material.

Under certain conditions specified in the law, libraries and archives are authorized to furnish a photocopy or other reproduction. One of these specified conditions is that the photocopy or reproduction is not to be "used for any purpose other than private study, scholarship, or research." If a, user makes a request for, or later uses, a photocopy or reproduction for purposes in excess of "fair use" that user may be liable for copyright infringement,

This institution reserves the right to refuse to accept a copying order if, in its judgment, fulfillment of the order would involve violation of copyright law.

Please Note: The author retains the copyright while the New Jersey Institute of Technology reserves the right to distribute this thesis or dissertation

Printing note: If you do not wish to print this page, then select "Pages from: first page # to: last page #" on the print dialog screen

Order Number 9401729

Minimum redundancy array structure for interference cancellation

Chen, Wan-Ling, Ph.D.

New Jersey Institute of Technology, 1993

U·M·I
300 N. Zeeb Rd.
Ann Arbor, MI 48106

MINIMUM REDUNDANCY ARRAY STRUCTURE

FOR

INTERFERENCE CANCELLATION

by

Wan-Ling Chen

A Dissertation
Submitted to the Faculty of
New Jersey Institute of Technology
in Partial Fulfillment of the Requirements for the Degree of
Doctor of Philosophy

Department of Electrical and Computer Engineering

May 1993

ABSTRACT

Minimum Redundancy Array Structure
for
Interference Cancellation

by

Wan-Ling Chen

Adaptive antenna arrays are widely used in many advanced radar, sonar, and communication systems because of their effectiveness in cancelling intentional or unintentional interferers. A uniformly spaced linear array, referred to as a Uniform Regular Array (URA), is the usual structure used for interference cancellation. The Minimum Redundancy Array (MRA) structure proposed in this work is a special kind of thinned array whose application was limited in the past to direction finding. MRAs with the same number of array elements can resolve directions of much more closely spaced signals than URAs.

The URA structure is customarily utilized for interference cancellation, and the Minimum Noise Variance (MNV) criterion is a common performance measure for deriving optimum weights, provided that the desired signal is absent during adaptation. The MNV criterion is to minimize the combined sum of the interference and background noise power.

Another approach to interference cancellation using the URA structure is the eigencanceling method. This method, which is based on the eigenstructure of the spatial autocorrelation matrix, when compared to the conventional beamforming method, has the following advantages: 1) deeper interference cancellation 2) inde-

pendence of the interfers' power, and 3) faster optimum weight convergence. In this work, both the conventional beamforming and eigencanceling methods were applied to the MRA structure and investigated analytically. Performance of the MRAs were studied and compared to that of the URAs.

For uncorrelated interferers, the cancellation depth of the MRA in the main beam region was almost the same as that of the URA with the same aperture and many more elements. When the eigencanceling technique was applied, it was found that the convergence rate of the MRA was about four times faster than that of the URA.

This work also contains other topics, such as the relation between the eigenspaces of the MRA structure and its corresponding URA. Preliminary results on planar MRA structures are also included. For an array application with a large aperture requirement in terms of the number of array elements, the MRA proved to be a much better choice than the URA in achieving interference cancellation.

APPROVAL PAGE

Minimum Redundancy Array Structure

For

Interference Cancellation

Wan-Ling Chen

Dr. Yeheskel Bar-Ness, Dissertation Advisor (date)
Director of Center for Communications and Signal Processing Research
Distinguished Professor of Electrical Engineering
New Jersey Institute of Technology

Dr. Nirwan Ansari, Committee Member (date)
Assistant Professor of Electrical Engineering
New Jersey Institute of Technology

Dr. Alexander Haimovich, Committee Member (date)
Associate Professor of Electrical Engineering
New Jersey Institute of Technology

Dr. Zoran Siveski, Committee Member (date)
Assistant Professor of Electrical Engineering
New Jersey Institute of Technology

Dr. Michael Porter, Committee Member (date)
Associate Professor of Mathematics
New Jersey Institute of Technology

Dr. Jack Winters, Committee Member (date)
Member of Technical Staff, Network Systems Research Department
AT & T Bell Laboratories, Holmdel, NJ

BIOGRAPHICAL SKETCH

Author: Wan-Ling Chen
Degree: Doctor of Philosophy in Electrical Engineering
Date: May 1993

Undergraduate and Graduate Education:

- Doctor of Philosophy in Electrical Engineering,
  New Jersey Institute of Technology, Newark, NJ, 1993
- Master of Science in Systems Engineering,
  Case Western Reserve University, Cleveland, OH, 1988
- Master of Science in Electrical Engineering,
  Michigan Technological University, Houghton, MI, 1986
- Bachelor of Science in Electrical Engineering,
  National Tsing-Hua University, Hsin-Chu, Taiwan, R.O.C., 1984

Major: Electrical Engineering

Presentations and Publications:

Y. Bar-Ness, E. Panayirci and W.-L. Chen, "Eigenanalysis for Interference Cancellation with Minimum Redundancy Array Structure," IEEE SSAP workshop proceeding, pp 50-53, Oct. 1992.

Y. Bar-Ness, E. Panayirci and W.-L. Chen, "Conventional and Eigenanalysis Interference Cancellation with Minimum Redundancy Array Structure," Final Report to Naval Ocean System Center, July, 1992.

E. Panayirci, Y. Bar-Ness and W.-L. Chen, "Conventional Interference Cancellation for Minimum Redundancy Array Structure," ICASSP proceeding pp IV-541 - IV-544, March, 1992.

W.-L. Chen and Y. Bar-Ness, "Minimum Redundancy Array Structure For Interference Cancellation," International IEEE AP-S symposium, pp 121-124, May, 1991.

This dissertation is dedicated to

my family

ACKNOWLEDGMENTS

The author wishes to express her sincere gratitude to her supervisor, Professor Yeheskel Bar-Ness, for his guidance, help and consultation throughout this research.

Special thanks to Professors Nirwan Ansari, Alexander Haimovich, Zoran Siveski, Michael Porter, and Dr. Jack Winters from AT&T Bell Laboratories for serving as members of the dissertation committee. Professor Michael Porter and Dr. Jack Winters have devoted an enormous amount of time and effort in suggesting and discussing technical matters during the developement of this dissertation. Special thanks to Professor Erdal Panayırcı from Istanbul Technical University for his suggestions during his stay as a visiting professor at NJIT.

The author wishes to acknowledge the Naval Ocean System Center for the initial funding of this research, and to the Center for Communications and Signal Processing Research for providing further funding. The author is also grateful to Professor Kenneth Sohn and Ms. Brenda Walker of the Electrical and Computer Engineering Department at NJIT for their moral support during the last few years.

The author appreciates the timely help from Ms. Lisa Fitton for proofreading the entire dissertation; Mr. Chris Peckham and Mr. Raafat Kamel for their help with the computers; and Mr. Zhiqing Zhang for modifying the LaTeX style file to fit the NJIT standard.

Special thanks to my husband Ming-Wan Young, and the babysitter, Estela Martinez for assisting me with little Philip and Eric. Without their help, this work would never have been completed. And finally, a thank you is due to my parents and in-laws for their full support throughout the years.

TABLE OF CONTENTS

Chapter	Page
1 INTRODUCTION	1
2 SYSTEM MODEL AND FORMULATION	6
2.1 System Model of Linear Array	6
2.2 Properties of the Autocorrelation Matrix	8
2.3 Formulation of the Optimization Problem	9
2.3.1 Conventional Beamforming Formulation	10
2.3.2 Formulation using Eigencanceling Technique	11
2.3.3 The MRA Weight Constraint	12
2.4 The Recursive Formula for the Inverse of the Autocorrelation Matrix	16
2.5 Examples of the Recursive Inversion Formula	18
2.5.1 The Single-Interferer Case	18
2.5.2 The Dual-Interferer Case	18
2.6 System Model of Planar Square Array	19
3 PERFORMANCE EVALUATION	24
3.1 Conventional Beamforming Technique	25
3.1.1 The Single-Interferer Case	26
3.1.2 The Dual-Interferer Case	29
3.1.3 Numerical Examples	31
3.2 Eigencanceling Technique	33
3.2.1 The Single-Interferer Case	37
3.2.2 The Dual-Interferer Case	40
3.3 Examples of the MRA Eigencanceler	45
3.3.1 Three-Element Minimum Redundancy Array (MRA-3)	46
3.3.2 Four-Element Minimum Redundancy Array (MRA-4)	48

Chapter **Page**

3.4 Eigenvalue Spread Comparison 52
4 EIGENSPACE TRANSFORMATION BETWEEN THE URA AND THE MRA STRUCTURES 56
4.1 Analytical Formula for the Matrix Inverse 57
4.2 Transformation between the Eigenspaces of the URA and the MRA . . 59
4.2.1 Transformation between the Noise Subspaces 60
4.2.2 Transformation between the Eigenspaces 60
4.2.3 Diagonalized Transformation Matrix 61
4.3 Formulation of the MRA using the Eigenspace Transformation Matrix . 62
4.4 Performance Comparison 64
5 NUMERICAL RESULTS 68
5.1 Conventional Beamforming 69
5.1.1 The Single-Interferer Case 69
5.1.2 The Dual-Interferer Case 70
5.2 Eigencanceling Technique 71
5.2.1 The Single-Interferer Case 71
5.2.2 The Dual-Interferer Case 73
5.3 Planar Square Array Case 74
6 CONCLUSIONS 112
APPENDIX A 117
APPENDIX B 122
APPENDIX C 134
APPENDIX D 138
REFERENCES 143

LIST OF FIGURES

Figure		Page
1	The URA square array element arrangement.	20
2	All the possible MRA-3 square array layout.	23
3	Magnitude of $\mid \rho \mid^2$ as a function of the angle difference between two interferers for the URA-4 and the MRA-4.	55
4	The MNVV comparison between the MRA-3, the URA-3, and the URA-4.	75
5	The MNVV ratio as a function of the interferer's direction of the URA-3 to the MRA-3, and of the MRA-3 to the URA-4.	76
6	The MNVV comparison between the MRA-3, the URA-3, and the URA-4.	77
7	The MNVV ratio as a function of interferer's direction of the URA-3 to the MRA-3, and of the MRA-3 to the URA-4.	78
8	The MNVV comparison between the MRA-4, the URA-4, and the URA-7.	79
9	The MNVV ratio as a function of interferer's direction of the URA-4 to the MRA-4, and of the MRA-4 to the URA-7.	80
10	The MNVV comparison between the MRA-5, the URA-5, and the URA-10.	81
11	The MNVV of the MRA-5, the URA-5 and the URA-10. The location for the MRA-5 is (0, 1, 4, 7, 9).	82
12	The MNVV ratio as a function of interferer's darection of the URA-5 to the MRA-5.	83
13	The MNVV comparison between the MRA-6, the URA-6, and the URA-14.	84
14	The MNVV of the MRA-6 is compared to the URA-6 and the URA-14. The location for the MRA-6 is (0, 1, 4, 5, 11, 13).	85
15	The MNVV of the MRA-6 is compared to the URA-6 and the URA-14. The location for the MRA-6 is (0, 1, 6, 9, 11, 13).	86
16	The MNVV ratio as a function of interferer's direction for the URA-6 to the MRA-6.	87
17	The effect of different interference to noise ratio (INR) on the MNVV for the URA-4 and the MRA-4. The interference power was taken as 1.	88
18	The effect of different interference to noise ratio (INR) on the noise variance ratio between the URA-4 and the MRA-4.	89
19	The NMNVV for the URA-5 with two interferers using conventional beamforming method and $(\sigma^2, p_1, p_2) = (1, 100, 10)$.	90

Figure **Page**

20 The NMNVV for the MRA-5 with two interferers using conventional beamforming method and (σ^2, p_1, p_2) =(1,100,10). 91

21 The NMNVV ratio of the URA-5 to the MRA-5 with two interferers using conventional beamforming method and (σ^2, p_1, p_2) = (1, 100, 10). 92

22 Contour plot of the NMNVV for the URA-5 with two interferers using conventional beamforming method and (σ^2, p_1, p_2) =(1, 100, 10). 93

23 Contour plot of the NMNVV for the MRA-5 with two interferers using conventional beamforming method and (σ^2, p_1, p_2) =(1, 100, 10). 94

24 Contour plot of the NMNVV ratio of the URA-5 to the MRA-5 with two interferers using conventional beamforming method and (σ^2, p_1, p_2) =(1, 100, 10). 95

25 The MNVV for the URA-4 with two interferers. 96

26 The MNVV for the MRA-4 with two interferers. 97

27 The MNVV comparison for three-element arrays the URA-3 and the MRA-3 using both conventional beamforming and eigencanceling methods. . . . 98

28 Convergence rate comparison for optimum weight using conventional beamforming and eigencanceling methods. 99

29 The NMNVV for the URA-5 with two interferers using eigencanceling method and (σ^2, p_1, p_2) =(1,100,10). 100

30 The NMNVV for the MRA-5 with two interferers using eigencanceling method and (σ^2, p_1, p_2) =(1,100,10). 101

31 The NMNVV ratio of the URA-5 and the MRA-5 with two interferers using eigencanceling method and (σ^2, p_1, p_2) =(1,100,10). 102

32 Contour plot of the NMNVV for the URA-5 with two interferers using eigencanceling method and (σ^2, p_1, p_2) =(1,100,10). 103

33 Contour plot of the NMNVV for the MRA-5 with two interferers using eigencanceling method. Note that (σ^2, p_1, p_2) =(1,100,10). 104

34 Contour plot of the NMNVV ratio of the URA-5 and the MRA-5 with two interferers using eigencanceling method and (σ^2, p_1, p_2) =(1,100,10). . . . 105

35 Contour plot of the MNVV for the URA-3 square array with single interferer using the conventional beamforming method and (σ^2, p_1) =(1,10). . . . 106

36 Contour plot of the MNVV for the MRA-3 square array with single interferer using the conventional beamforming method and (σ^2, p_1) =(1,10). . . . 107

37 Contour plot of the MNVV ratio for the URA-3 and the MRA-3 square array with single interferer using the conventional beamforming method and (σ^2, p_1) =(1,10). 108

Figure **Page**

38 Contour plot of the MNVV for the URA-3 square array with single interferer using eigencanceling method and (σ^2, p_1) =(1,10). 109

39 Contour plot of the MNVV for the MRA-3 square array with single interferer using eigencanceling method and (σ^2, p_1) =(1,10). 110

40 Contour plot of the MNVV ratio for the URA-3 and the MRA-3 square array with single interferer using eigencanceling method and (σ^2, p_1) =(1,10). . 111

CHAPTER 1

INTRODUCTION

Adaptive linear arrays are widely used in advanced radar, sonar and communication systems because of their effectiveness in cancelling strong interferers in sidelobe beams [1]. In an adaptive linear antenna system, it is customary to assume that the array is composed of equally spaced elements. This reduces the so-called aliasing or grating lobes in the antenna pattern. The spaces between the elements are assumed to be of half wave length $\lambda/2$. This array structure is referred to as the Uniform Regular Array (URA). The operation of an adaptive URA can be qualitatively understood by visualizing a main-beam pattern that is modified by subtracting an auxiliary beam pattern centered on the interferer. If all the array elements are used to form the auxiliary beam then the adapted antenna contains a well formed notch at the interference direction of arrival with no spurious lobes or attenuation of the desired signal. However, the cost and complexity of a fully adaptive URA is prohibitive for some applications which require a large number of array elements.

The main objective in this study is to investigate the interference cancellation capability of a class of adaptive arrays whose element locations are selected by a particular non-uniform thinning technique. It achieves better cancellation beam resolution than the URA, but with fewer array elements. Haimovich used an eigenanalysis technique (referred in this work as the eigencanceling technique) for the URA to achieve superior interference cancellation [2, 3]. The same technique will also be applied to this class of arrays.

It is known that for a given number of array elements, there is a class of arrays called "Minimum Redundancy Arrays" (MRAs) which achieve the highest possible

resolution by reducing the number of redundant spacings. By minimum redundancy we mean the array autocorrelation matrix $\mathbf{R}$ contains the minimum possible number of repeatable entries [4]. For example, with a three-element array, instead of locating the elements at $(0, \lambda/2, 2\lambda/2)$ to form a URA, we locate these elements at $(0, \lambda/2, 3\lambda/2)$ to form the corresponding MRA. We refer to such an array as having an aperture of 3 instead of $3\lambda/2$. Notice that the MRA has an aperture of 3 instead of 2 for the corresponding three-element URA, which is advantageous when considering resolution. For a four-element MRA we locate the elements at $(0, \lambda/2, 4\lambda/2, 6\lambda/2)$ with aperture of 6 instead of 3 for the four-element URA. The autocorrelation matrices of these two examples are

$$\mathbf{R}_{MRA-3} = \begin{bmatrix} r(0) & r(1) & r(3) \\ r^*(1) & r(0) & r(2) \\ r^*(3) & r^*(2) & r(0) \end{bmatrix} \quad \mathbf{R}_{URA-3} = \begin{bmatrix} r(0) & r(1) & r(4) & r(6) \\ r^*(1) & r(0) & r(3) & r(5) \\ r^*(4) & r^*(3) & r(0) & r(2) \\ r^*(6) & r^*(5) & r^*(2) & r(0) \end{bmatrix}.$$

Note that these matrices are Hermitian but not Toeplitz (A Toeplitz matrix is one for which all the elements along the same subdiagonal take on the same value.). These matrices have no redundancy in the upper triangle part of the autocorrelation matrix except for the repeatable $r(0)$ in the main diagonal, and there is only one off-diagonal term for each correlation lag. For arrays with more than four elements, a suitable structure can be found, but with some redundancy. The problem of finding the array configuration with the lowest possible redundancy was examined by Leech [5]. He gave a single configuration of each MRA for the number of array elements less than 12. Through an exhaustive search program, the locations of the elements giving maximum aperture and minimum redundancy can be found. Table 1 depicts the results of such a search for all possible array configurations. In this table, N is the number of elements and $L-1$ is the corresponding array aperture. Much research has been devoted to finding the relation between N and L [6,7,8]. Clearly for a URA, the aperture is always $N-1$. The column entitled "MRA configuration"

shows the locations of elements from the left most referenced element in units of $\lambda/2$. The column marked "Redundancy" shows the correlation lags which are repeated (in the parenthesis). Notice that for some N we can have different configurations. This means that for a given number of array elements, different configurations with different correlation lag repetitions are possible. In this table, the "mirror image" of each array location is not listed. For example, the three-element MRA configuration was listed as (0,1,3) and its "mirror image" has the configuration of (0,2,3). It can be seen that the mirror image will only result in the relocation of the autocorrelation matrix entries but the number of redundant correlation lags is the same. Pearson [9] developed a constructive procedure that creates a restrictive difference base. Furthermore he has shown that for N>3, it is always possible to choose an MRA configuration such that $N^2/(L-1) < 3$.

Table 1 The MRA configuration with a given number of array elements.

N	L-1	MRA configuration	Redundancy
3	3	0 1 3	None
4	6	0 1 4 6	None
5	9	0 1 2 6 9	$2r(1)$
		0 1 4 7 9	$2r(3)$
6	13	0 1 2 6 10 13	$2r(1,4)$
		0 1 4 5 11 13	$2r(1,4)$
		0 1 6 9 11 13	$2r(2,5)$
7	17	0 1 2 3 8 13 17	$2r(2,5)$, $3r(1)$
		0 1 2 6 10 14 17	$2r(1,8)$, $3r(4)$
		0 1 2 8 12 14 17	$2r(1,2,6,12)$
		0 1 2 8 12 15 17	$2r(1,2,7,15)$
		0 1 8 11 13 15 17	$2r(4,7)$, $3r(2)$
8	23	0 1 2 11 15 18 21 23	$2r(1,2,3,10,21)$
		0 1 4 10 16 18 21 23	$2r(2,3,5,6,17)$
9	29	0 1 2 14 18 21 24 27 29	$2r(1,2,6,13,27)$, $3r(3)$
		0 1 3 6 13 20 24 28 29	$2r(1,3,4,5,7,23,28)$
		0 1 4 10 16 22 24 27 29	$2r(2,3,5,12,23,28)$
10	36	0 1 3 6 13 20 27 31 35 36	$2r(1,3,4,5,14,30,35)$
11	43	0 1 3 6 13 20 27 34 38 42 43	$2r(1,3,4,5,21,37,42)$,$3r(14)$, $4r(7)$

The idea of exploiting the advantages of the MRA structure was first proposed for direction finding to increase the number of signals that could be resolved with a given number of array elements [10,11]. In this approach the autocorrelation matrix was augmented to a Toeplitz matrix by repeating the different correlation lags along the corresponding subdiagonals [12]. By doing so, we get a 4×4 Toeplitz matrix for the three-element MRA structure instead of a 3×3. A 7×7 Toeplitz matrix would be obtained for the four-element MRA structure while its original autocorrelation matrix is only 4×4. Therefore the three-element MRA can resolve three directions as apposed to two directions with a URA. The second MRA structure, with four elements, can resolve six directions instead of only three. The MRA principle and its application for direction finding using the MUSIC algorithm was reported in [13]. Some other variations of the MUSIC algorithm were also applied to the MRA structure for direction finding, and are cited in [14,15,16,17].

In this work, we discuss using the MRA structure for interference cancellation. Different optimization criteria are customarily used in the literature to derive the adaptive optimal weights which control the array response. Our attention will be concentrated on the noise variance performance of the MRAs operating in a multiple narrow-band interference environment. This is the most suitable approach for radar applications where the desired signal is assumed absent or has been previously removed. The term "Minimum Noise Variance value" (MNVV) is referred as the value of the noise variance when the optimum weight vector is obtained from the Minimum Noise Variance (MNV) criterion optimization problem. To gain an understanding of the interference cacellation ability of the MRA structure without becoming overwhelmed by the numerical results, most of the attention is focused on the single- and dual-interferer problems. It is assumed in this study that a suitable constraint was employed to prevent main beam cancellation [18], so that efforts can be concentrated

on sidelobe interferers. The MNV criterion, to be used in our study, is first defined and then analytical solutions are derived for the optimal weights. Conditions on the direction of interferers for which the MRA performs better or worse than the URA will also be derived.

For bearing estimation problems, eigenanalysis techniques are shown to provide an asymptotically unbiased solution [19]. A comparison between superresolution methods can be found in [20]. The eigenspace of the autocorrelation matrix can be decomposed into two orthogonal subspaces one corresponding to the interference signal and the other to the noise of the process [21]. The main objective of the eigencanceler is to construct the optimum weight vector to be in the noise subspace which results in the total cancellation of the interference [22]. Besides offering total interference cancellation, the eigencanceler has a remarkable convergence rate to the optimum weight vector. It is also immune to the interference-to-noise power ratio but does suffer from higher sidelobes and sensitivity to a change in the interference angle. The same constraint for the weight to lie in the noise subspace was also posed for the MRA cases. We present a comparison between the URA and the MRA using conventional beamforming and the eigencanceling technique using the MNVV as a performance measurement. The MRA was compared to the URA with the same number of elements and to the URA with the same aperture.

The planar sparse array with the structure similar to the linear MRA will be discussed in this research. In the past, the planar sparse array was used only for direction finding [23]. Bucker found that a sparse planar array with a structure similar to the MRA has higher resolution due to its large aperture [24]. The ability of the MRA planar array structure for interference cancellation will be formulated and briefly examined.

CHAPTER 2

SYSTEM MODEL AND FORMULATION

This chapter describes the system model and the assumptions used for the process. The optimization problem and its solution for the cases of conventional beamforming and eigencanceling techniques are presented. The treatment of the augmented autocorrelation matrix for the MRA structure and the constraint for processing the MRA signals are also discussed. The non-augmented autocorrelation matrix used to reduce the processing dimension of the MRA is also provided. A recursive formula for calculating the inverse of the autocorrelation matrix is employed, and the single- and dual-interferer cases are given as examples.

2.1 System Model of Linear Array

Let r be the number of interferers in the form of planar waves impinging at the array from different directions $\theta_l (l = 1, 2, \ldots, r)$ relative to broadside. The interferers, $s_l (l = 1, 2, \ldots, r)$ are assumed zero-mean uncorrelated narrow-band processes. Let the number of array elements be N and define the array output vector by $\mathbf{x} \triangleq [x_1, x_2, \ldots, x_N]^T$. Uncorrelated white Gaussian noise with zero mean and variance σ^2 is added at the array output. The signal received at the n-th element is given by

$$x_n = \sum_{l=1}^{r} s_l e^{ji_{n-1}\omega_l} + \nu_n \qquad n = 1, 2, \ldots, N \qquad i_0 = 0 \tag{2.1}$$

where ν_n is the added noise and ω_l is related to the direction angle θ_l by

$$\omega_l = d\frac{\omega_0}{c}\sin(\theta_l) \tag{2.2}$$

and ω_0 is the center frequency of the signal. The spacing between array elements is d and the wave speed is c. For the URA, the integers i_n take the values $i_0 = 0, i_1 = 1, \ldots,$

$i_{N-1} = N - 1$, while for MRA structures, they are chosen according to Table 1.

Equation (2.1) can be written in a vector form as follows:

$$\mathbf{x} = \mathbf{D}_r \mathbf{s} + \boldsymbol{\nu} \tag{2.3}$$

where

$$\mathbf{D}_r = [\mathbf{d}_1, \mathbf{d}_2, \ldots, \mathbf{d}_r], \tag{2.4}$$

is an $N \times r$ matrix, and for each interferer, its correspoonding direction vector is:

$$\mathbf{d}_l = [1, e^{-ji_1\omega_l}, e^{-ji_2\omega_l}, \ldots, e^{-ji_{N-1}\omega_l}]^T. \tag{2.5}$$

The signal power vector is

$$\mathbf{s} = [s_1, s_2, \ldots, s_r]^T$$

and the noise vector is

$$\boldsymbol{\nu} = [\nu_1, \nu_2, \ldots, \nu_N]^T.$$

The array autocorrelation matrix $\mathbf{R}$ is easily computed from Eq. (2.3) as follows:

$$\begin{aligned} \mathbf{R} &= E[\mathbf{x}\mathbf{x}^H] \\ &= \mathbf{D}_r E[\mathbf{s}\mathbf{s}^H]\mathbf{D}_r^H + E[\nu\nu^H] \\ &= \mathbf{D}_r \mathbf{S} \mathbf{D}_r^H + \sigma^2 \mathbf{I}_N \end{aligned} \tag{2.6}$$

where $\mathbf{S} = E[\mathbf{s}\mathbf{s}^H]$ is a diagonal matrix. If s_l is written as $s_l = b_l(t)e^{-j(\omega_0 t + \phi_l)}$ where $b_l(t)$ and ϕ_l are the amplitude and phase functions of these signals, then the elements of the diagonal matrix $\mathbf{S}$ are given by $p_l = E[\mid b_l(t) \mid^2]$, the power of these signals. It is easy to see that the autocorrelation matrix $\mathbf{R}$ is Hermitian and, for the URA structure, it is also Toeplitz.

2.2 Properties of the Autocorrelation Matrix

In this section various properties of the autocorrelation matrix are presented. These properties are applicable to both the URA and the MRA structures.

For an N element array with r interferers:

- There are $(N-r)$ eigenvalues with value of σ^2.

  Discussion : From Eq. (2.6),

  $$\mathbf{R} = \mathbf{D}_r \mathbf{S} \mathbf{D}_r^H + \sigma^2 \mathbf{I}_N$$

  $\mathbf{D}_r$ is an $N \times r$ matrix, the rank of $\mathbf{D}_r \mathbf{S} \mathbf{D}_r^H$ is r. $\mathbf{R}$ is of full rank N, which implies that there are $(N-r)$ eigenvectors of $\mathbf{R}$ corresponding to the eigenvalue σ^2.

- The interference and noise subspaces of $\mathbf{R}$ are orthogonal.

  Discussion : The noise subspace $\mathbf{G}_\nu$ is the span of all the eigenvectors of $\mathbf{R}$ corresponding to the eigenvalue σ^2. The collection of all these eigenvectors as bases of $\mathbf{G}_\nu$ formed a matrix $\mathbf{E}_\nu$. The interference subspace $\mathbf{G}_r$ is the span of all the eigenvectors of $\mathbf{R}$ with eigenvalues greater than σ^2. The collection of all these eigenvectors as bases of $\mathbf{G}_r$ form a matrix $\mathbf{E}_r$. In the Jordan form (for repeated roots case), not all bases of $\mathbf{G}_\nu$ are orthogonal to each other, but any basis in $\mathbf{G}_r$ is orthogonal to any basis in $\mathbf{G}_\nu$.

- The smallest eigenvalue of $\mathbf{R}$ is σ^2.

  Proof : Assume that e_i is an eigenvector of $\mathbf{R}$, from the previous property we have the following fact: for an eigenvector $e_i \subset \mathbf{G}_\nu$, is orthogonal to any vectors in the interference subspace $\mathbf{G}_r$ which can also be spanned by the interference signal vectors $\mathbf{d}_1, \mathbf{d}_2, ...\mathbf{d}_r$. It leads to

  $$\mathbf{D}_r^H e_i = 0$$

for $e_i \subset \mathbf{G}_\nu$. From the definition of $\mathbf{R}$ in Eq.(2.6) and the fact that

$$\begin{aligned} \lambda_i &= \frac{e_i^H \mathbf{R} e_i}{e_i^H e_i}, \\ &= e_i^H (\mathbf{D}_r \mathbf{S} \mathbf{D}_r^H + \sigma^2 \mathbf{I}_N) e_i, \\ &\geq \sigma^2. \end{aligned}$$

The equality sign holds when $e_i \subset \mathbf{G}_\nu$.

- For the single interferer case (r=1), the autocorrelation matrix of the URA and the MRA are *similar* (i.e. they have the same eigenvalues).

  Proof : From reference [22],

  $$\text{trace}[\mathbf{R}] = \sum_{i=1}^{N} \lambda_i = N \left(\text{trace}[\mathbf{S}] + \sigma^2 \right) = N(p_1 + \sigma^2).$$

  Thus, there are N-1 eigenvalues with the value of σ^2. The eigenvalue corresponding to the interferer is $Np_1 + (N-1)\sigma^2$ for both the URA and the MRA. With all the eigenvalues the same, the two matrices are similar (the eigenvectors are in general different).

2.3 Formulation of the Optimization Problem

Minimum Mean Square Error (MMSE), Maximum Signal to Noise Ratio (MSNR) and Minimum Noise Variance (MNV) are some of the common performance measures which have been proposed to evaluate the adaptive process [23]. The optimum weight vector obtained by these different criteria differs only by a scaling factor for the narrow band signal case. For radar applications where the desired signal is absent, the MNV criterion is the most suitable approach. In a linearly constrained minimum output power array, the main lobe constraint only affects the beam pattern. The influence of the constraint decreases rapidly as distance from the look

direction increases [27, 28]. The absence of the main lobe constraint allows the null to form exactly in the direction of the desired signal. This may have the disastrous consequence of canceling both the desired and interference signals [29, 30, 31]. In this section, the formulation of the optimization problem using both the conventional beamformer and the eigencanceling techniques will be discussed.

2.3.1 Conventional Beamforming Formulation

We concentrate now on the MNV criterion with constraints on the array pattern that it have prescribed gain in certain directions. Note that concentrating on the MNV criterion is not restrictive since the optimal weight vectors obtained for different criteria differ from one another by only a scale factor. Thus, we are interested in finding the optimal weights (or weight vector) which satisfy:

$$\begin{aligned} \min \quad & \mathbf{w}^H\mathbf{R}\mathbf{w} \\ \text{subject to} \quad & \mathbf{w}^H\mathbf{A}_p = \mathbf{g}^H \end{aligned}$$

where $\mathbf{A}_p = [\mathbf{a}_{p_1}, \mathbf{a}_{p_2}, \ldots, \mathbf{a}_{p_p}]$; $\mathbf{a}_{p_i}$, $i = 1, 2, \ldots, p$ are the preassigned directions and $\mathbf{g}^H = [g_1, g_2, \ldots, g_p]$; g_i, $i = 1, 2, \ldots, p$ are the required gains in the direction of $\mathbf{a}_{p_i}$.

Using a Lagrange multiplier vector $\boldsymbol{\lambda}$, we have the following unconstrained optimization problem:

$$\min J = \mathbf{w}^H\mathbf{R}\mathbf{w} + \boldsymbol{\lambda}^\tau(\mathbf{A}_p^H\mathbf{w} - \mathbf{g}) + (\mathbf{w}^H\mathbf{A}_p - \mathbf{g}^H)\boldsymbol{\lambda}.$$

Taking the gradient of J with respect to $\mathbf{w}$ we get

$$\nabla_{\mathbf{w}} J = 2\mathbf{R}\mathbf{w} + 2\mathbf{A}_p\boldsymbol{\lambda}. \tag{2.7}$$

Equating Eq. (2.7) to zero we then have,

$$\mathbf{w}_{op} = -\mathbf{R}^{-1}\mathbf{A}_p\boldsymbol{\lambda}. \tag{2.8}$$

But from the constraint,

$$\begin{aligned} \mathbf{g}^H &= \mathbf{w}_{op}^H \mathbf{A}_p = -\boldsymbol{\lambda}^\tau (\mathbf{A}_p^H \mathbf{R}^{-1} \mathbf{A}_p) \\ \Rightarrow \qquad \boldsymbol{\lambda}^\tau &= -\mathbf{g}^H (\mathbf{A}_p^H \mathbf{R}^{-1} \mathbf{A}_p)^{-1}. \end{aligned}$$

Finally substituting in Eq. (2.8), we find the optimum weight to be

$$\mathbf{w}_{op} = \mathbf{R}^{-1} \mathbf{A}_p (\mathbf{A}_p^H \mathbf{R}^{-1} \mathbf{A}_p)^{-1} \mathbf{g} \tag{2.9}$$

where we used the fact that $\mathbf{R}$, and hence $\mathbf{R}^{-1}$, is Hermitian.

For the case of a single desired direction $\mathbf{A}_p = \mathbf{a}_p$ and assuming the array gain in that direction to be unity, *i.e.* $\mathrm{g} = 1$, then

$$\mathbf{w}_{op} = \frac{\mathbf{R}^{-1} \mathbf{a}_p}{\mathbf{a}_p^H \mathbf{R}^{-1} \mathbf{a}_p}.$$

2.3.2 Formulation using Eigencanceling Technique

Recall that the eigenvectors of the autocorrelation matrix can be divided into two sets, the set $\mathbf{E}_\nu$ corresponding to the noise eigenvector and the set $\mathbf{E}_r$ corresponding to the interference eigenvectors [32, 33, 34]. When using the eigencanceling technique, the weight vector is restricted to the noise subspace. The eigenvalues μ and eigenvectors $\mathbf{e}$ are related by

$$\mathbf{R}\mathbf{e} = \mu \mathbf{e}. \tag{2.10}$$

Clearly $\mathbf{D}_r$ defined in Eq. (2.4) is the interference subspace spanned by the r interferers' position vectors. Let $\mathbf{E}_r = [\mathbf{e}_l, l = 1, 2, \ldots, r]$ be the matrix of r eigenvectors corresponding to the r dominant (largest) eigenvalues of $\mathbf{R}$. Then one can show that

$$\text{span } (\mathbf{e}_1, \mathbf{e}_2, \ldots \mathbf{e}_r) = \text{ span } (\mathbf{d}_1, \mathbf{d}_2, \ldots, \mathbf{d}_r). \tag{2.11}$$

If $\mathbf{E}_\nu = [\mathbf{e}_l, l = r+1, \ldots, N]$ are the $N-r$ eigenvectors corresponding to the smallest eigenvalues σ^2, then

$$\text{span } (\mathbf{e}_{r+1}, \mathbf{e}_{r+2}, \ldots, \mathbf{e}_N) \perp \text{ span } (\mathbf{d}_1, \mathbf{d}_2, \ldots, \mathbf{d}_r). \tag{2.12}$$

To obtain total cancellation of the interferers we must confine the weight vector to lie in the noise subspace $\mathbf{G}_\nu$. Equivalently we choose the optimal weight to be orthogonal to vectors in the interference subspace $\mathbf{G}_r$

$$\mathbf{w}_{op}^H \mathbf{E}_r = \mathbf{0}. \tag{2.13}$$

Therefore from Eq. (2.13), we get $\mathbf{w}_{op}^H \mathbf{b} = 0$; for any vector $\mathbf{b}$ in the span of the interference subspace $\mathbf{G}_r$ and, in particular, for all the direction vectors of the interferers. This means that such weight vectors will totally cancel all interferers regardless of their signal to background power ratios. This is, what is termed a superresolution estimator or eigencanceler. The optimization problem will be as follows:

$$\begin{aligned} \min \quad & \mathbf{w}^H \mathbf{R} \mathbf{w} \\ \text{subject to} \quad & \mathbf{w}^H \mathbf{A}_p = \mathbf{g}^H \\ & \mathbf{w}^H \mathbf{E}_r = \mathbf{0}. \end{aligned} \tag{2.14}$$

Define $\tilde{\mathbf{A}}_p = [\mathbf{A}_p \mid \mathbf{E}_r]$ and $\tilde{\mathbf{g}}^H = [\mathbf{g}^H \mid \mathbf{0}]$ then the optimum weight vector in this case will have the solution form given in Eq. (2.9) for a conventional beamformer:

$$\tilde{\mathbf{w}}_{op} = \mathbf{R}^{-1} \tilde{\mathbf{A}}_p (\tilde{\mathbf{A}}_p^H \mathbf{R}^{-1} \tilde{\mathbf{A}}_p)^{-1} \tilde{\mathbf{g}}. \tag{2.15}$$

2.3.3 The MRA Weight Constraint

Traditionally the MRA output correlation lags were arranged in a Toeplitz matrix fashion to resemble a URA output structure. This involved choosing the right constraints to properly reflect the MRA structure.

When using the augmented matrix in defining the optimization problem for an MRA, the dimension of the weight vector is that of the augmented matrix. However, fewer outputs (when compared to the URA with the same aperture) are available for processing. Therefore, one might impose a constraint on the optimal weight vector to have zero entries at locations where there is no corresponding element in the MRA structure [36]. In our previous examples; the three-element MRA requires that the third entry of the four dimensional weight vector be zero while the four-element MRA requires that the second, the third and the fifth entries be zeroes. These zero entries can be obtained using the following second or first order constraint on the extended weight vector $\mathbf{w}$:

1. Second order weight constraint:

   $\mathbf{w}^H\mathbf{C}\mathbf{w} = 0$

   where $\mathbf{C}$=diagonal(0,0,k_1, 0, $k_2, \ldots, k_M$).

2. First order weight constraint:

   $\mathbf{w}^H\mathbf{c}_{k_i} = 0$

   where $\mathbf{c}_{k_i} = e^{(k_i)}_{L\mathrm{X}1}$

In the above constraints, e^{k_i} is the unit vector. We pick k_i to represent the locations where the entries of the weight vector must be suppressed $i = 1, 2, \ldots, M$. The value of M is given by $L - N$.

With the augmented autocorrelation matrix, the reformulation of the optimization problem will be discussed here. The MNV criterion is still used and the array pattern is constrained to be constant at certain directions. The constrained optimization problem for an MRA structure with second-order weight constraint becomes:

$$\begin{aligned} \min \quad & \mathbf{w}^H\mathbf{R}\mathbf{w} \\ \text{subject to} \quad & \mathbf{w}^H\mathbf{A}_p = \mathbf{g}^H \\ & \mathbf{w}^H\mathbf{C}\mathbf{w} = \mathbf{0}. \end{aligned} \tag{2.16}$$

With the first order weight constraint, the optimization problem became:

$$\begin{aligned} \min \quad & \mathbf{w}^H\mathbf{R}\mathbf{w} \\ \text{subject to} \quad & \mathbf{w}^H\mathbf{A}_p = \mathbf{g}^H \\ & \mathbf{w}^H\tilde{\mathbf{C}} = \mathbf{0} \end{aligned} \tag{2.17}$$

where $\tilde{\mathbf{C}} = [\mathbf{c}_{k_1}, \mathbf{c}_{k_2}, \ldots, \mathbf{c}_{k_M}]$. Thus, the cost function corresponding to the two different weight constraints will be given by

1. $f_1(\mathbf{w}) = \mathbf{w}^H\mathbf{R}\mathbf{w} + \alpha\mathbf{w}^H\mathbf{C}\mathbf{w} + \boldsymbol{\lambda}^\tau(\mathbf{A}_p^H\mathbf{w} - \mathbf{g}) + (\mathbf{w}^H\mathbf{A}_p - \mathbf{g}^H)\boldsymbol{\lambda}$
2. $f_2(\mathbf{w}) = \mathbf{w}^H\mathbf{R}\mathbf{w} + \boldsymbol{\lambda}^\tau(\hat{\mathbf{A}}_p^H\mathbf{w} - \hat{\mathbf{g}}) + (\mathbf{w}^H\hat{\mathbf{A}}_p - \hat{\mathbf{g}}^\tau)\boldsymbol{\lambda}$

where $\mathbf{A}_p = [\mathbf{a}_{p_1}, \mathbf{a}_{p_2}, \ldots, \mathbf{a}_{p_p}]$, $\mathbf{g}=[g_1, g_2, \ldots, g_D]$ and $\hat{\mathbf{A}}_\mathbf{p} = [\mathbf{A}_\mathbf{p} \mid \tilde{\mathbf{C}}]$ with $\tilde{\mathbf{C}}=[\mathbf{c}_{k_1}, \mathbf{c}_{k_2}, \ldots, \mathbf{c}_{k_M}]$ and $\hat{\mathbf{g}} = [\mathbf{g} \mid \mathbf{0}]$. Here α and $\boldsymbol{\lambda}$ are Lagrange multipliers.

The optimal weight vector for these two different cases is given by:

1. $\mathbf{w}_{op} = (\mathbf{R} + \alpha\mathbf{C})^{-1}\mathbf{A}_p[\mathbf{A}_p^H(\mathbf{R} + \alpha\mathbf{C})^{-1}\mathbf{A}_p]\mathbf{g}$
   where α can be eliminated using $\mathbf{w}_{op}^H\mathbf{C}\mathbf{w}_{op} = \mathbf{0}$
2. $\mathbf{w}_{op} = \mathbf{R}^{-1}\hat{\mathbf{A}}_p(\hat{\mathbf{A}}_p^H\mathbf{R}^{-1}\hat{\mathbf{A}}_p)^{-1}\hat{\mathbf{g}}$

In fact, one can show that eliminating α makes these two solutions equivalent. That is $\mathbf{C} = \tilde{\mathbf{C}}\tilde{\mathbf{C}}$. To simplify the analytical calculation, we consider the case of a

three-element array, then $\tilde{\mathbf{C}} = \mathbf{c}_{k_1} = [0,0,1,0]^T = \mathbf{c}$. Also we impose a constraint that the broadside gain be unity, *i.e.* $\mathbf{g} = \mathbf{1}$. For this case:

$$\mathbf{w}_{op} = \frac{\mathbf{R}^{-1}[(\mathbf{c}^H\mathbf{R}^{-1}\mathbf{c})\mathbf{a}_p - (\mathbf{c}^H\mathbf{R}^{-1}\mathbf{a}_p)\mathbf{c}]}{(\mathbf{c}^H\mathbf{R}^{-1}\mathbf{c})(\mathbf{a}_p^H\mathbf{R}^{-1}\mathbf{a}_p) - \mid \mathbf{a}_p^H\mathbf{R}^{-1}\mathbf{c} \mid^2} \tag{2.18}$$

and the corresponding Minimum Noise Variance value is:

$$\mathbf{w}_{op}^H\mathbf{R}\mathbf{w}_{op} = \frac{\mathbf{c}^H\mathbf{R}^{-1}\mathbf{c}}{(\mathbf{c}^H\mathbf{R}^{-1}\mathbf{c})(\mathbf{a}_p^H\mathbf{R}^{-1}\mathbf{a}_p) - \mid \mathbf{a}_p^H\mathbf{R}^{-1}\mathbf{c} \mid^2}. \tag{2.19}$$

The Minimum Noise Variance value (MNVV) is the value obtained from $\mathbf{w}_{op}^H\mathbf{R}\mathbf{w}_{op}$ using the MNV criterion. For the URA with three-element one can show that

$$\hat{\mathbf{w}}_{op} = \frac{\hat{\mathbf{R}}^{-1}\hat{\mathbf{a}}_p}{\hat{\mathbf{a}}_p^H\hat{\mathbf{R}}^{-1}\hat{\mathbf{a}}_p}, \tag{2.20}$$

and

$$\hat{\mathbf{w}}_{op}^H\hat{\mathbf{R}}\hat{\mathbf{w}}_{op} = \frac{1}{\hat{\mathbf{a}}_p^H\hat{\mathbf{R}}^{-1}\hat{\mathbf{a}}_p}, \tag{2.21}$$

where $\hat{\mathbf{R}}$ is the 3×3 upper left corner of the augmented autocorrelation matrix $\mathbf{R}$ and $\hat{\mathbf{a}}_p$ is the corresponding constraint vector. Similarly for a four-element URA

$$\tilde{\mathbf{w}}_{op} = \frac{\mathbf{R}^{-1}\mathbf{a}_p}{\mathbf{a}_p^H\mathbf{R}^{-1}\mathbf{a}_p} \tag{2.22}$$

and its noise variance is

$$\tilde{\mathbf{w}}_{op}^H\mathbf{R}\tilde{\mathbf{w}}_{op} = \frac{1}{\mathbf{a}_p^H\mathbf{R}^{-1}\mathbf{a}_p}, \tag{2.23}$$

where $\mathbf{a}_p$ and $\mathbf{R}$ are the same as in Eq. (2.18) and Eq. (2.19).

The optimum weight vector found using either first or second order weight constraints is the same since the constraints are equivalent. Furthermore the optimum weight vector obtained using the augmented autocorrelation matrix for the MRA will produce zeros for the entries which correspond to "missing" array elements. The result is the same as performing row and column reduction on the augmented autocorrelation matrix at the corresponding zero weight position. The autocorrelation

matrix of the MRA will yield exactly the same MNVV as when the non-augmented autocorrelation matrix is used. This finding allows one to greatly reduces the size of the matrix for the MRA case. It is especially beneficial when searching for the eigenvectors or calculating the inverse of the autocorrelation matrix. That is to say the augmentation is not necessary for obtaining the optimum weight vector for the MNV criteria. All the autocorrelation matrix properties derived before can be directly applied to the non-augmented MRA case. One must bear in mind that when the augmented matrix is no longer needed for the interference cancellation application, the number of interferers that can be cancelled by the MRA structure is the same as the URA with the same number of array elements. However, due to the larger aperture of the MRA structure, the resolution for cancelling the closely spaced interferers is improved.

2.4 The Recursive Formula for the Inverse of the Autocorrelation Matrix

In order to find the MNVV, the inverse of the autocorrelation matrix is needed. One can simply avoid the direct computation of the matrix inverse. In the following we obtain a recursive formula for computing the inverse of the URA autocorrelation matrix.

From Eq. (2.6) and the definition of $\mathbf{D}_r$ we can write

$$\mathbf{R}_r = \sigma^2 \mathbf{I}_N + \sum_{l=1}^{r} p_l \mathbf{d}_l \mathbf{d}_l^H \tag{2.24}$$

or

$$\mathbf{R}_r = \mathbf{R}_{r-1} + p_r \mathbf{d}_r \mathbf{d}_r^H, \tag{2.25}$$

where $\mathbf{R}_{r-1}$ is the array output autocorrelation matrix when $r-1$ interfering plane waves impinge on the array. Similarly $\mathbf{R}_r$ is the autocorrelation matrix when another

interferer is added. That is,

$$\mathbf{R}_{r-1} = \sigma^2 \mathbf{I}_N + \sum_{l=1}^{r-1} p_l \mathbf{d}_l \mathbf{d}_l^H. \tag{2.26}$$

To simplify Eq. (2.25) using the inversion lemma [29] given by

$$(\mathbf{A}^{-1} + \mathbf{C}\mathbf{B}^{-1}\mathbf{C}^H)^{-1} = \mathbf{A} - \mathbf{A}\mathbf{C}(\mathbf{B} + \mathbf{C}^H\mathbf{A}\mathbf{C})^{-1}\mathbf{C}^H\mathbf{A}, \tag{2.27}$$

with

$$\begin{aligned} \mathbf{R}_{r-1} &= \mathbf{A}^{-1}, \\ \mathbf{d}_r &= \mathbf{C}, \\ \text{and} \quad p_r &= \mathbf{B}^{-1}, \end{aligned}$$

then

$$\begin{aligned} \mathbf{R}_r^{-1} &= (\mathbf{R}_{r-1} + p_r \mathbf{d}_r \mathbf{d}_r^H)^{-1} \\ &= \mathbf{R}_{r-1}^{-1} - \mathbf{R}_{r-1}^{-1}\mathbf{d}_r(\frac{1}{p_r} + \mathbf{d}_r^H \mathbf{R}_{r-1}^{-1}\mathbf{d}_r)^{-1}\mathbf{d}_r^H \mathbf{R}_{r-1}^{-1}. \end{aligned}$$

Therefore, in general,

$$\mathbf{R}_i^{-1} = \mathbf{R}_{i-1}^{-1} - \frac{p_i \mathbf{R}_{i-1}^{-1}\mathbf{d}_i \mathbf{d}_i^H \mathbf{R}_{i-1}^{-1}}{1 + p_i \mathbf{d}_i^H \mathbf{R}_{i-1}^{-1}\mathbf{d}_i}. \tag{2.28}$$

This is a recursion formula with which we can obtain the inverse of $\mathbf{R}_i^{-1}$ from $\mathbf{R}_{i-1}^{-1}$ and the power and the direction vector of the added interferer. Certain algebraic manipulation performed in appendix [A-1] lead to

$$\mathbf{R}_i^{-1} = \mathbf{R}_{i-1}^{-1}\left[\frac{(2 + p_i \mathbf{d}_i^H \mathbf{R}_{i-1}^{-1}\mathbf{d}_i)\mathbf{R}_{i-1}^{-1} - \mathbf{R}_i}{1 + p_i \mathbf{d}_i^H \mathbf{R}_{i-1}^{-1}\mathbf{d}_i}\right]\mathbf{R}_{i-1}^{-1}, \tag{2.29}$$

with

$$\mathbf{R}_0 = \sigma^2 \mathbf{I}_N.$$

One may note that this is a generalized form for computing the inverse of the autocorrelation matrix for both the URA and the MRA structures [39]. It can be applied to any matrix with the properties of Eq. (2.25).

2.5 Examples of the Recursive Inversion Formula

In the next two subsections, the recursive form for finding the inverse of the auto-correlation matrix is applied. Note that the mirror image and other configurations of an MRA with the same number of array elements require no special treatment. They have been embedded in the incoming interference signal vector $\mathbf{d}_i$.

2.5.1 The Single-Interferer Case

For this case equation (2.29) becomes

$$\mathbf{R}_1^{-1} = \mathbf{R}_0^{-1}\left[\frac{(2+p_1\mathbf{d}_1^H\mathbf{R}_0^{-1}\mathbf{d}_1)\mathbf{R}_0^{-1}-\mathbf{R}_1}{1+p_1\mathbf{d}_1^H\mathbf{R}_0^{-1}\mathbf{d}_1}\right]\mathbf{R}_0^{-1} \tag{2.30}$$

with

$$\mathbf{R}_0 = \sigma^2\mathbf{I}_N. \tag{2.31}$$

Again, certain algebraic manipulations performed in Appendix [A-2] give

$$\mathbf{R}_1^{-1} = \frac{(2\gamma_1+N)\mathbf{I}_N - \mathbf{R}_1/p_1}{\sigma^2(\gamma_1+N)}, \tag{2.32}$$

where $\gamma_1 = \sigma^2/p_1$ is the noise-to-interference ratio.

Also, directly from Eq. (2.28) we can write for the single interferer case, after substituting for $\mathbf{R}_0$,

$$\mathbf{R}_1^{-1} = \sigma^{-2}\left[\mathbf{I} - \frac{\mathbf{d}_1\mathbf{d}_1^H}{\gamma_1+N}\right]. \tag{2.33}$$

2.5.2 The Dual-Interferer Case

From Eq. (2.28), for interferers coming from the direction of $\mathbf{d}_1$ and $\mathbf{d}_2$, we have

$$\mathbf{R}_2^{-1} = \mathbf{R}_1^{-1} - \frac{p_2\mathbf{R}_1^{-1}\mathbf{d}_2\mathbf{d}_2^H\mathbf{R}_1^{-1}}{1+p_2\mathbf{d}_2^H\mathbf{R}_1^{-1}\mathbf{d}_2}. \tag{2.34}$$

Following the derivation in Appendix [A-3]

$$\mathbf{R}_2^{-1} = \sigma^{-2}\left[\mathbf{I} - \alpha_1 \mathbf{d}_1 \mathbf{d}_1^H - \alpha_2 \mathbf{d}_2 \mathbf{d}_2^H + 2\alpha_{12} Re\{\rho \mathbf{d}_1 \mathbf{d}_2^H\}\right] \tag{2.35}$$

where

$$\alpha_1 = \frac{N+\gamma_2}{\beta}, \tag{2.36}$$

$$\alpha_2 = \frac{N+\gamma_1}{\beta}, \tag{2.37}$$

$$\alpha_{12} = \frac{N}{\beta}, \tag{2.38}$$

$$\beta = \gamma_1\gamma_2 + N(\gamma_1+\gamma_2) + N^2(1-\mid \rho \mid^2), \tag{2.39}$$

$$\text{and} \quad \rho = \frac{\mathbf{d}_1^H \mathbf{d}_2}{N}. \tag{2.40}$$

The quantity ρ is the complex correlation coefficient of the interferer direction vectors $\mathbf{d}_1$ and $\mathbf{d}_2$. The quantities γ_1 and γ_2 constitute the noise-to-interference ratio of the respective interferers.

2.6 System Model of Planar Square Array

Consider a square-shaped planar array, the inter-element spacings are d_x and d_y for the x and y axis respectively as shown in Figure 1. We take $d_x = d_y$ to avoid grating lobes.

The field at a distant point P in the free space contributed by the column coincident with the x axis is [37]

$$E_0 = f(\theta,\phi)\sum_{m=1}^{N} s_{m0} e^{j(mkd_x \sin\theta\cos\phi + \alpha_x)}, \tag{2.41}$$

where $f(\theta,\phi)$ is the element pattern function, s_{m0} is the amplitude excitation of the mth element in the column $y = 0$, α_x is the associated phase excitation, and $k = 2\pi/\lambda$.

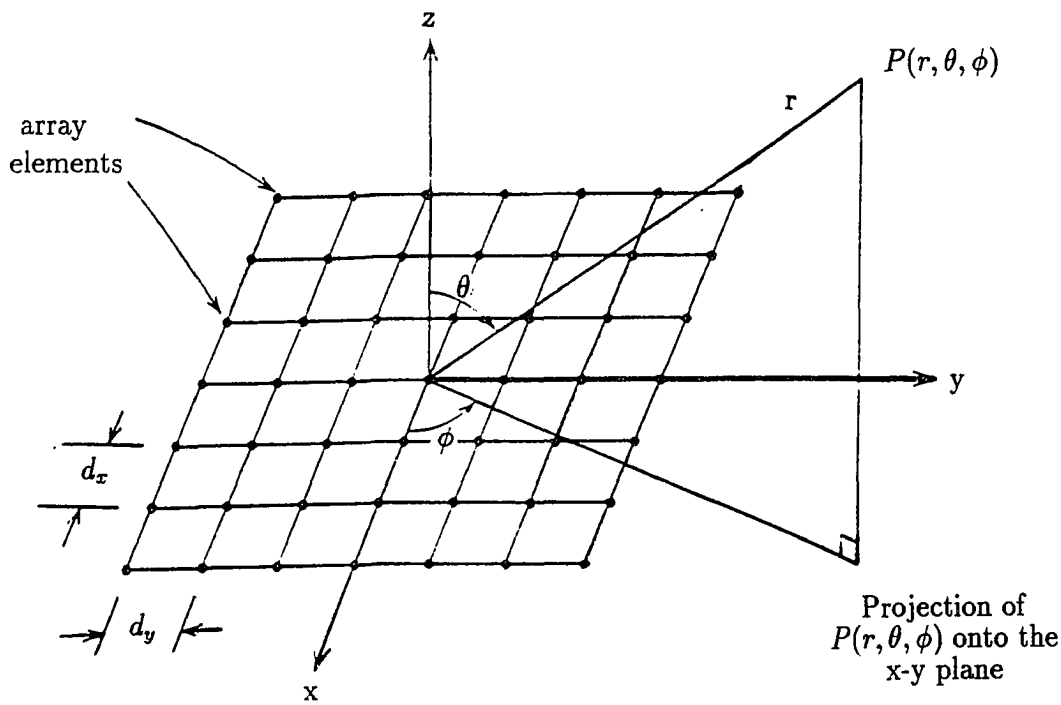

Figure 1 The URA square array element arrangement.

It is seen that the output signal depends on both the projected azimuth angle ϕ and the elevation angle θ. Only the pattern in the xz plane has an expression comparable to the linear array. When the amplitude excitations for elements in other columns are proportional to those for corresponding elements on the x axis,

$$s_{mn} = s_{m0}s_{0n}. \tag{2.42}$$

The total phaser sum of signal contributions from all array elements is given by

$$\begin{aligned} E(\theta,\phi) &= \sum_{n=1}^{N_y} E_n \\ &= f(\theta,\phi)S_xS_y, \end{aligned} \tag{2.43}$$

where

$$S_x = \sum_{m=1}^{N_x} s_{m0} e^{j(mkd_x \sin\theta \cos\phi + \alpha_x)} \tag{2.44}$$

$$S_y = \sum_{n=1}^{N_y} s_{n0} e^{j(nkd_x \sin\theta \sin\phi + \alpha_y)}. \tag{2.45}$$

The quantities s_{mn} and $\alpha_x + \alpha_y$ may be considered as the total amplitude and phase excitations of the (m,n)th element in the array. From Eq. (2.43), the pattern of the square array is the product of array factors of two linear arrays, one along the x axis and the other along the y axis [38].

The quantities α_x and α_y can be arbitrarily adjusted so that the position of the main beam of S_x is different from S_y [26]. Assuming that the main beams do point to the same position (θ_0, ϕ_0) and that the elements are progressively phased, we can determine the required α_x and α_y as follows:

$$\alpha_x = -mkd_x \sin\theta_0 \cos\phi_0 \tag{2.46}$$

$$\alpha_y = -mkd_y \sin\theta_0 \sin\phi_0. \tag{2.47}$$

Since $\sin\theta = \sin(\pi - \theta)$, we can see from Eq. (2.44) and Eq. (2.45) that both S_x and S_y are generally bidirectional in any vertical plane given by ϕ=constant. This represents two *pencil beams*, with one above and one below the array plane. The one below the array plane can be eliminated by a proper choice of the element pattern function $f(\theta, \phi)$ or it can be reflected by the use of a ground plane.

When $s_{m0}, s_{n0}, N_x, N_y, d_x, d_y, \theta_0$ and ϕ_0 are all specified, the characteristics such as the beamwidth, sidelobe levels, and positions can be analyzed in the same manner as that for linear arrays.

With the above formulation, the output of the (m,n)th element is given by

$$x_{m,n} = \sum_{l=1}^{r} s_{mn} e^{j(i_{m-1} k d_x \sin\theta \cos\phi + i_{n-1} d_x \sin\theta \sin\phi)} + \nu_{m,n} \tag{2.48}$$

where r is the number of interferers, $\nu_{m,n}$ is the added noise assumed uncorrelated from sensor to sensor, and i_m and i_n are integers representing the location of the elements. For the URA case, i_m=m and i_n=n for m, n=0, 1,...,N-1. For the MRA case, i_m and i_n are chosen according to Table 1 as before.

Using an arrangement similar to that of the linear array case, the output was written in the vector form

$$\begin{aligned} \mathbf{x} &= [x_{1,1}, x_{1,2}, ..., x_{1,N}; x_{2,1}, x_{2,2}, .; ., x_{N,N}] \\ &\quad + [\nu_{1,1}, \nu_{1,2}, ..., \nu_{1,N}, \nu_{2,1}, \nu_{2,2}, ..., \nu_{N,N}]_{N^2 \times 1}. \end{aligned} \tag{2.49}$$

In this arrangement, the autocorrelation matrix is still in the form of Eq. (2.6)

$$\mathbf{R}_s = E[\mathbf{x}\mathbf{x}^H]. \tag{2.50}$$

The eigenvalues and eigenvectors of this autocorrelation matrix can be partitioned into two subsets, as in the linear array case. There are r eigenvectors corresponding to the interference subspace with eigenvalues larger than σ^2 and $N^2 - r$ eigenvectors corresponding to the noise subspace with the eigenvalue of σ^2. All the properties of the autocorrelation matrix for the linear array case can be applied to the planar array cases. Conventional beamforming and eigencanceling methods can both be used for the planar array case with a different autocorrelation matrix for interference cancellation purposes. The optimum weight vector for the planar array using the conventional beamforming method has exactly the same form as Eq. (2.9):

$$\mathbf{w}_{op} = \mathbf{R}_s^{-1} \mathbf{A}_p (\mathbf{A}_p^H \mathbf{R}_s^{-1} \mathbf{A}_p)^{-1} \mathbf{g} \tag{2.51}$$

where $\mathbf{A}_p$ and $\mathbf{g}$ are the preassigned directions and their respective gains.

For the planar array using the eigencanceling method, the optimum weight is in

exactly the same form as Eq. (2.15):

$$\tilde{\mathbf{w}}_{op} = \mathbf{R}_s^{-1}\check{\mathbf{A}}_p(\check{\mathbf{A}}_p^H\mathbf{R}_s^{-1}\check{\mathbf{A}}_p)^{-1}\tilde{\mathbf{g}} \tag{2.52}$$

with $\check{\mathbf{A}}_p = [\mathbf{A}_p \mid \mathbf{E}_{s_r}]$ and $\tilde{\mathbf{g}}^H = [\mathbf{g}^H \mid 0]$, where $\mathbf{E}_{s_r}$ is the collection of all eigenvectors spanning the interference subspace. $\mathbf{A}_p$ is the matrix of preassigned directions, with gain $\mathbf{g}^H$.

Note that just as in the linear array case, the reference point chosen for the square array structure does not affect the autocorrelation matrix. According to Table 1, with a given number of linear array elements N, there exist M configurations (not counting the mirror images). In the case of the MRA square array, there exist $4M^2$ possible configurations for these N^2 elements. The possible nine-element MRA square array configurations are shown in Figure 2.

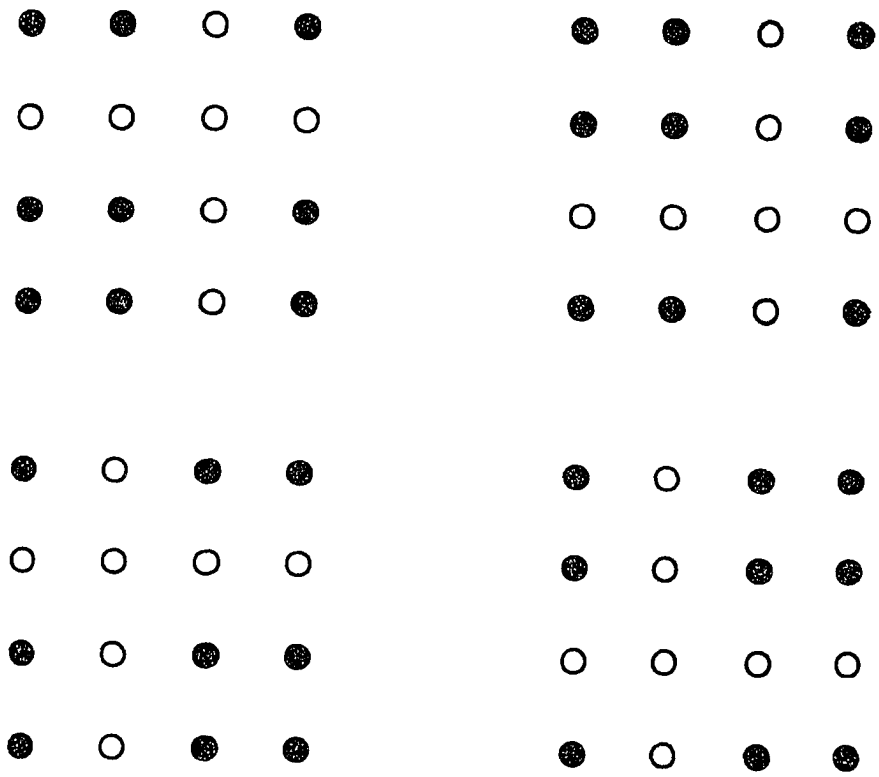

Figure 2 All the possible MRA-3 square array configurations.

CHAPTER 3

PERFORMANCE EVALUATION

In this chapter, the linear Minimum Redundancy Array (MRA) structure and Uniform Regular Array (URA) structure are compared using the Minimum Noise Variance (MNV) criteria as the performance measure. The Minimum Noise Variance Value (MNVV) is the value of $\mathbf{w}_{op}^H \mathbf{R} \mathbf{w}_{op}$. First the conventional beamforming technique is applied to both the URA and the MRA structures. The formulas for calculating the MNVV of single- and dual-interferer are derived. The performance comparison follows. The second part of this chapter carries out the performance evaluation for both the URAs and the MRAs using the eigencanceling technique. Since the extra constraint imposed on the original optimization problem for the eigencanceling technique requires the calculation of the eigenvectors of the autocorrelation matrix, the reformulation of the problem is presented. A similar situation for calculating an inverse matrix of the modified optimization problem exists, but a recursive formula is derived for solving the dual-interferer case here. The explicit results of the single- and dual-interferer cases followed by the performance comparison between the URA and the MRA are also included. Since the eigenvalue spread plays an important role in the convergence rate of the optimization process, it is investigated at the end of this chapter.

With the preassigned directional gain constraint $\mathbf{w}_{op}^H \mathbf{a}_p = 1$ imposed, the result of the MNVV obtained is equivalent to assuming zero dB desired signal power. Furthermore, since with this criterion we use the fact that the desired signal has been previously removed, then $\mathbf{w}_{op}^H \mathbf{R} \mathbf{w}_{op}$ gives the total interference plus noise power at the output of the array. Therefore $1/\mathbf{w}_{op}^H \mathbf{R} \mathbf{w}_{op}$ is the signal-to-interference plus noise ratio (SINR) for a zero dB desired signal power.

3.1 Conventional Beamforming Technique

Following the optimization problem formulation from the previous chapter for the conventional beamforming, with the optimum weight vector obtained from Eq. (2.9) the MNVV becomes

$$\mathbf{w}_{op}^H \mathbf{R} \mathbf{w}_{op} = \mathbf{g}^H (\mathbf{A}_p^H \mathbf{R}^{-1} \mathbf{A}_p)^{-1} \mathbf{A}_p^H \mathbf{R}^{-1} \mathbf{A}_p (\mathbf{A}_p^H \mathbf{R}^{-1} \mathbf{A}_p)^{-1} \mathbf{g}. \tag{3.1}$$

For the case of a single desired direction $\mathbf{A}_p = \mathbf{a}_p$ with gain of unity, $\mathbf{g} = 1$, the Eq. (3.1) becomes,

$$\begin{aligned} \mathbf{w}_{op}^H \mathbf{R} \mathbf{W}_{op} &= \frac{\mathbf{a}_p^H \mathbf{R}^{-1}}{\mathbf{a}_p^H \mathbf{R}^{-1} \mathbf{a}_p} \mathbf{R} \frac{\mathbf{R}^{-1} \mathbf{a}_p}{\mathbf{a}_p^H \mathbf{R}^{-1} \mathbf{a}_p} \\ &= \frac{1}{\mathbf{a}_p^H \mathbf{R}^{-1} \mathbf{a}_p}. \end{aligned} \tag{3.2}$$

Using Eq. (2.28) we have

$$\mathbf{a}_p^H \mathbf{R}_i^{-1} \mathbf{a}_p = \mathbf{a}_p^H \mathbf{R}_{i-1}^{-1} \mathbf{a}_p - \frac{p_i \mid \mathbf{a}_p^H \mathbf{R}_{i-1}^{-1} \mathbf{a}_i \mid^2}{1 + p_i \mathbf{a}_i^H \mathbf{R}_{i-1}^{-1} \mathbf{a}_i}. \tag{3.3}$$

This shows that the SINR decreases as a result of an added interference signal.

Without loss of generality, we will take the direction of the desired signal to be at broadside [39], i.e.

$$\mathbf{a}_p = [1, 1, \ldots, 1]^T. \tag{3.4}$$

In this case the MNVV from Eq. (3.2) becomes

$$\mathbf{w}_{op}^H \mathbf{R} \mathbf{w}_{op} = \frac{1}{\mathbf{1}^\tau \mathbf{R}^{-1} \mathbf{1}} \triangleq \frac{1}{\|\mathbf{R}^{-1}\|_b} \tag{3.5}$$

where for any matrix A, $\|A\|_b$ denotes the sum of all elements.

3.1.1 The Single-Interferer Case

For an N element array with noise-to-interference ratio of $\gamma_1 = \sigma^2/p_1$ and the interferer direction given by $\mathbf{d}_1$, from Eq. (2.33)

$$\|\mathbf{R}_1^{-1}\|_b = \sigma^{-2}\left[N - \frac{\|\mathbf{d}_1\mathbf{d}_1^H\|_b}{\gamma_1 + N}\right]. \tag{3.6}$$

But

$$\|\mathbf{d}_1\mathbf{d}_1^H\|_b = N + \sum_{i=1}^{N}\sum_{j=1,j\neq i}^{N}\gamma_{ij} \tag{3.7}$$

where $\gamma_{ij}; i \neq j$ are the off diagonal entries of the matrix $\mathbf{d}_1\mathbf{d}_1^H$. Since $\mathbf{d}_1\mathbf{d}_1^H$ is Hermitian, the off diagonal terms are complex conjugate pairs. Therefore,

$$\|\mathbf{d}_1\mathbf{d}_1^H\|_b = N + 2Re\left\{\sum_{i=1}^{N}\sum_{j=i+1}^{N}\gamma_{ij}\right\}. \tag{3.8}$$

Substituting Eqs. (3.8) and (3.6) into Eq. (3.5) the MNVV is now

$$\mathbf{w}_{op}^H\mathbf{R}\mathbf{w}_{op} = \frac{\sigma^2(N+\gamma_1)}{N(N+\gamma_1-1) - 2Re\left\{\sum_{i=1}^{N}\sum_{j=i+1}^{N}\gamma_{ij}\right\}}, \tag{3.9}$$

where the summation is over the off diagonal terms of $\mathbf{d}_1\mathbf{d}_1^H$.

Performance Comparison for the URA and the MRA

For the URA,

$$\mathbf{d}_1 = [1, e^{-j\omega_1}, e^{-j2\omega_1}, \ldots, e^{-j(N-1)\omega_1}].$$

The matrix $\Gamma = \mathbf{d}_1\mathbf{d}_1^H$, besides being Hermitian, is also Toeplitz. In particularly, the matrix Γ has elements $\gamma_{i,j}$ with

$$\gamma_{i,i+n} = e^{jn\omega_l}, \qquad n = 1, 2, \ldots, N-1.$$

Each of these subdiagonals has $N-n$ elements, $n = 1, 2, \ldots, N-1$. Using Eq. (3.9), for the URA

$$\mathbf{w}_{op}^H \mathbf{R} \mathbf{w}_{op} = \frac{\sigma^2(N+\gamma_1)}{N(N+\gamma_1-1) - 2\sum_{n=1}^{N-1}(N-n)\cos(n\omega_1)}. \tag{3.10}$$

For the MRA, the matrix $\mathbf{d}_1\mathbf{d}_1^H$ is Hermitian, but not Toeplitz. In fact, for the zero redundancy cases, all the entries above the main diagonal are different and are given by $e^{jn\omega_l}, n = 1, 2, \ldots, L-1$ where L is the dimension of the augmented matrix, $L - 1 = N(N-1)/2$. This is the case for three-element and for four-element arrays (see Table 1). In other cases,

$$L - 1 < \frac{N(N-1)}{2}. \tag{3.11}$$

For example, when $N = 5, L-1 = 9 < N(N-1)/2 = 10$. In these cases the elements above the main diagonal are not all different; some of them are repeated. Therefore using these facts in Eq. (3.9), for the MRA structure

$$\mathbf{w}_{op}^H \mathbf{R} \mathbf{w}_{op} = \frac{\sigma^2(N+\gamma_1)}{N(N+\gamma_1-1) - 2\sum_{n=1}^{L-1} e_n \cos(n\omega_1)}, \tag{3.12}$$

where e_n is the number of times of $e^{jn\omega_l}$ appears in the off diagonal terms of $\mathbf{d}_1\mathbf{d}_1^H$. From Eqs. (3.10) and (3.12) we have

$$\frac{(\text{SINR})_{URA}}{(\text{SINR})_{MRA}} = \frac{N(N+\gamma_1-1) - 2\sum_{n=1}^{N-1}(N-n)\cos(n\omega_1)}{N(N+\gamma_1-1) - 2\sum_{n=1}^{L-1} e_n \cos(n\omega_1)}, \tag{3.13}$$

where as mentioned before SINR stands for signal-to-interference plus noise ratio and γ_1 is the noise-to-interference ratio.

Therefore, for the MRA to perform better we must have

$$\sum_{n=1}^{N-1}(N-n)\cos(n\omega_1) > \sum_{n=1}^{L-1} e_n \cos(n\omega_1). \tag{3.14}$$

Clearly the MNVV of both the URA and the MRA using the conventional beamforming technique is a function of the noise-to-interference ratio.

Equivalent Relations

We now derive equivalent relations of Eqs. (3.10) and (3.12) for the URA and the MRA respectively. By definition

$$\begin{aligned} \|\mathbf{d}_1\mathbf{d}_1^H\|_b &= (\mathbf{1}^T\mathbf{d}_1)(\mathbf{d}_1^H\mathbf{1}) \\ &= |\,\mathbf{1}^T\mathbf{d}_1\,|^2 \end{aligned}$$

where again $\mathbf{d}_1 = [1, e^{-ji_1\omega_1}, e^{-ji_2\omega_1}, \ldots, e^{-ji_{N-1}\omega_1}]^T$.

• The URA case:

$$\begin{aligned} \mathbf{1}^T\mathbf{d}_1 &= \sum_{n=0}^{N-1} e^{jn\omega_1} \\ &= e^{j\frac{N-1}{2}\omega_1}\frac{\sin(N\omega_1/2)}{\sin(\omega_1/2)}, \end{aligned} \tag{3.15}$$

$$\begin{aligned} \|\mathbf{d}_1\mathbf{d}_1^H\|_b &= \frac{\sin^2(N\omega_1/2)}{\sin^2(\omega_1/2)} \\ &= g_N^2(\omega_1) \end{aligned} \tag{3.16}$$

where

$$g_N(\omega_1) = \sin(N\omega_1/2)/\sin(\omega_1/2). \tag{3.17}$$

Substituting Eqs. (3.16) and (3.6) into Eq. (3.5), the resulting MNVV is

$$\mathbf{w}_{op}^H \mathbf{R} \mathbf{w}_{op} = \frac{\sigma^2(N+\gamma_1)}{N(N+\gamma_1) - \sin^2(N\omega_1/2)/\sin^2(\omega_1/2)}. \tag{3.18}$$

- The MRA case:

In cases where all $e_n = 1$, by using Eq. (A.17) of Appendix [A-5] in Eq. (3.12), we get

$$\mathbf{w}_{op}^H \mathbf{R} \mathbf{w}_{op} = \frac{\sigma^2(N+\gamma_1)}{N(N+\gamma_1) + (1-N) - \sin(\frac{2L-1}{2}\omega_1)/\sin(\omega_1/2)}. \tag{3.19}$$

Comparing this result to Eqs. (3.6), (3.9) and (3.12) we can easily see that if all $e_n = 1$, then

$$\|\mathbf{d}_1 \mathbf{d}_1^H\|_b = N - 1 + \frac{\sin(\frac{2L-1}{2}\omega_1)}{\sin(\omega_1/2)}. \tag{3.20}$$

Obviously, if not all $e_n = 1$ then

$$\|\mathbf{d}_1 \mathbf{d}_1^H\|_b = N - 1 + \frac{\sin(\frac{2L-1}{2}\omega_1)}{\sin(\omega_1/2)} + \sum_{e_n \neq 1} (e_n - 1)\cos n\omega_1. \tag{3.21}$$

The extra term in the above equation should be subtracted from the denominator of Eq. (3.21) when not all $e_n = 1$.

3.1.2 The Dual-Interferer Case

From Eq. (2.35)

$$\|\mathbf{R}_2^{-1}\|_b = \sigma^{-2}\left[N - \alpha_1\|\mathbf{d}_1\mathbf{d}_1^H\|_b - \alpha_2\|\mathbf{d}_2\mathbf{d}_2^H\|_b + 2\alpha_{12} Re\left\{\rho\|\mathbf{d}_1\mathbf{d}_2^H\|_b\right\}\right] \tag{3.22}$$

where $\|\mathbf{d}_i\mathbf{d}_j^H\| = \mathbf{1}^T\mathbf{d}_i\mathbf{d}_j^H\mathbf{1}$ and $\alpha_1, \alpha_2, \alpha_{12}$ and ρ are previously defined in Eqs. (2.36–2.40).

From the last section we have:

$$\|\mathbf{d}_1\mathbf{d}_1^H\|_b = \begin{cases} N + 2\sum_{n=1}^{N-1}(N-n)\cos n\omega_1 & \text{for URA} \\ N + 2\sum_{n=1}^{L-1} e_n \cos n\omega_1 & \text{for MRA all } e_n = 1. \end{cases}$$

Or, equivalently, from Eq. (3.16) or Eq. (3.20)

$$\|\mathbf{d}_1\mathbf{d}_1^H\|_b = \begin{cases} \dfrac{\sin^2(N\omega_1/2)}{\sin^2(\omega_1/2)} & \text{for URA} \\ N - 1 + \dfrac{\sin(\frac{2L-1}{2}\omega_1)}{\sin(\omega_1/2)} & \text{for MRA all } e_n = 1. \end{cases}$$

Similar equations are obtained for $\|\mathbf{d}_2\mathbf{d}_2^H\|$.

From Eq. (2.40) and the definition of $\mathbf{d}_i$ in Eq. (2.5),

$$\rho = \frac{1}{N}\sum_{n=0}^{N-1} e^{ji_n(\omega_1-\omega_2)}. \tag{3.23}$$

For the URA case $i_n = n$, we get

$$\rho = \frac{1}{N} e^{j\frac{N-1}{2}(\omega_1-\omega_2)} \frac{\sin(N(\omega_1-\omega_2)/2)}{\sin((\omega_1-\omega_2)/2)} \tag{3.24}$$

$$|\rho|^2 = \frac{1}{N^2}\frac{\sin^2(N(\omega_1-\omega_2)/2)}{\sin^2((\omega_1-\omega_2)/2)}. \tag{3.25}$$

For the MRA case we have from Eq. (A.18) of Appendix [A-6],

$$|\rho|^2 = \frac{1}{N^2}\left(N + 2\sum_{n=1}^{L-1} e_n \cos n(\omega_1-\omega_2)\right) \tag{3.26}$$

or, equivalently, when using Eq. (A.17) of Appendix [A-5]

$$|\rho|^2 = \frac{1}{N^2}\left(N - 1 + \frac{\sin(\frac{2L-1}{2}(\omega_1 - \omega_2))}{\sin((\omega_1 - \omega_2)/2)}\right), \tag{3.27}$$

if all $e_n = 1$.

Finally from Eq. (3.22) together with Eqs. (2.36–2.40) for the URA with two interferers, we write,

$$\mathbf{w}_{op}^H \mathbf{R} \mathbf{w}_{op} = \frac{\sigma^2[\gamma_1\gamma_2 + N(\gamma_1 + \gamma_2) + N^2 - g_N^2(\omega_1 - \omega_2)]}{N - (N + \gamma_2)g_N^2(\omega_1) - (N + \gamma_1)g_N^2(\omega_2) + 2g_N(\omega_1)g_N(\omega_2)g_N(\omega_1 - \omega_2)}, \tag{3.28}$$

where

$$g_N(\omega) = \frac{\sin(N\omega/2)}{\sin(\omega/2)}. \tag{3.29}$$

For the MRA case with all $e_n = 1$

$$\mathbf{w}_{op}^H \mathbf{R} \mathbf{w}_{op} = \frac{\sigma^2[\gamma_1\gamma_2 + N(\gamma_1 + \gamma_2) + N^2 - g_L(\omega_1 - \omega_2)]}{N - (N + \gamma_2)g_L(\omega_1) - (N + \gamma_1)g_L(\omega_2) + 2Re\{\mathbf{d}_1^H \mathbf{d}_2)\|\mathbf{d}_1 \mathbf{d}_2^H\|_b\}} \tag{3.30}$$

where

$$g_L(\omega) = N - 1 + \frac{\sin(\frac{2L-1}{2}\omega)}{\sin(\omega/2)}. \tag{3.31}$$

Performance Comparison of the URA and the MRA

To compare the performance of these two arrays we must deal with equation (3.28) and (3.30). It is almost impossible to do this analytically for every condition. However, the contour plots obtained numerically are given for the dual-interferer case in Chapter 5.

3.1.3 Numerical Examples

In the following example it will be shown that there is an angle ω_t which marks the region where the MRA performs better than the URA when the interferers are

closer to broadside (the direction vector of the desired signal). Even though the URA performs better than the MRA for $\omega_1 > \omega_t$, improved performance only occurs in directions where both arrays already have sufficient cancellation. The degraded performance of the MRA in some directions is very small when compared to the cancellation depth at those directions.

Example 1. Three-element array (N=3)

From Eq. (3.10) for the URA,

$$\mathbf{w}_{op}^H \mathbf{R} \mathbf{w}_{op} = \frac{\sigma^2(3+\gamma_1)}{3(\gamma_1+2) - 2(2\cos\omega_1 + \cos 2\omega_1)}. \tag{3.32}$$

For the MRA with N=3 and L=4, each element above the diagonal of $\mathbf{d}_1\mathbf{d}_1^H$ appears only once *i.e.*, $e_1 = e_2 = e_3 = 1$. Therefore from Eq. (3.12)

$$\mathbf{w}_{op}^H \mathbf{R} \mathbf{w}_{op} = \frac{\sigma^2(3+\gamma_1)}{3(\gamma_1+2) - 2(\cos\omega_1 + \cos 2\omega_1 + \cos 3\omega_1)}. \tag{3.33}$$

The SINR can now be written as

$$\frac{(\text{SINR})_{URA}}{(\text{SINR})_{MRA}} = \frac{3(2+\gamma_1) - 2(2\cos\omega_1 + \cos 2\omega_1)}{3(2+\gamma_1) - 2(\cos\omega_1 + \cos 2\omega_1 + \cos 3\omega_1)}. \tag{3.34}$$

From Eq. (3.14) for the MRA to perform better than the URA, we must have,

$$\begin{aligned} \cos\omega_1 + \cos 2\omega_1 + \cos 3\omega_1 &< 2\cos\omega_1 + \cos 2\omega_1 \\ \cos 3\omega_1 &< \cos\omega_1. \end{aligned} \tag{3.35}$$

We show in Appendix [A-4] that the condition in Eq. (3.35) is satisfied for $\omega_1 < \pi/2$. To relate this to physical direction θ_1, we note from Eq. (2.2) by substituting $c = \lambda f_0$ and letting $d = \lambda/2$

$$\omega_1 = \frac{\lambda}{2}\frac{2\pi f_0}{\lambda f_0}\sin\theta_1 = \pi\sin\theta_l. \tag{3.36}$$

Thus, when $\omega_t = \pi/2, \theta_t = 30°$.

Example 2. Four-element array (N=4)

From Eq. (3.10) for the URA

$$\mathbf{w}_{op}^H \mathbf{R} \mathbf{w}_{op} = \frac{\sigma^2(4+\gamma_1)}{4(3+\gamma_1) - 2(3\cos\omega_1 + 2\cos 2\omega_1 + \cos 3\omega_1)}. \tag{3.37}$$

For the MRA, N=4, L=7, again $e_n = 1$, for $n = 1, 2, \ldots, 6$

$$\mathbf{w}_{op}^H \mathbf{R} \mathbf{w}_{op} = \frac{\sigma^2(4+\gamma_1)}{4(3+\gamma_1) - 2\sum_{n=1}^{6} \cos(n\omega_1)}. \tag{3.38}$$

From Eqs. (3.10) and (3.12)

$$\frac{(\mathrm{SINR})_{URA}}{(\mathrm{SINR})_{MRA}} = \frac{4(3+\gamma_1) - 2(3\cos\omega_1 + 2\cos 2\omega_1 + \cos 3\omega_1)}{4(3+\gamma_1) - 2\sum_{n=1}^{6} \cos(n\omega_1)}. \tag{3.39}$$

and from Eq. (3.14), for the MRA to perform no worse than the URA, we must have

$$\cos 4\omega_1 + \cos 5\omega_1 + \cos 6\omega_1 \leq 2\cos\omega_1 + \cos 2\omega_1. \tag{3.40}$$

Equality in the above equation occurs when $\omega_1 = \omega_t$, the limiting position vector angle. For ω_1 smaller than the angle ω_t, the MRA performs better than the URA.

3.2 Eigencanceling Technique

In this section, attention will remain focussed on the MNV performance of the MRA structure operating in a multiple narrow-band interference environment. This is the most suitable approach for radar applications where the desired signal is assumed not to exist during adaptation. In order to evaluate the performance of the eigencanceler using the MRA structure without being overwhelmed with numerical results, most of the attention will be focussed on the single- and dual-interferer problems. These

cases are sufficient to illustrate the interaction of multiple interferers and, at the same time, give insight into more complex cases. We have published earlier results in references [40, 41]. When using the eigencanceling technique, the optimization problem will be as follows:

$$\begin{aligned} \min \quad & \mathbf{w}^H\mathbf{R}\mathbf{w} && (3.41)\\ \text{subject to} \quad & \mathbf{w}^H\mathbf{A}_p = \mathbf{g}^H, && (3.42)\\ \text{and} \quad & \mathbf{w}^H\mathbf{E}_r = \mathbf{0} && (3.43) \end{aligned}$$

where $\mathbf{A}_p = [\mathbf{a}_{p_1}, \mathbf{a}_{p_2}, \ldots, \mathbf{a}_{p_p}]$; $\mathbf{a}_{p_i}$, $i = 1, 2, \ldots, p$ are the predefined directions and $\mathbf{g}^H = [g_1, g_2, \ldots, g_p]$; g_i, $i = 1, 2, \ldots, p$ are the preassigned gains in the direction $\mathbf{a}_{p_i}$ as described in the previous chapter for the conventional beamforming case. The column span of $\mathbf{E}_r$ is the interference subspace.

The optimization problem in Eqs. (3.41–3.43) is equivalent to

$$\begin{aligned} \min \quad & \mathbf{w}^H\mathbf{R}\mathbf{w} \\ \text{subject to} \quad & \mathbf{w}^H\mathbf{A}_p = \mathbf{g}^H, \\ \text{and} \quad & \mathbf{w} = \mathbf{E}_\nu\mathbf{c}. && (3.44) \end{aligned}$$

In fact, the condition in Eq. (3.44) reflects the requirement that the optimal weight be in the noise subspace $\mathbf{G}_\nu$ which is orthogonal to the interference subspace $\mathbf{G}_r$. By substituting Eq. (3.44) in Eqs. (3.41) and (3.42) we are able to remove the added constraint and obtain an equivalent form of the optimization problem

$$\begin{aligned} \min \quad & \mathbf{c}^H\mathbf{E}_\nu^H\mathbf{R}\mathbf{E}_\nu\mathbf{c}, && (3.45)\\ \text{subject to} \quad & \mathbf{c}^H\mathbf{E}_\nu^H\mathbf{A}_p = \mathbf{g}^H. && (3.46) \end{aligned}$$

From Eqs. (2.6) and (2.10) we have

$$\mathbf{R}\mathbf{E}_\nu = \sigma^2\mathbf{E}_\nu. \qquad (3.47)$$

Equation (3.47) also reflects the fact that $\mathbf{e}_l$, l=r+1,..., N are the eigenvectors of $\mathbf{R}$ corresponding to the eigenvalue σ^2. Substituting Eq. (3.47) in Eq. (3.45) our optimization problem becomes that of finding the vector $\mathbf{c}$ that minimizes

$$\sigma^2 \mathbf{c}^H \mathbf{E}_\nu^H \mathbf{E}_\nu \mathbf{c}, \tag{3.48}$$

$$\text{subject to} \quad \mathbf{c}^H \mathbf{E}_\nu^H \mathbf{A}_p = \mathbf{g}^H. \tag{3.49}$$

Using a Lagrange multiplier vector $\boldsymbol{\lambda}$ we have the following unconstrained optimization problem as solved in section 2.3.1,

$$\min J = \sigma^2 \mathbf{c}^H \mathbf{U} \mathbf{c} + \boldsymbol{\lambda}^\tau (\mathbf{A}_{pp}^H \mathbf{c} - \mathbf{g}) + (\mathbf{c}^H \mathbf{A}_{pp} - \mathbf{g}^H) \boldsymbol{\lambda} \tag{3.50}$$

where

$$\mathbf{U} = \mathbf{E}_\nu^H \mathbf{E}_\nu \tag{3.51}$$

$$\text{and } \mathbf{A}_{pp} = \mathbf{E}_\nu^H \mathbf{A}_p. \tag{3.52}$$

Taking the gradient of J with respect to $\mathbf{c}$ we get

$$\nabla_c J = 2\sigma^2 \mathbf{U} \mathbf{c} + 2\mathbf{A}_{pp} \boldsymbol{\lambda},$$

and equating this to zero we then have

$$\mathbf{c}_{op} = -\sigma^{-2} \mathbf{U}^{-1} \mathbf{A}_{pp} \boldsymbol{\lambda}. \tag{3.53}$$

But

$$\begin{aligned} \mathbf{g}^H &= \mathbf{c}_{op}^H \mathbf{A}_{pp} = -\sigma^{-2} \boldsymbol{\lambda}^\tau (\mathbf{A}_{pp}^H \mathbf{U}^{-1} \mathbf{A}_{pp}) \\ \Longrightarrow \boldsymbol{\lambda}^\tau &= -\sigma^2 \mathbf{g}^H (\mathbf{A}_{pp}^H \mathbf{U}^{-1} \mathbf{A}_{pp})^{-1} \end{aligned}$$

Finally substituting in Eq. (3.54), we get

$$\mathbf{c}_{op} = \mathbf{U}^{-1} \mathbf{A}_{pp} (\mathbf{A}_{pp}^H \mathbf{U}^{-1} \mathbf{A}_{pp})^{-1} \mathbf{g} \tag{3.54}$$

where we used the fact that $\mathbf{U}$, and hence $\mathbf{U}^{-1}$, is Hermitian.

For the case of a single desired direction $\mathbf{A}_{pp} = \mathbf{a} = \mathbf{E}_\nu^H \mathbf{a}_p$. Without loss of generality, we set $\mathbf{g} = \mathbf{1}$ and get

$$\mathbf{c}_{op} = \frac{\mathbf{U}^{-1}\mathbf{a}}{\mathbf{a}^H\mathbf{U}^{-1}\mathbf{a}} \tag{3.55}$$

where

$$\mathbf{a} = \mathbf{E}_\nu^H \mathbf{a}_p.$$

Using the MNV as an optimization criterion leads to the following conclusions:

1. The constraint Eq. (3.43) restricts the optimal weight to be in the span of the noise eigenvectors, enabling the array to do eigencanceling in the direction of interference.

2. Due to constraint Eq. (3.42), with g=1, our result is equivalent to assuming that the desired signal power at the output of the array is zero dB.

Since with such criterion we use the fact that the desired signal has been previously removed or is absent, then $\sigma^2 \mathbf{c}_{op}^H \mathbf{U} \mathbf{c}_{op}$ gives the optimal total interference plus noise at the output of the array. Therefore $(\sigma^2 \mathbf{c}_{op}^H \mathbf{U} \mathbf{c}_{op})^{-1}$ is the SINR for a zero dB desired signal power.

Using Eq. (3.48) with Eq. (3.55) for $\mathbf{c}_{op}$, after normalization to the quiescent noise σ^2, we get the "Normalized Minimum Noise Variance" value (NMNVV)

$$\frac{J_{min}}{\sigma^2} = \mathbf{c}_{op}^H \mathbf{U} \mathbf{c}_{op} = \frac{1}{\mathbf{a}^H\mathbf{U}^{-1}\mathbf{a}} \tag{3.56}$$

where again, $\mathbf{a} = \mathbf{E}_\nu^H \mathbf{a}_p$. To simplify our analysis, the direction of the desired signal $\mathbf{a}_p$ will be taken at broadside from now on. That is,

$$\mathbf{a}_p = [1, 1, \ldots, 1]^T. \tag{3.57}$$

In the next subsection we will discuss the performance of the MRA canceler. The elements are located at $i_n\lambda/2$, where i_n are integers, not necessarily consecutive.

3.2.1 The Single-Interferer Case

Since the matrix $\mathbf{U}$ is Hermitian and positive definite, its inverse can be expressed in terms of the following expansion

$$\mathbf{U}^{-1} = \sum_{n=1}^{N-1} \lambda_n^{-1} \mathbf{u}^{(n)} \mathbf{u}^{(n)H} \tag{3.58}$$

where λ_n's and $\mathbf{u}^{(n)}$'s; n=1,2,..., N-1 are the eigenvalues and eigenvectors of the matrix $\mathbf{U}$ respectively. Substituting Eq. (3.58) in Eq. (3.56), the normalized minimum noise variance can be expressed as follows:

$$\frac{J_{min}}{\sigma^2} = \frac{1}{\sum_{n=1}^{N-1} \lambda_n^{-1} \mid \mathbf{u}^{(n)H} \mathbf{a} \mid^2}. \tag{3.59}$$

We will determine the matrix $\mathbf{U}$ and find its eigenvalues and eigenvectors analytically. From Eq. (2.4) for $\mathbf{D}_r = \mathbf{d}_r = [\ 1,\ e^{-ji_1\omega_1},\ e^{-ji_2\omega_1},\ldots,\ e^{-ji_{N-1}\omega_1}]$, the correlation matrix takes the form

$$\mathbf{R} = p_1 \mathbf{d}_r \mathbf{d}_r^H + \sigma^2 \mathbf{I}_N. \tag{3.60}$$

Since there is only one interferer, the eigenvector of $\mathbf{R}$ corresponding to the interference subspace is in the direction of $\mathbf{d}_r$. Without loss of generality we simply take $\mathbf{e}_1 = \mathbf{d}_r$. Its corresponding eigenvalue can be easily determined from $\mathbf{R}\mathbf{e}_1 = \mu_1 \mathbf{e}_1$

as $\mu_1 = Np_1 + \sigma^2$. Let $\mathbf{E}_\nu = [\ \mathbf{e}_2, \mathbf{e}_3, \ldots, \mathbf{e}_N]$ be the matrix of N-1 eigenvectors corresponding to the N-1 smallest eigenvalues of $\mathbf{R}$. These vectors span the noise subspace. Since the noise subspace is orthogonal to the interference subspace, then $\mathbf{e}_n \perp \mathbf{e}_1$, for n=2, 3, ..., N, and these N-dimensional eigenvectors can be determined systematically as follows:

$$\mathbf{e}_2 = \begin{bmatrix} -1 \\ e^{-ji_1\omega_1} \\ 0 \\ \vdots \\ \vdots \\ 0 \end{bmatrix}_{N\times 1}, \mathbf{e}_3 = \begin{bmatrix} 0 \\ -1 \\ e^{-j(i_2-i_1)\omega_1} \\ 0 \\ \vdots \\ 0 \end{bmatrix}_{N\times 1} \ldots, \mathbf{e}_N = \begin{bmatrix} 0 \\ 0 \\ \vdots \\ 0 \\ -1 \\ e^{-j(i_{N-1}-i_{N-2})\omega_1} \end{bmatrix}_{N\times 1} \tag{3.61}$$

Note that these eigenvectors are orthogonal to $\mathbf{e}_1$, but not orthogonal to each other. The eigenvalues $\mu_2, \mu_3, \ldots, \mu_N$, corresponding to these eigenvectors, are simply $\mu_n = \sigma^2$ for n=2, ..., N.

Finally, the matrix $\mathbf{U}$ can be formed from $\mathbf{U} = \mathbf{E}_\nu^H \mathbf{E}_\nu$, where $\mathbf{E}_\nu = [\ \mathbf{e}_2, \mathbf{e}_3, \ldots, \mathbf{e}_N]$. The result is

$$\mathbf{U} = \begin{bmatrix} 2 & -e^{ji_1\omega_1} & 0 & \ldots & 0 & 0 \\ -e^{-ji_1\omega_1} & 2 & -e^{j(i_2-i_1)\omega} & \ldots & 0 & 0 \\ 0 & -e^{-j(i_2-i_1)\omega_1} & 2 & \ldots & 0 & 0 \\ 0 & 0 & -e^{-j(i_3-i_2)\omega_1} & \ldots & 0 & 0 \\ \vdots & \vdots & \vdots & \vdots & \vdots & \vdots \\ 0 & 0 & 0 & \ldots & -e^{j(i_{N-3}-i_{N-4})\omega_1} & 0 \\ 0 & 0 & 0 & \ldots & 2 & -e^{j(i_{N-2}-i_{N-3})\omega_1} \\ 0 & 0 & 0 & \ldots & -e^{-j(i_{N-2}-i_{N-3})\omega_1} & 2 \end{bmatrix}. \tag{3.62}$$

In Appendices [B-1] and [B-2], the eigenvalues λ_n, and eigenvector $\mathbf{u}^{(n)}$, n=1,2,..., N-1, respectively, are derived analytically as

$$\lambda_n = 2(1 - \cos\frac{\pi n}{N}) = 4\sin^2(\frac{\pi n}{2N}) \tag{3.63}$$

$$\text{and} \quad \mathbf{u}^{(n)} = [u_1^{(n)}, u_2^{(n)}, \ldots, u_{N-1}^{(n)}]^T$$

$$\text{where} \quad u_k^{(n)} = e^{-ji_{k-1}\omega_1} \frac{\sin(\pi nk/N)}{\sqrt{\sum_{n=1}^{N-1} \sin^2(\pi nk/N)}}. \tag{3.64}$$

As mentioned earlier, the value i_{k-1} are integers chosen appropriately for different array structures, and ω_1 is related to the directional angle θ_1 of the single interferer by Eq. (3.36) as $\omega_1 = \pi \sin\theta_1$.

Using Eq. (B.15) in Appendix [B-3] together with Eq. (3.59) we obtain

$$\sum_{n=1}^{N-1} \lambda_n^{-1} \mid \mathbf{u}^{(n)H}\mathbf{a} \mid^2 = \sum_{n=1}^{N-1} P_n \mid \sum_{k=1}^{N-1} Q_{nk}(e^{ji_k\omega_1} - e^{ji_{k-1}\omega_1}) \mid^2 \tag{3.65}$$

where

$$P_n = \frac{1}{4\sin^2(\frac{\pi n}{2N})}, \quad Q_{nk} = \frac{\sin(\pi nk/N)}{q_k}, \quad q_k = \sqrt{\sum_{n=1}^{N-1} \sin^2(\frac{\pi nk}{N})}. \tag{3.66}$$

Expanding the above equation, we prove in Appendix [B-4] (see Eq. (B.16)) that Eq. (3.65) is equivalent to

$$\begin{aligned} \sum_{n=1}^{N-1} P_n \quad \{ & \sum_{l=1}^{N-1} \sum_{k=l+1}^{N-1} [Q_{nl}Q_{nk}(e^{ji_l\omega_1} - e^{ji_{l-1}\omega_1})(e^{ji_k\omega_1} - e^{ji_{k-1}\omega_1}) \\ & + \text{complex conjugate}] + Q_{nl}Q_{nl} \mid e^{ji_l\omega_1} - e^{ji_{l-1}\omega_1} \mid^2\}. \end{aligned}$$

Using Eq. (3.65) in Eq. (3.59) we get the final form for the NMNVV

$$\begin{aligned} \frac{J_{min}}{\sigma^2} = 1 \quad / \quad & \{4 \sum_{l=1}^{N-1} P_{l,l} \sin^2(\frac{i_l - i_{l-1}}{2}\omega_1) \\ & + \quad 2 \sum_{l=1}^{N-1} \sum_{k>l}^{N-1} P_{l,k}[\cos(i_l - i_k)\omega_1 + \cos(i_{l-1} - l_{k-1})\omega_1 \\ & - \quad \cos(i_l - i_{k-1})\omega_1 - \cos(i_{l-1} - i_k)\omega_1]\} \end{aligned} \tag{3.67}$$

where

$$P_{l.k} \triangleq \sum_{n=1}^{N-1} P_n Q_{nk} Q_{nl}.$$

For the special case of the URA, we substitute $i_0 = 0, i_1 = 1, i_2 = 2, \ldots, i_{N-1} = N-1$ and get the following

$$\left(\frac{J_{min}}{\sigma^2}\right)_{URA} = 1 \;/\; \{4\sin^2\left(\frac{\omega_1}{2}\right)\sum_{l=1}^{N-1} P_{l,l} + 2\sum_{l=1}^{N-1}\sum_{k>l}^{N-1} P_{l,k}[2\cos(l-k)\omega_1 - \cos(l-k-1)\omega_1 - \cos(l-k+1)\omega_1]\}. \quad (3.68)$$

3.2.2 The Dual-Interferer Case

Let the two interference direction vectors be defined as

$$\mathbf{d}_1 = \begin{bmatrix} 1 \\ e^{-ji_1\omega_1} \\ e^{-ji_2\omega_1} \\ \vdots \\ e^{-ji_{N-1}\omega_1} \end{bmatrix}_{N\times 1} \qquad \mathbf{d}_2 = \begin{bmatrix} 1 \\ e^{-ji_1\omega_2} \\ e^{-ji_2\omega_2} \\ \vdots \\ e^{-ji_{N-1}\omega_2} \end{bmatrix}_{N\times 1}. \quad (3.69)$$

We can then determine the eigenvalues and eigenvectors of the correlation matrix $\mathbf{R} = \mathbf{D}_r\mathbf{S}\mathbf{D}_r^H + \sigma^2\mathbf{I}_N$. Let the vectors $\mathbf{e}_3, \mathbf{e}_4, \ldots, \mathbf{e}_N$ span the noise subspace of $\mathbf{R}$. It is then clear that the corresponding eigenvalues are

$$\mu_3 = \mu_4 = \ldots = \mu_N = \sigma^2.$$

Since the noise and interference subspaces are orthogonal, we have $\mathbf{e}_k \perp \mathbf{d}_1$ and $\mathbf{e}_k \perp \mathbf{d}_2$, for every k=3, 4, ..., N. Thus the noise eigenvectors can be chosen systematically as follows,

$$\mathbf{e}_3 = \begin{bmatrix} -1 \\ p_0 \\ q_0 \\ 0 \\ 0 \\ \vdots \\ 0 \end{bmatrix}_{N\times 1}, \mathbf{e}_4 = \begin{bmatrix} 0 \\ -1 \\ p_1 \\ q_1 \\ 0 \\ \vdots \\ 0 \end{bmatrix}_{N\times 1}, \ldots, \mathbf{e}_N = \begin{bmatrix} 0 \\ 0 \\ \vdots \\ 0 \\ -1 \\ p_{N-3} \\ q_{N-3} \end{bmatrix}_{N\times 1}. \quad (3.70)$$

These vectors are linearly independent, but not orthogonal. In order for these vectors to be orthogonal to $\mathbf{d}_1$ and $\mathbf{d}_2$, p_n and q_n must satisfy the equations:

$$-e^{ji_n\omega_1} + p_n e^{ji_{n+1}\omega_1} + q_n e^{ji_{n+2}\omega_1} = 0 \tag{3.71}$$

$$-e^{ji_n\omega_2} + p_n e^{ji_{n+1}\omega_2} + q_n e^{ji_{n+2}\omega_2} = 0 \tag{3.72}$$

or in matrix form

$$\begin{bmatrix} p_n \\ q_n \end{bmatrix} = \begin{bmatrix} z_1(i_{n+1}) & z_1(i_{n+2}) \\ z_2(i_{n+1}) & z_2(i_{n+2}) \end{bmatrix}^{-1} \begin{bmatrix} z_1(i_n) \\ z_2(i_n) \end{bmatrix} \tag{3.73}$$

with

$$z_i(i_n) \equiv e^{ji_n\omega_i} \quad i = 1, 2, \quad n = 0, 1, 2, ..., N-3 \quad i_0 \equiv 0.$$

Taking the inverse of the above matrix and solving for p_n and q_n, we have

$$p_n = \frac{z_1(i_n)z_2(i_{n+2}) - z_2(i_n)z_1(i_{n+2})}{\triangle_n}, \tag{3.74}$$

$$q_n = \frac{-z_1(i_n)z_2(i_{n+1}) + z_2(i_n)z_1(i_{n+1})}{\triangle_n}, \tag{3.75}$$

$$\text{with } \triangle_n = z_1(i_{n+1})z_2(i_{n+2}) - z_1(i_{n+2})z_2(i_{n+1}). \tag{3.76}$$

Note that for the case of the URA, substituting i_n=n, into Eqs. (3.74) and (3.75) yields

$$p_n = e^{-j\omega_1} + e^{-j\omega_2} \quad \text{and} \quad q_n = -e^{-j\omega_1}e^{-j\omega_2}. \tag{3.77}$$

Finally, the $\mathbf{U}$ matrix defined by $\mathbf{U}$= $\mathbf{E}_\nu^H\mathbf{E}_\nu$ where $\mathbf{E}_\nu$= [$\mathbf{e}_3$, $\mathbf{e}_4$, ..., $\mathbf{e}_N$] can be formed from Eq. (3.70) together with Eqs. (3.74–3.76) as follows

$$\mathbf{U} = \begin{bmatrix} \gamma_0 & a_0 & b_0 & 0 & 0 & 0 & 0 & \dots & 0 \\ a_0^* & \gamma_1 & a_1 & b_1 & 0 & 0 & 0 & \dots & 0 \\ b_0^* & a_1^* & \gamma_2 & a_2 & b_2 & 0 & 0 & \dots & 0 \\ 0 & b_1^* & a_2^* & \gamma_3 & a_3 & b_3 & 0 & \dots & 0 \\ \vdots & \vdots & \vdots & \vdots & \vdots & \vdots & \vdots & \vdots & \vdots \\ 0 & 0 & 0 & 0 & \dots & a_{N-6} & \gamma_{N-5} & a_{N-5} & b_{N-5} \\ 0 & \dots & \dots & \dots & 0 & b_{N-6}^* & a_{N-5}^* & \gamma_{N-4} & a_{N-4} \\ 0 & \dots & \dots & \dots & 0 & 0 & b_{N-5}^* & a_{N-4}^* & \gamma_{N-3} \end{bmatrix}_{(N-2)\times(N-2)}, \tag{3.78}$$

where one can show

$$\gamma_n = 1+ \mid p_n \mid^2 + \mid q_n \mid^2, \qquad n = 0, 1, \ldots, N-3 \tag{3.79}$$

$$a_n = -p_n^* + q_n^* p_{n+1}, \qquad n = 0, 1, \ldots, N-4 \tag{3.80}$$

$$b_n = -q_n^*, \qquad n = 0, 1, \ldots, N-5. \tag{3.81}$$

If Eqs. (3.73) and (3.74) is substituted in Eq. (3.79) we obtain

$$\gamma_n = 1 + \frac{4 - 2Re\{Z_n\}}{\mid \triangle_n \mid^2}, \tag{3.82}$$

where $Z_n \equiv z_1^*(i_n) z_2(i_n)[z_2^*(i_{n+2}) z_1(i_{n+2}) + z_2^*(i_{n+1}) z_1(i_{n+1})]$.

Substituting $z_1(i_n) = e^{j\omega_1 i_n}$ and $z_2(i_n) = e^{j\omega_2 i_n}$ into Eq. (3.82), yields

$$\gamma_n = 1 + \frac{2 - \cos[\triangle\omega(i_{n+2} - i_n)] - \cos[\triangle\omega(i_{n+1} - i_n)]}{1 - \cos[\triangle\omega(i_{n+2} - i_{n+1})]}, \tag{3.83}$$

where $\triangle\omega \equiv \omega_1 - \omega_2$. For the special case of the URA i.e. $i_0 = 0, i_n = n$, Eq. (3.83) reduces to

$$\gamma_n = 4 + 2\cos(\triangle\omega). \tag{3.84}$$

Substituting Eqs. (3.74–3.76) in equation (3.80) we obtain in Appendix [B-5], Eq. (B.19) and analytical expression for a_n

$$\begin{aligned} a_n = \; & - \{\frac{[z_1(i_{n+1} - i_n) - z_2(i_{n+1} - i_n)]}{[z_1(i_{n+3} - i_{n+2}) - z_2(i_{n+3} - i_{n+2})]} \\ & \times \frac{[z_1(i_{n+3} - i_{n+1}) - z_2(i_{n+3} - i_{n+1})]}{[z_1(i_{n+2} - i_{n+1}) - z_2(i_{n+2} - i_{n+1})]}\} \\ & - \frac{z_1(i_{n+2} - i_n) - z_2(i_{n+2} - i_n)}{[z_1(i_{n+2} - i_{n+1}) - z_2(i_{n+2} - i_{n+1})]}. \end{aligned} \tag{3.85}$$

For the case of the URA (see Eq. (B.20))

$$a_n = -2(e^{j\omega_1} + e^{j\omega_2}). \tag{3.86}$$

From Eq. (3.81) together with Eqs. (3.75), (3.76), and Eq. (B.21) derived in Appendix [B-6], the analytical expression for b_n is found to be

$$b_n = -z_1(i_{n+2} - i_{n+1}) z_2(i_{n+2} - i_{n+1}) \frac{z_2(i_{n+1} - i_n) - z_1(i_{n+1} - i_n)}{z_1(i_{n+2} - i_{n+1}) - z_2(i_{n+2} - i_{n+1})}, \tag{3.87}$$

and for the case of the URA, putting $i_n = n$ yields

$$b_n = -e^{j\omega_1} e^{j\omega_2}. \tag{3.88}$$

Finally, by taking the inverse of the matrix $\mathbf{U}$ defined by Eq. (3.78) and substituting the result in Eq. (3.56), the NMNVV can be evaluated as a function of the interferer directions.

Recursive Formula for Calculating $\mathbf{U}^{-1}$

Let us first define the $\mathbf{U}$ matrix iteratively as follows. From Eq. (3.78), it is clear that the (n+1)×(n+1) matrix $\mathbf{U}_{n+1}$ can be expressed in terms of the (n×n) matrix $\mathbf{U}_n$ as

$$\mathbf{U}_{n+1} = \left[\begin{array}{c|c} \mathbf{U}_n & \mathbf{v}_n \\ \hline \mathbf{v}_n^* & \gamma_n \end{array}\right], \qquad \mathbf{v}_n = \begin{bmatrix} 0 \\ 0 \\ \vdots \\ b_{n-2} \\ a_{n-1} \end{bmatrix}_{n\times 1}. \tag{3.89}$$

where $\gamma_n, a_{n-1}, b_{n-2}$ are given in Eqs. (3.79), (3.85) and (3.87) respectively.
Also for every n, we have

$$\mathbf{U}_n = \begin{bmatrix} \gamma_0 & a_0 & b_0 & 0 & 0 & 0 & 0 & \dots & 0 \\ a_0^* & \gamma_1 & a_1 & b_1 & 0 & 0 & 0 & \dots & 0 \\ b_0^* & a_1^* & \gamma_2 & a_2 & b_2 & 0 & 0 & \dots & 0 \\ 0 & b_1^* & a_2^* & \gamma_3 & a_3 & b_3 & 0 & \dots & 0 \\ \vdots & \vdots & \vdots & \vdots & \vdots & \vdots & \vdots & \vdots & \vdots \\ 0 & 0 & 0 & 0 & \dots & a_{n-4} & \gamma_{n-3} & a_{n-3} & b_{n-3} \\ 0 & \dots & \dots & \dots & 0 & b_{n-4}^* & a_{n-3}^* & \gamma_{n-2} & a_{n-2} \\ 0 & \dots & \dots & \dots & 0 & 0 & b_{n-3}^* & a_{n-2}^* & \gamma_{n-1} \end{bmatrix}_{n\times n}. \tag{3.90}$$

The term $\mathbf{a}^H\mathbf{U}^{-1}\mathbf{a}$ in the denominator of Eq. (3.56) can be computed as follows. Note that from Eqs. (3.57) and (3.70)

$$\mathbf{a} = \mathbf{E}_\nu^H \mathbf{1} = \begin{bmatrix} p_0^* + q_0^* - 1 \\ p_1^* + q_1^* - 1 \\ \vdots \\ p_{N-3}^* + q_{N-3}^* - 1 \end{bmatrix}_{(N-2)\times 1} . \tag{3.91}$$

Using the matrix inversion lemma for the matrix $\mathbf{U}_{n+1}$ in Eq. (3.89), we have,

$$\mathbf{U}_{n+1}^{-1} = \left[\begin{array}{c|c} \mathbf{U}_n^{-1} & \mathbf{0} \\ \hline \mathbf{0} & 0 \end{array}\right] + \left[\begin{array}{c} -\mathbf{U}_n^{-1}\mathbf{v}_n \\ \hline 1 \end{array}\right] \left[\begin{array}{c|c} -\mathbf{v}_n^H\mathbf{U}_n^{-1} & 1 \end{array}\right] \frac{1}{\gamma_n - \mathbf{v}_n^H\mathbf{U}_n^{-1}\mathbf{v}_n}. \tag{3.92}$$

Multiplying both sides of the above equation from left and right by $\mathbf{a}_{n+1}^H$ and $\mathbf{a}_{n+1}$, and noticing that $\mathbf{a}_{n+1}$ can be written in terms of $\mathbf{a}_n$ as

$$\mathbf{a}_{n+1} = \begin{bmatrix} p_0^* + q_0^* - 1 \\ p_1^* + q_1^* - 1 \\ \vdots \\ p_n^* + q_n^* - 1 \end{bmatrix}_{(n+1)\times 1} = \left[\begin{array}{c} \mathbf{a}_n \\ \hline p_n^* + q_n^* - 1 \end{array}\right], \tag{3.93}$$

we get, after some algebra, the following recursive expression for $\mathbf{a}^H\mathbf{U}^{-1}\mathbf{a}$

$$\begin{aligned} \mathbf{a}_{n+1}^H\mathbf{U}_{n+1}^{-1}\mathbf{a}_{n+1} = \mathbf{a}_n^H\mathbf{U}^{-1}\mathbf{a}_n \; &+ \; \{[\mathbf{a}_n^H\mathbf{U}_n^{-1}\mathbf{v}_n\mathbf{v}_n^H\mathbf{U}_n^{-1}\mathbf{a}_n \\ &- \; (p_n + q_n - 1)\mathbf{v}_n^H\mathbf{U}_n^{-1}\mathbf{a}_n \\ &- \; (p_n^* + q_n^* - 1)\mathbf{a}_n^H\mathbf{U}_n^{-1}\mathbf{v}_n + \mid p_n + q_n - 1 \mid^2] \\ &/ \; [\gamma_n - \mathbf{v}_n^H\mathbf{U}_n^{-1}\mathbf{v}_n]\}. \end{aligned} \tag{3.94}$$

Defining $\Gamma_n = \mathbf{a}_n^H\mathbf{U}_n^{-1}\mathbf{a}_n$, and $\xi_n = \mathbf{U}_n^{-1}\mathbf{v}_n$, the above expression can be rewritten as

$$\begin{aligned} \Gamma_{n+1} &= \Gamma_n + \frac{\|\mathbf{a}_n^H\xi_n\|^2 - 2Re\left\{(p_n^* + q_n^* - 1)\mathbf{a}_n^H\xi_n\right\} + \mid p_n + q_n - 1 \mid^2}{\gamma_n - \xi_n^H\mathbf{U}_n\xi_n}, \\ n &= 1, 2, \ldots, N-3 \end{aligned} \tag{3.95}$$

and

$$\Gamma_1 = \mathbf{a}_1^H \mathbf{U}_1^{-1} \mathbf{a}_1 = \gamma_0^{-1} \mid p_0 + q_0 - 1 \mid^2 . \tag{3.96}$$

The iterative Eq. (3.95) enables us to compute the NMNVV obtained from the eigencanceling for an N-element nonuniform array structure. The final expression for the NMNVV obtained from Eqs. (3.56) and (3.95) is

$$\frac{J_{min}}{\sigma^2} = \frac{1}{\Gamma_{N-2}}. \tag{3.97}$$

3.3 Examples of the MRA Eigencanceler

As mentioned earlier, for the MRA structure, we choose i_n in such a way that the integer differences $i_m - i_n$ for n, m = 0, 1, ... ,N-1 span the integer set (1, 2, 3, ..., L). In previous work, it was shown that for each array with a given number of elements N, there corresponds an L, with L $\leq$ N(N-1)/2 (but L >> N-1). For N=3 or N=4, L=N(N-1)/2, and there is only one MRA structure which has no redundant correlation lag. That is, the off-diagonal entries of the autocorrelation matrix are all different. For N$\geq$ 5, L < N(N-1)/2, there exist several MRA structures with some redundant elements in the autocorrelation matrix but with the redundant elements in different position. However, the number of these equal entries by definition is minimal for the MRA. In this section, the examples of three- and four-element URA and MRA using the eigencanceling technique are demonstrated. Both single- and dual-interferer cases are considered.

3.3.1 Three-Element Minimum Redundancy Array (MRA-3)

For this array structure $i_0 = 0, i_1 = 1$ and $i_2 = 3$.

The Single-Interferer case

When only a single interferer impinges on the array from the direction ω_1, we get from Eq. (3.67)

$$\begin{aligned}\frac{J_{min}}{\sigma^2} = 1 \;\; / \;\; & \{4\sum_{l=1}^{2} P_{l,l}\sin^2(\frac{i_l - i_{l-1}}{2}\omega_1) \\ & + \; 2P_{1,2}[\cos(i_1 - i_2)\omega_1 + \cos(i_0 - i_1)\omega_1 \\ & - \; \cos(i_1 - i_1)\omega_1 - \cos(i_0 - i_2)\omega_1]\} \\ = 1 \;\; / \;\; & 2[(P_{1,1} + P_{2,2} - P_{1,2}) + (P_{1,2} - P_{1,1})\cos\omega_1 \\ & + \; (P_{1,2} - P_{2,2})\cos 2\omega_1 - P_{1,2}\cos 3\omega_1]. \end{aligned} \tag{3.98}$$

But since $P_{l,k} = \sum_{n=1}^{2} P_n Q_{nk} Q_{nl}$ and by using Eq. (3.66) we get

$$P_{l,k} = \sum_{n=1}^{2} \frac{1}{4\sin^2(n\pi/6)} \cdot \frac{\sin(\pi nk/3)}{\sqrt{\sum_{n=1}^{2}\sin^2(\pi nk/3)}} \cdot \frac{\sin(\pi nl/3)}{\sqrt{\sum_{n=1}^{2}\sin^2(\pi nl/3)}}. \tag{3.99}$$

In the Appendix [B-7], we show that $P_{1,1} = P_{2,2} = P_{1,2} = \frac{2}{3}$. Hence, upon substituting these values in Eq. (3.98), we get for the MRA-3 with a single interferer:

$$\frac{J_{min}}{\sigma^2} = \frac{3/4}{1 - \cos 3\omega_1}. \tag{3.100}$$

For comparison, the result for the URA-3 NMNVV with a single interferer can be obtained from Eq. (3.68) as:

$$\frac{J_{min}}{\sigma^2} = \frac{1}{4(P_{1,1}+P_{2,2})\sin^2\frac{\omega_1}{2} + 2P_{1,2}(2\cos\omega_1 - \cos 2\omega_1 - 1)}$$

$$= \frac{3/4}{1-\cos 2\omega_1}. \tag{3.101}$$

The Dual-Interferer Case

For the dual-interferer case, there is only one noise eigenvector $\mathbf{e}^T = [-1, p_0, q_0]$ and by using Eq. (3.91)

$$a_1 = \mathbf{E}_\nu^H \cdot \mathbf{1} = \mathbf{e}^H \cdot \mathbf{1} = p_0^* + q_0^* - 1. \tag{3.102}$$

Also for the MRA-3, $\mathbf{U}_1 = [\gamma_0]$ and thus, $\mathbf{U}_1^{-1} = \gamma_0^{-1}$, where from Eq. (3.79), $\gamma_0 = 1 + \mid p_0 \mid^2 + \mid q_0 \mid^2$. Therefore, the NMNVV for this case can be written from Eq. (3.97) as

$$(\frac{J_{min}}{\sigma^2})_{MRA-3} = \frac{1}{\mid p_0 + q_0 - 1 \mid^2 \gamma_0^{-1}}. \tag{3.103}$$

Expanding Eq. (3.103) and substituting for γ_0 from Eq. (3.79) yields

$$(\frac{J_{min}}{\sigma^2})_{MRA-3} = \frac{1}{1 + \frac{2Re\{p_0 q_0^* - p_0 - q_0\}}{\mid p_0 \mid^2 + \mid q_0 \mid^2 + 1}} \tag{3.104}$$

Using Eqs. (3.74–3.76) for p_0 and q_0 respectively, we derive in Appendix [B-8] the relevant terms for Eq. (3.104). Then by using equations (B.24) and (B.25) in Eq. (3.104) with $i_0 = 0$, i_1=1, $i_2 = 3$, we finally obtain

$$
\begin{aligned}
(\frac{J_{min}}{\sigma^2})_{MRA-3} = 1 \quad / \quad & \{1 + [-\sum_{\gamma=1}^{3}(\cos\gamma\omega_1 + \cos\gamma\omega_2) \\
+ \quad & \cos(3\omega_2 - \omega_1) + \cos(3\omega_1 - \omega_2) + \cos(3\omega_2 - 2\omega_1) \\
+ \quad & \cos(3\omega_1 - 2\omega_2) + \cos(2\omega_2 + \omega_1) + \cos(2\omega_1 + \omega_2)] \\
/ \quad & [3 - \cos(\Delta\omega) - \cos(2\Delta\omega) - \cos(3\Delta\omega)]\}. \qquad (3.105)
\end{aligned}
$$

For comparison, the URA-3 performance with two interferers can be obtained by substituting equations (B.24) and (B.25) with $i_0 = 0$, i_1=1 and i_2=2 into Eq. (3.104);

$$
\begin{aligned}
(\frac{J_{min}}{\sigma^2})_{URA-3} = 1 \quad / \quad & \{1 + [-\sum_{\gamma=1}^{2}(3-\gamma)(\cos\gamma\omega_1 + \cos\gamma\omega_2) \\
+ \quad & 2\cos(2\omega_1 - \omega_2) + 2\cos(2\omega_2 - \omega_1) \\
+ \quad & 2\cos(\omega_1 + \omega_2)] \\
/ \quad & [3 - 2\cos(\Delta\omega) - \cos(2\Delta\omega)]\}. \qquad (3.106)
\end{aligned}
$$

3.3.2 Four-Element Minimum Redundancy Array (MRA-4)

For this array structure $i_0 = 0, i_1 = 1, i_2 = 4$ and $i_3 = 6$

The Single-Interferer Case

When a single interferer impinges on the array from the direction ω_1, we get from Eq. (3.67),

$$\begin{aligned}
\frac{J_{min}}{\sigma^2} = 1 \;/\; & \{4\sum_{l=1}^{3} P_{l,l}\sin^2(\frac{i_l - i_{l-1}}{2}\omega_1) \\
& + 2P_{1,2}[\cos(i_1 - i_2)\omega_1 + \cos(i_0 - i_1)\omega_1 \\
& - \cos(i_1 - i_1)\omega_1 - \cos(i_0 - i_2)\omega_1] \\
& + 2P_{1,3}[\cos(i_1 - i_3)\omega_1 + \cos(i_0 - i_2)\omega_1 \\
& - \cos(i_1 - i_2)\omega_1 - \cos(i_0 - i_3)\omega_1] \\
& + 2P_{2,3}[\cos(i_2 - i_3)\omega_1 + \cos(i_1 - i_2)\omega_1 \\
& - \cos(i_2 - i_2)\omega_1 - \cos(i_1 - i_3)\omega_1] \\
= 1 \;/\; & 2[(P_{1,1} + P_{2,2} + P_{3,3} - P_{1,2} - P_{2,3}) \\
& + (P_{1,2} - P_{1,1})\cos\omega_1 + (P_{2,3} - P_{3,3})\cos 2\omega_1 \\
& + (P_{1,2} + P_{2,3} - P_{1,3} - P_{2,2})\cos 3\omega_1 \\
& + (P_{1,3} - P_{1,2})\cos 4\omega_1 + (P_{1,3} - P_{2,3})\cos 5\omega_1 \\
& - P_{1,3}\cos 6\omega_1]. \qquad (3.107)
\end{aligned}$$

But $P_{l,k} = \sum_{n=1}^{2} P_n Q_{nk} Q_{nl}$. Then by using Eq. (3.66)

$$P_{l,k} = \sum_{n=1}^{3} \frac{1}{4\sin^2(n\pi/8)} \cdot \frac{\sin(\pi nk/4)}{\sqrt{\sum_{n=1}^{3}\sin^2(\pi nk/4)}} \cdot \frac{\sin(\pi nl/4)}{\sqrt{\sum_{n=1}^{3}\sin^2(\pi nl/4)}}. \qquad (3.108)$$

In the Appendix [B-9] we show that $P_{1,1} = \frac{3}{4}, P_{2,2} = 1$, $P_{3,3} = \frac{3}{4}, P_{1,2} = \frac{1}{2}, P_{1,3} = \frac{1}{4}$, $P_{2,3} = \frac{1}{2}$. Hence, upon substituting these values in Eq. (3.107), we get the NM-NVV of the MRA-4 with single interferer as

$$\frac{J_{min}}{\sigma^2} = \frac{2}{6 - \sum_{n=1}^{6}\cos n\omega_1}. \qquad (3.109)$$

For comparison, the URA-4 performance can be obtained from Eq. (3.68)

$$\begin{aligned}\frac{J_{min}}{\sigma^2} = 1 \;\; / \;\; & [4(P_{1,1}+P_{2,2}+P_{3,3})\sin^2\frac{\omega_1}{2} \\ & + 2P_{1,2}(2\cos\omega_1 - \cos 2\omega_1 - 1) \\ & + 2P_{1,3}(2\cos 2\omega_1 - \cos 3\omega_1 - \cos\omega_1) \\ & + 2P_{2,3}(2\cos\omega_1 - \cos 2\omega_1 - 1)] \\ = 1 \;\; / \;\; & 2[(P_{1,1}+P_{2,2}+P_{3,3}-P_{1,2}-P_{2,3}) \\ & + (2P_{2,3}+2P_{1,2}-P_{1,3}-P_{1,1}-P_{2,2}-P_{3,3})\cos\omega_1 \\ & + (2P_{1,3}-P_{1,2}-P_{2,3})\cos 2\omega_1 \\ & - P_{1,3}\cos 3]\omega_1 \\ = \quad & \frac{2}{6-\sum_{n=1}^{3}(4-n)\cos n\omega_1}. \end{aligned} \tag{3.110}$$

The Dual-Interferer Case

For this case there are two noise eigenvectors from Eq. (3.70) given by

$$\mathbf{E}_\nu = \begin{bmatrix} -1 & 0 \\ p_0 & -1 \\ q_0 & p_1 \\ 0 & q_1 \end{bmatrix}.$$

Therefore, it is clear that

$$\mathbf{a}_2 = \mathbf{E}_\nu^H \cdot \mathbf{1} = \begin{bmatrix} p_0^* + q_0^* - 1 \\ p_1^* + q_1^* - 1 \end{bmatrix} \quad \text{and} \quad \mathbf{U}_2 = \begin{bmatrix} \gamma_0 & a_0 \\ a_0^* & \gamma_1 \end{bmatrix}.$$

Using Eq. (3.97) $J_{min}/\sigma^2 = 1/\Gamma_2$, where Γ_2 can be computed from the recursion in Eq. (3.95), with n=1. From Eq. (3.89), $\mathbf{v}_1 = a_0$ and from Eq. (3.91), $\mathbf{a}_1 = p_0^* + q_0^*$-1. Also, $\mathbf{U}_1^{-1} = \gamma_0^{-1}$ implies $\xi_1 = \gamma_0^{-1}a_0$, so that

$$\mathbf{a}_1^H \xi_1 = (p_0 + q_0 - 1)\gamma_0^{-1}a_0. \tag{3.111}$$

Substituting in Eq. (3.95) we get

$$\Gamma_2 = \Gamma_1 + [\quad |\gamma_0^{-1}a_0(p_0+q_0-1)|^2$$

$$
\begin{aligned}
&- \quad 2Re\{(p_1^* + q_1^* - 1)a_0\gamma_0^{-1}(p_0 + q_0 - 1)\} \\
&+ \quad |\, p_1 + q_1 - 1 \,|^2]/(\gamma_1 - a_0^*\gamma_0^{-1}a_0) \qquad (3.112)
\end{aligned}
$$

and

$$
\Gamma_1 = \mathbf{a}_1^H \mathbf{U}_1^{-1}\mathbf{a}_1 = \gamma_0^{-1} \,|\, p_0 + q_0 - 1 \,|^2 . \qquad (3.113)
$$

After some algebraic manipulation we get

$$
\begin{aligned}
\Gamma_2 = \; & [\gamma_1 \,|\, p_0 + q_0 - 1 \,|^2 \\
& - \quad 2Re\{(p_0 + q_0 - 1)a_0(p_1^* + q_1^* - 1)\} \\
& + \quad \gamma_0 \,|\, p_1 + q_1 - 1 \,|^2]/(\gamma_0\gamma_1 - \,|\, a_0 \,|^2) \\
= \; & [\gamma_0^{-1} \,|\, p_0 + q_0 - 1 \,|^2 \\
& - \quad 2\gamma_0^{-1}\gamma_1^{-1}Re\{(p_0 + q_0 - 1)a_0(p_1^* + q_1^* - 1)\} \\
& + \quad \gamma_1^{-1} \,|\, p_1 + q_1 - 1 \,|^2]/(1 - \gamma_0^{-1}\gamma_1^{-1} \,|\, a_0 \,|^2) \qquad (3.114)
\end{aligned}
$$

where from Eqs. (3.74–3.76)

$$
\begin{aligned}
p_n &= \frac{e^{ji_{n+2}\omega_2}e^{ji_n\omega_1} - e^{ji_n\omega_2}e^{ji_{n+2}\omega_1}}{\triangle_n}, \\
q_n &= \frac{e^{ji_n\omega_2}e^{ji_{n+1}\omega_1} - e^{ji_{n+1}\omega_2}e^{ji_n\omega_1}}{\triangle_n}, \\
\triangle_n &= e^{ji_{n+2}\omega_2}e^{ji_{n+1}\omega_1} - e^{ji_{n+1}\omega_2}e^{ji_{n+2}\omega_1}.
\end{aligned}
$$

Also

$$
\begin{aligned}
\gamma_i &= 1 + |\, p_i \,|^2 + |\, q_i \,|^2 \qquad i = 0, 1 \\
\text{and} \qquad a_0 &= -p_0^* + q_0^* p_1. \qquad (3.115)
\end{aligned}
$$

Again recall that for the MRA-4, $i_0 = 0$, i_1=1, i_2=4 and i_3=6. Finally from Eq. (3.97) $J_{min}/\sigma^2 = 1/\Gamma_2$.

For the URA-4 structure, i_0=0, i_1=1, i_2=2 and i_3=3. From equations (3.77), (3.84) and (3.86) we obtain the following, independent of the n parameter,

$$\begin{aligned} p_0 &= p_1 = e^{-j\omega_1} + e^{-j\omega_2}, \\ q_0 &= q_1 = -e^{-j\omega_1} e^{-j\omega_2}, \\ \gamma_0 &= \gamma_1 = 4 + 2\cos(\Delta\omega), \\ \text{and } a_0 &= -2(e^{j\omega_1} + e^{j\omega_2}). \end{aligned}$$

Substituting these values in Eq. (3.114) and after some algebra, we get

$$\left(\frac{J_{min}}{\sigma^2}\right)_{URA-4} = \frac{2 + 2\cos(\Delta\omega) + \cos^2(\Delta\omega)}{4[2 + \cos(\Delta\omega) + \cos\omega_1 + \cos\omega_2](1 - \cos\omega_1)(1 - \cos\omega_2)}. \quad (3.116)$$

The General Case

The eigencanceling technique for nonuniform arrays with two interferers having more than four array elements is more involved and it becomes impractical to obtain an exact analytical expression. However, in this case, the iterative formula given by Eqs. (3.89),(3.95–3.96) can be used to calculate the NMNVV for the performance evaluation. If there are more than two interferers, it becomes very difficult to obtain an explicit analytical expression for the inverse of the matrix **U**. In this case, the performance analysis may be carried out numerically by computer.

3.4 Eigenvalue Spread Comparison

With two interferers, the autocorrelation matrix $\mathbf{R}_2$ given by Eq. (2.24) has two eigenvalues greater than σ^2 which are [44],

$$\lambda_1, \lambda_2 = \sigma^2 + \frac{N}{2}(p_1 + p_2 \pm \sqrt{(p_1 - p_2)^2 + 4p_1p_2 \mid \rho \mid^2}) \quad (3.117)$$

where ρ is defined as $\rho = \mathbf{d}_1^H \mathbf{d}_2/N$ from equation (2.40). The quantities p_1 and p_2 are the power of the interferers.

The ratio $C = \lambda_{max}/\lambda_{min}$ plays an important role in the rate of solution convergence. For example, in the implementation of a sampled-data adaptive array system, the response time, which is measured in sample periods, is given by $\tau \leq C/2$ [45].

From the exact expression of $\mid \rho \mid^2$ in Eqs. (3.25) and (3.27), for the URA and the MRA respectively, it is clear that

$$0 \leq \mid \rho_{URA} \mid^2 \leq 1 \quad \text{and} \quad \frac{N-1}{N^2} + \varepsilon \leq \mid \rho_{MRA} \mid^2 \leq 1, \tag{3.118}$$

where

$$\varepsilon = \min_{\omega_0} \frac{\sin(\frac{2L-1}{2}\omega_0)}{N^2(\sin\omega_0/2)}.$$

It can be shown that ε has a negative value that occurs at points ω_0 and that satisfies the equation

$$\frac{L}{L-1} = \frac{\sin L\omega_0}{\sin(L-1)\omega_0}. \tag{3.119}$$

The eigenvalue spreads for the URA and the MRA can be easily determined from Eq. (3.117) as

$$\frac{1+N/\min(\gamma_1,\gamma_2)}{1+N/\max(\gamma_1,\gamma_2)} \leq C_{URA} \leq 1+N(\frac{1}{\gamma_1}+\frac{1}{\gamma_2})$$

$$\frac{1+\frac{N}{2}(\frac{1}{\gamma_1}+\frac{1}{\gamma_2}+\sqrt{(\frac{1}{\gamma_1}-\frac{1}{\gamma_2})^2+4(\frac{(N-1)}{N^2}+\varepsilon)\frac{1}{\gamma_1\gamma_2}})}{1+\frac{N}{2}(\frac{1}{\gamma_1}+\frac{1}{\gamma_2}-\sqrt{(\frac{1}{\gamma_1}-\frac{1}{\gamma_2})^2+4(\frac{(N-1)}{N^2}+\varepsilon)\frac{1}{\gamma_1\gamma_2}})} \leq C_{MRA} \leq 1+N(\frac{1}{\gamma_1}+\frac{1}{\gamma_2}) \tag{3.120}$$

where as before $\gamma_k = \sigma^2/p_k, \quad k = 1,2.$

It can also be shown numerically that the lower bound of C_{MRA} is greater than the lower bound of C_{URA}. For example, if $(\sigma^2, p_1, p_2) = (1, 100, 10)$, then for N=3,

which implies L=4, we get,

$$9.71 \leq C_{URA} \leq 331$$

$$10.20 \leq C_{MRA} \leq 331.$$

We can also compare directly the eigenvalue spreads of the URA and the MRA. Since from Eq. (3.117),

$$C = \frac{\lambda_{max}}{\lambda_{min}} = \frac{\lambda_1}{\lambda_2} = \frac{1 + \frac{N}{2}(\frac{1}{\gamma_1} + \frac{1}{\gamma_2} + \sqrt{(\frac{1}{\gamma_1} - \frac{1}{\gamma_2})^2 + \mid \rho \mid^2 \frac{1}{\gamma_1 \gamma_2}})}{1 + \frac{N}{2}(\frac{1}{\gamma_1} + \frac{1}{\gamma_2} - \sqrt{(\frac{1}{\gamma_1} - \frac{1}{\gamma_2})^2 + \mid \rho \mid^2 \frac{1}{\gamma_1 \gamma_2}})}. \tag{3.121}$$

It is easy to notice that for a given σ^2, p_1, p_2, the resulting ratio C is larger if and only if $\mid \rho \mid^2$ is larger and therefore,

$$C_{URA} \gtrless C_{MRA} \quad \Longleftrightarrow \quad \mid \rho_{URA} \mid^2 \gtrless \mid \rho_{MRA} \mid^2 \tag{3.122}$$

where $\mid \rho_{URA} \mid^2$ and $\mid \rho_{MRA} \mid^2$ are obtained from Eqs. (3.25) and (3.27). For N=4, $\mid \rho_{URA} \mid^2$ and $\mid \rho_{MRA} \mid^2$ are plotted in Figure 3, from which we conclude that for $\Delta\omega = \omega_1 - \omega_2$ less than 58°, the MRA has a smaller eigenvalue spread.

The General Case : r-interferers ($r > 2$)

In the presence of r interferers, with direction vectors

$$\mathbf{d}_k = [1, e^{-ji_1\omega_k}, e^{-ji_2\omega_k}, \ldots, e^{-ji_{N-1}\omega_k}]^T, \qquad k = 1, 2, \ldots, r$$

the term $\|\mathbf{R}_r^{-1}\|_b$ in Eq. (3.5) can be computed recursively by means of Eq. (2.28), as follows:

$$\begin{aligned} \|\mathbf{R}_i^{-1}\|_b &= \|\mathbf{R}_{i-1}^{-1}\|_b - \frac{p_i \mid \mathbf{1}^T \mathbf{R}_{i-1}^{-1} \mathbf{d}_i \mid^2}{1 + p_i \mathbf{d}_i^H \mathbf{R}_{i-1}^{-1} \mathbf{d}_i} \qquad i = 1, 2, \ldots, r \\ \|\mathbf{R}_0^{-1}\|_b &\equiv \sigma^{-2} \|\mathbf{I}\|_b = \sigma^2 N \end{aligned}$$

with the MNVV expression given by Eq. (3.5).

The key conclusion of this eigenvalue spread comparison is that with the same number of array elements used, the MRA will not degrade the eigenvalue spread of the correspondence URA structure. For the dual-interferer case, the eigenvectors corresponding to the interference subspace were obtained explicitly in terms of the interferers' power and the direction vector of the interferers in Appendix C.

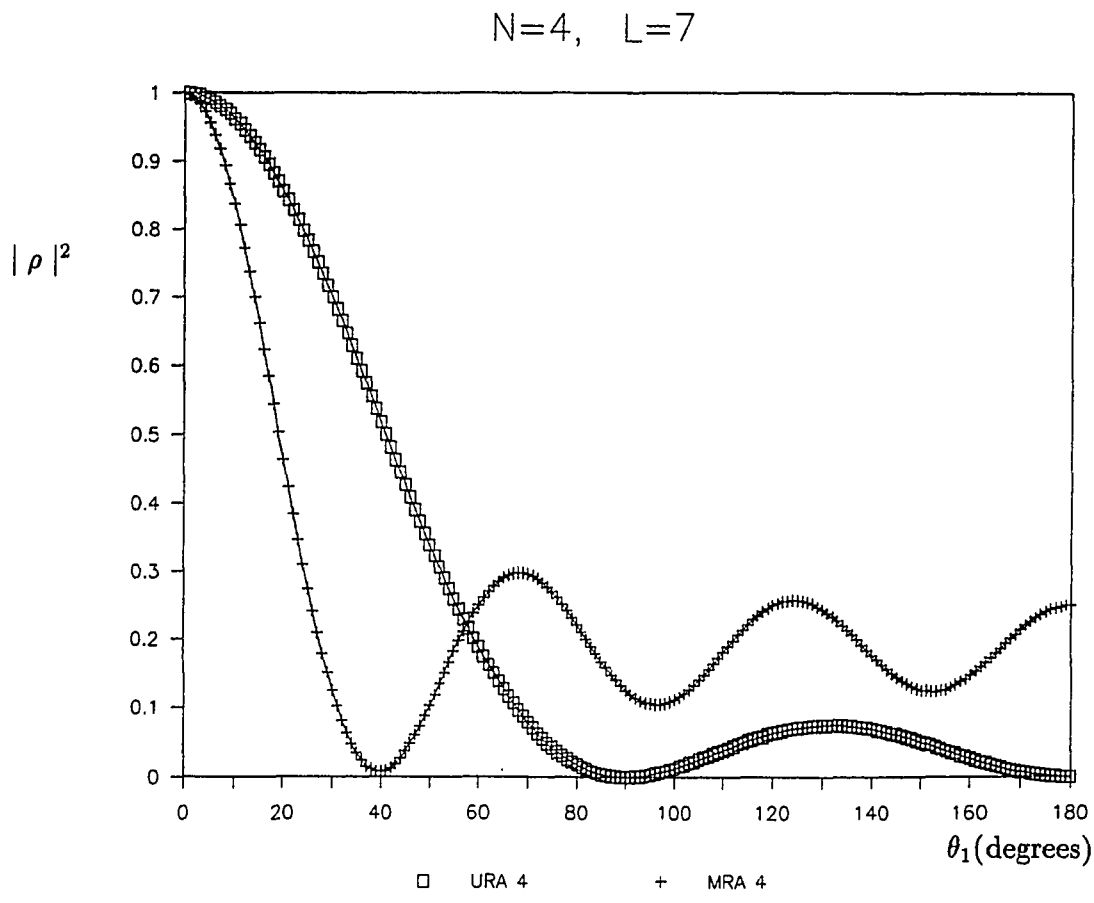

Figure 3 Magnitude of $|\ \rho\ |^2$ as a function of the angle difference between two interferers ($\Delta\omega = \omega_1 - \omega_2 = 2\pi \sin\theta$) for the URA-4 and the MRA-4.

CHAPTER 4

EIGENSPACE TRANSFORMATION BETWEEN THE URA AND THE MRA STRUCTURES

In this chapter an attempt is made to relate the eigenspaces of the URA and the MRA structures. This analysis provides another approach to gain further understanding of the operation of the MRA eigencanceler. The analysis of the MRA performance in the previous chapter was quite tedious even for the dual-interferer case. The idea of performing the eigenspace transformation started when considering that the vector space spanned by the eigenvectors of the URA and the MRA structures is exactly the same. Thus, the URA results obtained should be able to be transformed to the respective MRA vector space through some kind of transformation matrix. In this chapter, this idea is examined and the results are presented. In order not to be confused by all the manipulations, the simplest case is studied as an example. The single-interferer case for the URA with the eigencanceling technique is used as a basis for all analyses. The optimization problem is still the same as formulated in equation (2.14):

$$\begin{aligned} \min \quad & \mathbf{w}^H \mathbf{R} \mathbf{w} \\ \text{subject to} \quad & \mathbf{w}^H \mathbf{A}_p = \mathbf{g}^H \\ & \mathbf{w}^H \mathbf{E}_r = \mathbf{0}. \end{aligned} \tag{4.1}$$

The constraint in Eq. (4.1) which restricts the optimum weight to be orthogonal to the interference subspace $\mathbf{w}^H \mathbf{E}_r = \mathbf{0}$ is equivalent to requiring that the weight vector lies in the noise subspace. In this case, as mentioned in section 3.2, the optimum weight vector can be written as a linear combination of the noise subspace vectors. From Eq. (3.44), it will take the form of

$$\mathbf{w} = \mathbf{E}_\nu \mathbf{c}. \tag{4.2}$$

Rewriting the optimization problem as in Eqs. (3.45) and (3.46), we obtain

$$\begin{aligned} \min \quad & \sigma^2 \mathbf{c}^H \mathbf{U} \mathbf{c} \\ \text{subject to} \quad & \mathbf{c}^H \mathbf{A}_{pp} = \mathbf{g}^H \end{aligned} \tag{4.3}$$

where $\mathbf{U} = \mathbf{E}_\nu^H \mathbf{E}_\nu$, $\mathbf{A}_{pp} = \mathbf{E}_\nu^H \mathbf{A}_p$, and $\mathbf{E}_\nu$ is the noise subspace of $\mathbf{R}$.

The optimum solution for the above problem is as given in Eq. (3.54):

$$\mathbf{c}_{op} = \mathbf{U}^{-1}\mathbf{A}_{pp}[\mathbf{A}_{pp}^H \mathbf{U}^{-1}\mathbf{A}_{pp}]^{-1}\mathbf{g}. \tag{4.4}$$

When constraining the signal to come from broadside i.e. $\mathbf{a}_p = \mathbf{1}$ and with unity gain g=1, define $\mathbf{a} = \mathbf{E}_\nu^H \mathbf{a}_p$,

$$\sigma^2 \mathbf{c}_{op}^H \mathbf{U} \mathbf{c}_{op} = \frac{\sigma^2}{\mathbf{a}^H \mathbf{U}^{-1} \mathbf{a}} \tag{4.5}$$

$$c_{op} = \frac{\mathbf{U}^{-1}\mathbf{a}}{\mathbf{a}^H \mathbf{U}^{-1} \mathbf{a}}. \tag{4.6}$$

4.1 Analytical Formula for the Matrix Inverse

The inverse of the aforementioned matrix $\mathbf{U}$ for the single-interferer URA structure using the eigencanceling technique can be calculated explicitly. The procedure is as follows. Define an $N \times (N-1)$ matrix $\mathbf{E}_\nu$ as a collection of the noise eigenvectors of the autocorrelation matrix for a URA with N array elements and a single interferer:

$$\mathbf{E}_\nu = \begin{bmatrix} -1 & 0 & \dots & \dots & 0 \\ e^{-j\omega_1} & -1 & \dots & \dots & 0 \\ 0 & e^{-j\omega_1} & -1 & \dots & 0 \\ \vdots & \vdots & \vdots & \vdots & \vdots \\ 0 & 0 & \dots & \dots & e^{-j\omega_1} \end{bmatrix}. \tag{4.7}$$

Note that the eigenvectors are not orthogonal to each other but $\mathbf{E}_\nu$ satisfies $\mathbf{R}\mathbf{E}_\nu = \sigma^2\mathbf{E}_\nu$. Restricting the signal coming from broadside yields $\mathbf{a}_p = \mathbf{1}$. The cost function for the new optimization problem becomes:

$$\begin{aligned} J_{min} &= \frac{\sigma^2}{\mathbf{a}^H\mathbf{U}^{-1}\mathbf{a}} \\ &= \frac{\sigma^2}{(\mathbf{E}_\nu^H\mathbf{1})^H\mathbf{U}^{-1}(\mathbf{E}_\nu^H\mathbf{1})} \\ &= \frac{\sigma^2}{(e^{-j\omega_1}-1)(e^{j\omega_1}-1)\mathbf{1}^H\mathbf{U}^{-1}\mathbf{1}} \\ &= \frac{\sigma^2}{(e^{-j\omega_1}-1)(e^{j\omega_1}-1)\|\mathbf{U}^{-1}\|_b} \end{aligned} \tag{4.8}$$

where again $\|\cdot\|_b$ denotes for the sum of all the matrix elements.

Now take a look at the form of the $\mathbf{U}$ matrix before finding its inverse. From Eq. (3.62) with i_n=n for n=0, 1, ..., N-2

$$\mathbf{U} = \mathbf{E}_\nu^H\mathbf{E}_\nu$$

$$= \begin{bmatrix} -1 & e^{j\omega_1} & 0 & \dots & 0 \\ 0 & -1 & e^{j\omega_1} & \dots & 0 \\ 0 & 0 & -1 & \dots & 0 \\ \vdots & \vdots & \vdots & \vdots & \vdots \\ 0 & 0 & \dots & -1 & e^{j\omega_1} \end{bmatrix} \begin{bmatrix} -1 & 0 & \dots & \dots & 0 \\ e^{-j\omega_1} & -1 & \dots & \dots & 0 \\ 0 & e^{-j\omega_1} & -1 & \dots & 0 \\ \vdots & \vdots & \vdots & \vdots & \vdots \\ 0 & 0 & \dots & \dots & e^{-j\omega_1} \end{bmatrix}$$

$$= \begin{bmatrix} 2 & -e^{j\omega_1} & 0 & \dots & 0 \\ -e^{-j\omega_1} & 2 & -e^{j\omega} & \dots & 0 \\ 0 & -e^{-j\omega_1} & 2 & \dots & 0 \\ \vdots & \vdots & \vdots & \vdots & \vdots \\ 0 & 0 & \dots & -e^{-j\omega_1} & 2 \end{bmatrix}. \tag{4.9}$$

Through the process of induction in Appendix D, the general form for $\mathbf{U}^{-1}$ becomes:

$$\mathbf{U}^{-1} = \frac{1}{N}\begin{bmatrix} N-1 & (N-2)e^{j\omega_1} & (N-3)e^{2j\omega_1} & \dots & 2e^{(N-3)j\omega_1} & e^{(N-2)j\omega_1} \\ (N-2)e^{-j\omega_1} & 2(N-2) & 2(N-3)e^{j\omega_1} & \dots & 4e^{(N-4)j\omega_1} & 2e^{(N-3)j\omega_1} \\ (N-3)e^{-2j\omega_1} & 2(N-3)e^{-j\omega_1} & 2(N-2) & \dots & \dots & 3e^{(N-4)j\omega_1} \\ \vdots & \vdots & \vdots & \vdots & \vdots & \vdots \\ 2e^{-(N-3)j\omega_1} & 4e^{-(N-4)j\omega_1} & 6e^{-(N-5)j\omega_1} & \dots & 2(N-2) & (N-2)e^{j\omega_1} \\ e^{-(N-2)j\omega_1} & 2e^{-(N-3)j\omega_1} & 3e^{-(N-4)j\omega_1} & \dots & (N-2)e^{-j\omega_1} & N-1 \end{bmatrix}. \tag{4.10}$$

Also

$$\|\mathbf{U}^{-1}\| = \frac{1}{N}\sum_{k=0}^{N-2}[2(N-1-k)+2(N-2-k)(N-3-k)]\cos(k\omega_1). \tag{4.11}$$

The explicit expression for the MNVV of the URA using the eigencanceling method is

$$J_{min} = \frac{\sigma^2}{(e^{-j\omega_1}-1)(e^{j\omega_1}-1)\|\mathbf{U}^{-1}\|_b} \tag{4.12}$$

$$= \frac{N\sigma^2}{(2-2\cos\omega_1)\sum_{k=0}^{N-2}[2(N-1-k)+2(N-2-k)(N-3-k)]\cos(k\omega_1)}$$

where N is the number of array elements.

4.2 Transformation between the Eigenspaces of the URA and the MRA

The following notation is used in this section. We write $\mathbf{E}_u = [\mathbf{E}_{u_r} \mid \mathbf{E}_{u_\nu}]$ and $\mathbf{E}_m = [\mathbf{E}_{m_r} \mid \mathbf{E}_{m_\nu}]$ where

- $\mathbf{E}_u$ and $\mathbf{E}_m$ denote the eigenvectors of the URA and the MRA autocorrelation matrices with the same number of array elements N.
- $\mathbf{E}_{u_r}$ and $\mathbf{E}_{m_r}$ denote the eigenvectors corresponding to the bases of the interference subspace for the URA and the MRA respectively.

- $\mathbf{E}_{u_\nu}$ and $\mathbf{E}_{m_\nu}$ denote the eigenvectors corresponding to the bases of the noise subspace for the URA and the MRA.

4.2.1 Transformation between the Noise Subspaces

Since the noise subspace plays a major role in the eigencanceling technique, a direct transformation between the URA and the MRA noise subspace bases is most desirable. Unfortunately it does not exist.

Proof : Assume that there exists $\mathbf{T}_1$ such that $\mathbf{E}_{m_\nu} = \mathbf{T}_1\mathbf{E}_{u_\nu}$. In order to find $\mathbf{T}_1$, the pseudoinverse [35] of $\mathbf{E}_{u_\nu}$ is needed, where

$$\mathbf{T}_1 = \mathbf{E}_{m_\nu}\mathbf{E}_{u_\nu}{}^H(\mathbf{E}_{u_\nu}\mathbf{E}_{u_\nu}{}^H)^{-1}$$

Note that $\mathbf{E}_{u_\nu}\mathbf{E}_{u_\nu}{}^H$ is an $N \times N$ matrix with rank r, where r is the number of interferers. Its inverse does not exist, because $r < N$. Therefore, the transformation matrix between $\mathbf{E}_{u_\nu}$ and $\mathbf{E}_{m_\nu}$ does not exist.

4.2.2 Transformation between the Eigenspaces

Even though the previous result is disappointing, one may still hope a transformation exists between the URA and the MRA eigenspaces. A direct matrix transformation does exist between $\mathbf{E}_u$ and $\mathbf{E}_m$ for the single-interferer case due to the fact that all eigenvalues of the URA and the MRA autocorrelation matrices are the same. The matrices $\mathbf{E}_u$ and $\mathbf{E}_m$ are thus similar as shown in Chapter 2 (autocorrelation matrix properties). That is, there exists a matrix transformation $\mathbf{T}_2$ such that $\mathbf{E}_m = \mathbf{T}_2\mathbf{E}_u$. The matrix $\mathbf{E}_u$ has the following special structure:

$$\mathbf{E}_u = \left[\begin{array}{c|cccc} 1 & -1 & 0 & \dots & 0 \\ e^{-1j\omega_1} & e^{-j\omega_1} & -1 & \dots & 0 \\ e^{-2j\omega_1} & 0 & e^{-j\omega_1} & \dots & 0 \\ \vdots & \vdots & \vdots & \vdots & \vdots \\ e^{-(N-1)j\omega_1} & 0 & 0 & \dots & e^{-j\omega_1} \end{array}\right]. \qquad (4.13)$$

Through a recursive calculation similar to that given for finding $\mathbf{U}^{-1}$, the $\mathbf{E}_u^{-1}$ can be written as follows:

$$\mathbf{E}_u^{-1} = \frac{1}{N}\begin{bmatrix} 1 & e^{j\omega_1} & e^{2j\omega_1} & \dots & e^{(N-2)j\omega_1} & e^{(N-1)j\omega_1} \\ 1-N & e^{j\omega_1} & e^{2j\omega_1} & \dots & e^{(N-2)j\omega_1} & e^{j(N-1)\omega_1} \\ (2-N)e^{-j\omega_1} & 2-N & 2e^{j\omega_1} & \dots & 2e^{(N-3)j\omega_1} & 2e^{(N-2)j\omega_1} \\ (3-N)e^{-j\omega_1} & (3-N)e^{-j\omega_1} & 3-N & \dots & 3e^{(N-4)j\omega_1} & 3e^{(N-3)j\omega_1} \\ \vdots & \vdots & \vdots & \vdots & \vdots & \vdots \\ -2e^{-(N-3)j\omega_1} & -2e^{-(N-2)j\omega_1} & \dots & -2 & (N-2)e^{j\omega_1} & (N-2)e^{2j\omega_1} \\ -e^{-(N-2)j\omega_1} & -e^{-(N-3)j\omega_1} & \dots & -e^{-j\omega_1} & -1 & (N-1)e^{j\omega_1} \end{bmatrix}. \tag{4.14}$$

Let the distance between two adjacent array elements be a sequence denoted as d_1, d_2,..., d_{N-1}. Let the distance between the i-th element and the reference element be i_1, i_2, ,...i_{N-1}. i.e., $d_0 = i_0 = 0$. Also

$$i_n = \sum_{j=1}^{n} d_j \qquad n = 1, 2, \ ,\dots N-1. \tag{4.15}$$

The collection of the eigenvectors of the MRA becomes:

$$\mathbf{E}_m = \left[\begin{array}{c|cccc} 1 & -1 & 0 & \dots & 0 \\ e^{-i_1 j\omega_1} & e^{-d_1 j\omega_1} & -1 & \dots & 0 \\ e^{-i_2 j\omega_1} & 0 & e^{-d_2 j\omega_1} & \dots & 0 \\ \vdots & \vdots & \vdots & \vdots & \vdots \\ e^{-i_{N-1} j\omega_1} & 0 & 0 & \dots & e^{-d_{N-1} j\omega_1} \end{array}\right]. \tag{4.16}$$

The transformation matrix $\mathbf{T}_2$ can be found through

$$\mathbf{T}_2 = \mathbf{E}_m \mathbf{E}_u^{-1}$$

where both $\mathbf{E}_u$ and $\mathbf{E}_m$ have full rank N.

4.2.3 Diagonalized Transformation Matrix

The transformation matrix found above does not have a diagonal structure. The following procedure defines a diagonalized transformation matrix between the eigenspaces, $\mathbf{E}_u$ of the URA and $\mathbf{E}_m$ of the MRA.

Let i_n, $n = 1, 2, \ldots, N-1$ be defined as in Eq. (4.15) and consider an $N \times N$ transformation matrix $\mathbf{T}$,

$$\mathbf{T} = \begin{bmatrix} e^{-(i_0)j\omega_1} & 0 & 0 & \ldots & 0 \\ 0 & e^{-(i_1-1)j\omega_1} & 0 & \ldots & 0 \\ 0 & 0 & e^{-(i_2-2)j\omega_1} & \ldots & 0 \\ \vdots & \vdots & \vdots & \vdots & \vdots \\ 0 & 0 & 0 & \ldots & e^{-(i_{N-1}-(N-1))j\omega_1} \end{bmatrix}. \tag{4.17}$$

With $\mathbf{E}_m^{new} = \mathbf{R}\mathbf{E}_u$, the matrix of eigenvectors of the MRA becomes:

$$\mathbf{E}_m^{new} = \left[\begin{array}{c|ccc} 1 & -1 & 0 & \ldots & 0 \\ e^{-s_1 j\omega_1} & e^{-(s_1-1)j\omega_1} & -e^{-(s_1-1)j\omega_1} & \ldots & 0 \\ e^{-s_2 j\omega_1} & 0 & e^{-(s_2-1)j\omega_1} & \ldots & 0 \\ \vdots & \vdots & \vdots & \vdots & \vdots \\ e^{-s_{N-1} j\omega_1} & 0 & 0 & \ldots & e^{-(s_{N-1}-(N-2))j\omega_1} \end{array}\right]. \tag{4.18}$$

Notice that the only difference between $\mathbf{E}_m$ and $\mathbf{E}_m^{new}$ is that besides the first two columns, all the new eigenvectors are scaled by the factor $e^{(i_{n-2}-1)j\omega_1}$ for $n = 4, 5, \ldots, N-1$. The reason the first two columns remain unchanged is because $i_0 = 0$ and $i_1 = d_1$.

4.3 Formulation of the MRA using the Eigenspace Transformation Matrix

We next discuss the optimization problem of an MRA with the eigencanceling technique using the diagonalized eigenspace transformation matrix.

Recall that for the single-interferer case

$$\mathbf{R}_m = p_1 \mathbf{d}_1 \mathbf{d}_1^H + \sigma^2 I_N,$$

where

$$\mathbf{d}_1^T = \left[1, e^{-s_1 j\omega_1}, e^{-s_2 j\omega_1}, \ldots, e^{-s_{N-1} j\omega_1}\right].$$

The noise variance for an MRA has an identical expression as that for a URA. The MRA autocorrelation matrix uses the subscript m to distinguish it from the URA one. We obtain

$$\begin{aligned} \min \quad & \mathbf{w}^H \mathbf{R}_m \mathbf{W} \\ \text{subject to} \quad & \mathbf{w}^H \mathbf{A}_p = \mathbf{g}^H \\ & \mathbf{w}^H \mathbf{E}_{mr} = \mathbf{0}. \end{aligned} \tag{4.19}$$

Using Eq. (4.2),

$$\begin{aligned} \mathbf{w}^H \mathbf{R}_m \mathbf{W} &= \sigma^2 \mathbf{c}^H (\mathbf{E}_{m_\nu}^H \mathbf{E}_{m_\nu}) \mathbf{c} \\ &= \sigma^2 \mathbf{c}^H \mathbf{U}_m \mathbf{c}, \end{aligned} \tag{4.20}$$

$$\begin{aligned} \mathbf{w}^H \mathbf{a}_p &= \mathbf{c}^H \mathbf{E}_{m_\nu}^H \mathbf{a}_p \\ &= \mathbf{c}^H \mathbf{A}_m = \mathbf{g}. \end{aligned} \tag{4.21}$$

Using the transformation matrix $\mathbf{T}$ found in the previous section, we can write

$$\mathbf{E}_{m_\nu} = \mathbf{T}\mathbf{E}_{u_\nu}.$$

From the definition of $\mathbf{T}$ in Eq. (4.17),

$$\mathbf{T}^H \mathbf{T} = \mathbf{I}_N.$$

We then calculate $\mathbf{U}_m$ and $\mathbf{A}_m$ as follows:

$$\begin{aligned} \mathbf{U}_m &= \mathbf{E}_{m_\nu}^H \mathbf{E}_{m_\nu} \\ &= (\mathbf{E}_{u_\nu}^H \mathbf{T}^H) \mathbf{T} \mathbf{E}_{u_\nu} \end{aligned}$$

$$= \mathbf{E}_{u_\nu}^H \mathbf{E}_{u_\nu}$$

$$= \mathbf{U} \tag{4.22}$$

$$\mathbf{A}_m = \mathbf{E}_{m_\nu}^H \mathbf{a}_p$$

$$= (\mathbf{T}\mathbf{E}_{u_\nu})^H \mathbf{a}_p. \tag{4.23}$$

With $\mathbf{a}_p = \mathbf{1}$ for the desired signal coming from broadside with unit gain, the MNVV for the MRA using the eigencanceling technique becomes:

$$J_{min} = \frac{\sigma^2}{\mathbf{A}_m^H \mathbf{U}^{-1} \mathbf{A}_m}. \tag{4.24}$$

The $\mathbf{U}$ matrix for the MRA is the same as the matrix for the URA. This means there is no need to derive a separate $\mathbf{U}^{-1}$ for the MRA structure. But the constraint equations are slightly modified.

4.4 Performance Comparison

This section compares the performance of the URA and the MRA using the eigencanceling technique with the eigenspace transformation matrix.

The noise variance is used as a measure to compare the performance of the URA and the MRA. For the single-interferer case, the general expressions of the MNVV for the URA and the MRA using the conventional beamforming technique from Eqs. (3.10) and (3.12) are:

$$J_{URA} = \frac{\sigma^2(N+\gamma_1)}{N(N+\gamma_1-1) - 2\sum_{n=1}^{N-1}(N-n)\cos(n\omega_1)} \tag{4.25}$$

$$J_{MRA} = \frac{\sigma^2(N+\gamma_1)}{N(N+\gamma_1-1) - 2\sum_{n=1}^{L-1} e_n \cos(n\omega_1)}. \quad (4.26)$$

Here e_n is some number related to the redundant correlation lag in the MRA structure, as mentioned in Eq. (3.12).

The MNVV of the URA and the MRA using the eigencanceling method are:

$$J_{URA_e} = \frac{\sigma^2 N}{N(N-1) - 2\sum_{n=1}^{N-1} (N-n)\cos(n\omega_1)} \quad (4.27)$$

$$J_{MRA_e} = \frac{\sigma^2 N}{N(N-1) - 2\sum_{n=1}^{L-1} e_n \cos(n\omega_1)} \quad (4.28)$$

where N is the number of array elements and L-1 is the aperture of the MRA with N elements. The equivalent relation of Eq. (4.12) and Eq. (4.27) is derived in Appendix D.

A simple three-element array using the above equations, equations (4.25) through (4.28), was chosen to demonstrate the effect of the eigencanceling technique. The noise variance is selected as a measure of the difference between a URA and an MRA with both conventional beamforming and the eigencanceling technique.

- With the conventional beamforming from Eqs. (4.25) and (4.26):

$$J_{URA} = \frac{\sigma^2(3+\gamma_1)}{3(\gamma_1+2) - 2(2\cos\omega_1 + \cos 2\omega_1)} \quad (4.29)$$

$$J_{MRA} = \frac{\sigma^2(3+\gamma_1)}{3(\gamma_1+2) - 2(\cos\omega_1 + \cos 2\omega_1 + \cos 3\omega_1)}. \quad (4.30)$$

- With the eigencanceling method from Eqs. (4.27) and (4.28):

$$J_{URA_e} = \frac{3\sigma^2}{6 - 2(2\cos\omega_1 + \cos 2\omega_1)} \tag{4.31}$$

$$J_{MRA_e} = \frac{3\sigma^2}{6 - 2(\cos\omega_1 + \cos 2\omega_1 + \cos 3\omega_1)}. \tag{4.32}$$

Note that the condition for the MRA to outperform the URA, with either conventional beamforming or eigencanceling technique is the same. The following inequality has to be satisfied:

$$2\cos\omega_1 + \cos 2\omega_1 > \cos\omega_1 + \cos 2\omega_1 + \cos 3\omega_1, \tag{4.33}$$

which leads to

$$\omega_1 < \frac{\pi}{2}.$$

Using the relationship

$$\omega_1 = \pi \sin\theta \Longrightarrow \theta < 30°.$$

Thus the region for an MRA to perform better than a URA using either conventional beamforming or eigencanceling will be exactly the same. Another important property is when comparing Eqs. (4.29) through (4.32), the noise variance of the array using the eigencanceling will not be affected by the noise-to-interference power ratio γ_1. The noise variance using the eigencanceling technique can be obtained by bringing the noise-to-interference ratio γ_1 to zero from the conventional beamforming case.

A key point emerges from this discussion: after calculating the NMNVV for the URA structure using the conventional beamforming technique, the NMNVV of the corresponding MRA with the same number of array elements can be obtained through the transformation matrix found in Eq. (4.17). To obtain the minimum noise variance of the optimization problem using the eigencanceling technique, we

only have to set γ_1, the noise-to-interference ratio, to zero in the conventional beamforming problem.

When the number of interferers is larger than one, the analysis is not so straight forward. The eigenvectors derived in Appendix C for the dual-interferer case will help in finding the transformation matrix. The remaining steps will be similar to those developed in section 3.2.2.

CHAPTER 5

NUMERICAL RESULTS

In this chapter, the performance of the URAs and the MRAs is studied through a computer program using the formulas obtained in Chapter 3. The performance using the MNVV as a measurement is compared between the MRA and the URA with the same number of array elements. The URA and the MRA with the same aperture is also evaluated. The conventional beamforming and the eigencanceling techniques are applied to both the single- and dual-interferer cases.

Recall that due to the constraint imposed on the MNV criterion, $\mathbf{w}^H\mathbf{a}_p = \mathbf{1}$, the preassigned array pattern gain at broadside is chosen to be unity. The result obtained is equivalent to assuming zero dB desired signal power. Therefore, the noise variance $\mathbf{w}_{op}^H\mathbf{R}\mathbf{w}_{op}$ can be interpreted as the interference plus noise-to-signal ratio (1/SINR) for a zero dB desired signal power. At θ_1=0, the interference direction is the same as that of the desired signal. When using conventional beamforming, the array has no cancellation effect in the desired signal direction. Applying Eq. (3.18) for the single-interferer case we find the MNVV to be $\mathbf{w}_{op}^H\,\mathbf{R}\mathbf{w}_{op}= p_1 + \sigma^2/N$ in the desired signal direction. For the dual-interference case from Eq. (3.28) the MNVV is $p_1 + p_2 + \sigma^2/N$ for $\theta_1 = \theta_2 = 0$.

In all figures listed, the terminology URA-N refers to the Uniform Regular Array with N elements and with aperture N-1. The terminology of MRA-N refers to a Minimum Redundancy Array with N elements and aperture L-1, where N and L are related by Table 1 in Chapter 1. The MNVV comparison for the single-interferer cases was done between the URA and the MRA with the same number of elements, and the URA and the MRA with the same aperture. For the dual-interferer cases,

the MNVV comparison was made between a URA and an MRA with the same number of array elements. The configuration of the MRA used for the calculation is listed as the second title of each figure.

5.1 Conventional Beamforming

5.1.1 The Single-Interferer Case

In Figure 4, the MRA-3 (with 3 elements and aperture 3) was compared to the URA-3 (with the same number of array elements as the MRA-3) and to the URA-4 (with aperture 3) as a function of the arriving angle of a single interferer. The interference-to-noise ratio (INR) is taken as 10 dB. Notice that the crossover point is at $\theta = 30°$ as given in Eq. (3.35). Therefore the MRA-3 performs better than the URA-3 for $\theta < 30°$, and almost as well as the URA-4 for $\theta < 15°$. For $\theta > 30°$, the URA-3 performs better than the MRA-3. The performance ratio between the URA-3 to the MRA-3 and the MRA-3 to the URA-4 are depicted in Figure 5. The maximum gain in the main beam region for the MRA-3 is 3 dB higher than the URA-3, while the maximum loss of almost 2 dB occurred at around $\theta = 44°$. The effect of varying the INR for the same array is plotted in Figure 6 and 7. The increase of INR does not change the crossover point of the MNVV curves. Instead it increases the gain for the MRA-3 over the URA-3 in the main beam region is increased, while the performance beyond the main beam remains unchanged.

Figure 8 depicts the noise variance performance of the MRA-4 when compared to the URA-4 and the URA-7. The characteristics seen in the three elements array case become even more distinct now. The gain for the MRA-4 over the URA-4 as revealed in Figure 9 becomes almost 5.5 dB while the maximum degradation is only

about 1.5dB. Figures 10 and 11 show the effect of differently configurated MRAs with the same INR. The crossover point is slightly different, as can be seen in Figure 12, for different configurations. The MRA-5 gained more than 6dB in the main beam region when compared to the URA-5 and the degradation was bounded within 1.5dB. To ensure that the observation was not unique for the five-element array case, the six-element cases were also investigated. The MRA-6 structure has three different configurations. With INR equal to 10dB, the MNVV is compared to the URA-6 and the URA-14 in Figure 13, 14 and 15. The gain in the main beam for the MRA structure is now well over 7 dB while the degradation is reduced to almost within 1dB, as shown in Figure 16.

The difference in performance between the MRA-4 and the URA-4 with the INR as a parameter is shown in Figure 17. The interference power was taken to be unity. The MNVV ratio between the URA-4 and the MRA-4 with different values of the INR is depicted in Figure 18. The INR seemed to affect only the cancellation depth in the main beam region for the single-interferer case. It had no effect on the position of the crossover point nor the noise variance beyond the crossover point when the conventional beamforming technique was applied.

5.1.2 The Dual-Interferer Case

The performance of an MRA in comparison to a URA with more than one interferer was also studied. Figures 19 and 20 show the performance of a URA and an MRA with five elements and two interferers. The same procedure of taking the ratio between the URA-5 and the MRA-5 was performed, and the result is shown in Figure 21. In order to visualize the three dimensional plots better, their contours are shown in Figures 22, 23 and 24 respectively. Interference-to-noise ratios of 20 dB and 10dB

were used in the computation, i.e. $(\sigma^2,\ p_1,\ p_2) = (1, 100, 10)$. One should pay special attention to the zero dB line in Figure 24, which bounds the shaded region where the MRA outperforms the URA. As before in the single-interferer case, the MRA structure has a deeper cancellation ability in the main beam region.

We check the sensitivity of the MNVV in terms of the angle separation between two interferers. Figures 25 and 26 illustrate the results of the URA-4 and the MRA-4 structure. The first interferer is used as a reference and the second interferer is 2°, 5° and 10° apart from the first one. In these two figures, the MNVV at $\theta_1 = 0°$ will not be equal to $p_1 + p_2 + \sigma^2/N$, as mentioned before, since $\theta_2 \neq 0$ at this point.

5.2 Eigencanceling Technique

5.2.1 The Single-Interferer Case

Only a three-element array was used in the calculation carried out in the last section of Chapter 4. Figure 27 shows that the crossover point of the URA-3 and the MRA-3 did not change despite the difference of the optimization problem formulation. The additional constraint that the optimum weight vector lies in the noise subspace which was used in the eigencanceling technique causes a reduction of the feasible solution domain. The performance in terms of the MNVV is therefore expected to degrade. In Figure 27, the eigencanceling technique did not degrade the performance of the system much except in the look direction region. The extremely poor interference cancellation in the desired signal direction is due to the conflict between the two constraints posed in the optimization problem.

Recall that from Eqs. (3.41) through (3.43), the formulation for the eigen-

canceling technique for either the URA or the MRA case was,

$$\min \qquad \mathbf{w}^H\mathbf{R}\mathbf{w} \tag{5.1}$$

$$\text{subject to} \quad \mathbf{w}^H\mathbf{A}_p = \mathbf{g}^H \tag{5.2}$$

$$\text{and} \qquad \mathbf{w}^H\mathbf{E}_r = \mathbf{0}. \tag{5.3}$$

In the calculation, $\mathbf{A}_p$ was assigned to be from the broadside which meant $\theta_1 = 0$. The gain in this direction was constrained to be unity, i.e. g= 1. When the interference was exactly from the broadside where the desired signal was located, the following equality held:

$$\mathbf{E}_r = \alpha(\mathbf{A}_p),$$

where α is a scalar while $\mathbf{g} \neq \mathbf{0}$. When applying the eigencanceling technique, the optimum weight vector was always a linear combination of the noise space vectors, as shown in Eq. (3.44). The MNVV in the look direction can also be seen directly from Eq. (3.100) for the MRA-3 and Eq. (3.101) for the URA-3 cases,

$$\text{MRA-3} \qquad \frac{J_{min}}{\sigma^2} = \frac{3/4}{1-\cos 3\omega_1},$$

$$\text{URA-3} \qquad \frac{J_{min}}{\sigma^2} = \frac{3/4}{1-\cos 2\omega_1}.$$

When ω_1 approaches zero, the NMNVV approaches infinity.

Depending on the requirement of the particular application, some adjustment should be made. One way to avoid the overshoot of the NMNVV is to "turn off" the eigencanceling process when the interference is too close to the desired signal, and switch to a conventional beamformer or some other eigen-based technique. The "turn off" point should be determined by the inner product of the matrices $\mathbf{A}_p^H\mathbf{E}_r$. The MRA structure will have the advantage of a lower angle of "turn off" point than

the URA with a given number of array elements and a given noise variance value.

Haimovich [22] has concluded that for the URA case, the eigencanceling technique converges faster than the conventional beamforming method. For the case of the MRA, Pillai [46] has suggested that for the augmented autocorrelation matrix of an MRA, the convergence rate is roughly half that of a URA with the same number of array elements. The numerical result for the transient response of an eight-element array with three interferers is given in Figure 28. The eigencanceling method for both the URA and the MRA did converge faster than the same array using conventional beamforming. The convergence rate for a URA and an MRA using conventional beamforming is about the same when the non-augmented autocorrelation matrix was employed for the MRA. The most striking fact is that the MRA using the eigencanceling method converges to its steady state value in an extremely small number of snapshots.

5.2.2 The Dual-Interferer Case

The three-dimensional plots for the five-element array with dual interferers are shown in Figures 29 and 30 for the URA and the MRA structures respectively. The noise variance ratio is depicted in Figure 31. Contour plots are shown in Figures 32, 33 and 34. In Figure 34, the shaded region, which is closer to the main beam, shows where the MRA outperforms the URA. It is clearly visible that the region where the MRA outperforms the URA has shifted from the one obtained using the conventional beamforming method. This is a different behavior from what was seen in the single-interferer case.

5.3 Planar Square Array Case

Using the formulation derived in Chapter 2, the nine-element square array is examined here. Since the interference signal had to be specified in two dimensions (elevation θ and azimuth angle ϕ), only the single-interferer case can be examined here graphically. There exists only one configuration (plus its mirror image) for the linear MRA-3 structure. For the square array case, there are four configurations, as sketched in Figure 2. Note that the MRA-3 square array referred in Figure 2 actually consists of $3^2 = 9$ elements. For the MRA structure with a given number of linear configurations M, there exists $4M^2$ square array configurations.

Since the three-dimensional image will only cause confusion in visualizing the actual implication of the noise variance value, only the contour plots are shown. Figures 35 and 36 show the contours of MNVV for the nine-element the URA-3 and the MRA-3 square array using conventional beamforming technique. The ratio of the noise variance of the two structures is depicted in Figure 37. The zero dB line again marks the shaded region closer to the main beam in which the MRA outperforms the URA. Again, the contour plots for the URA-3 and the MRA-3 square arrays using the eigencanceling method are shown in Figures 38 and 39. Figure 40 depicts the NMNVV ratio for the square array of the URA-3 and the MRA-3 using the eigencanceling technique. As in the linear array case, the zero dB line is unchanged for the single-interferer case regardless of either the conventional beamforming or the eigencanceling technique used.

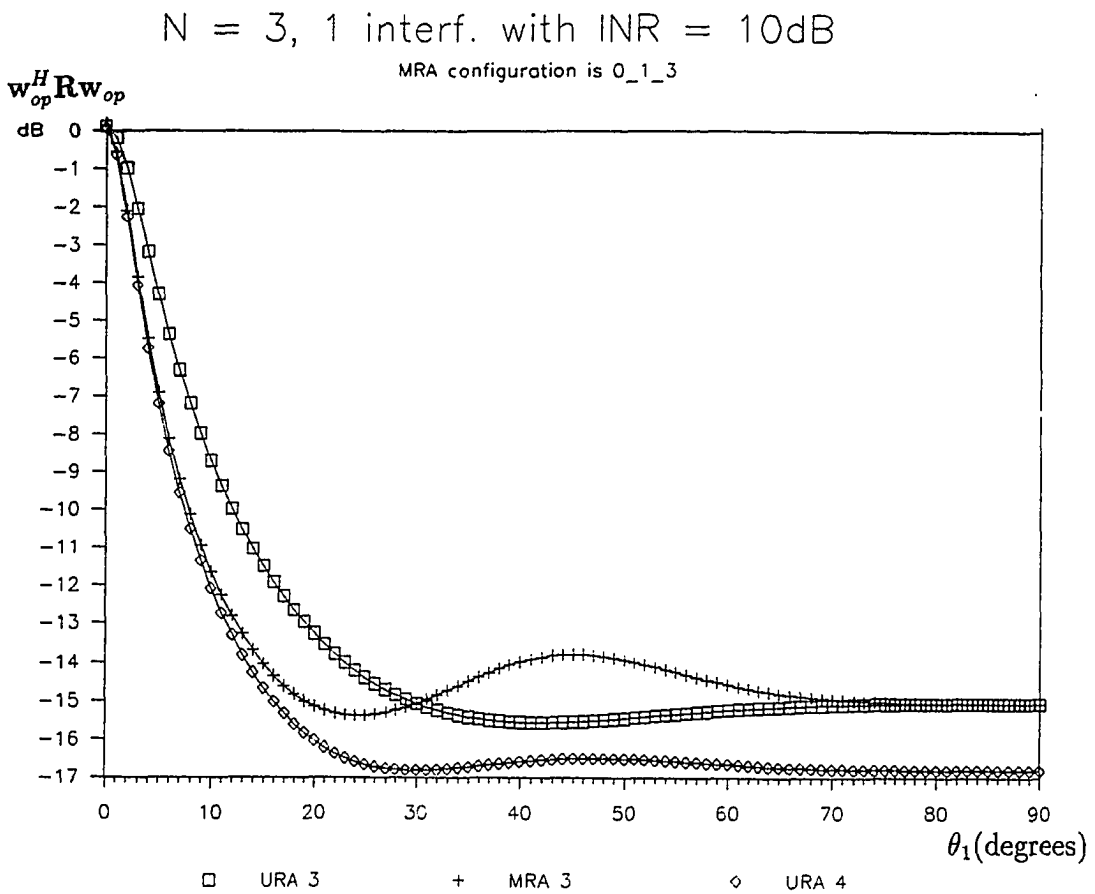

Figure 4 The MNVV comparison between the MRA-3, the URA-3, and the URA-4. Note that the URA-3 and the MRA-3 have the same number of elements while the MRA-4 and the URA-4 have the same aperture. The location for the MRA-3 is (0, 1, 3). The noise and the interferer power were taken as (σ^2, p_1)=(0.1,1).

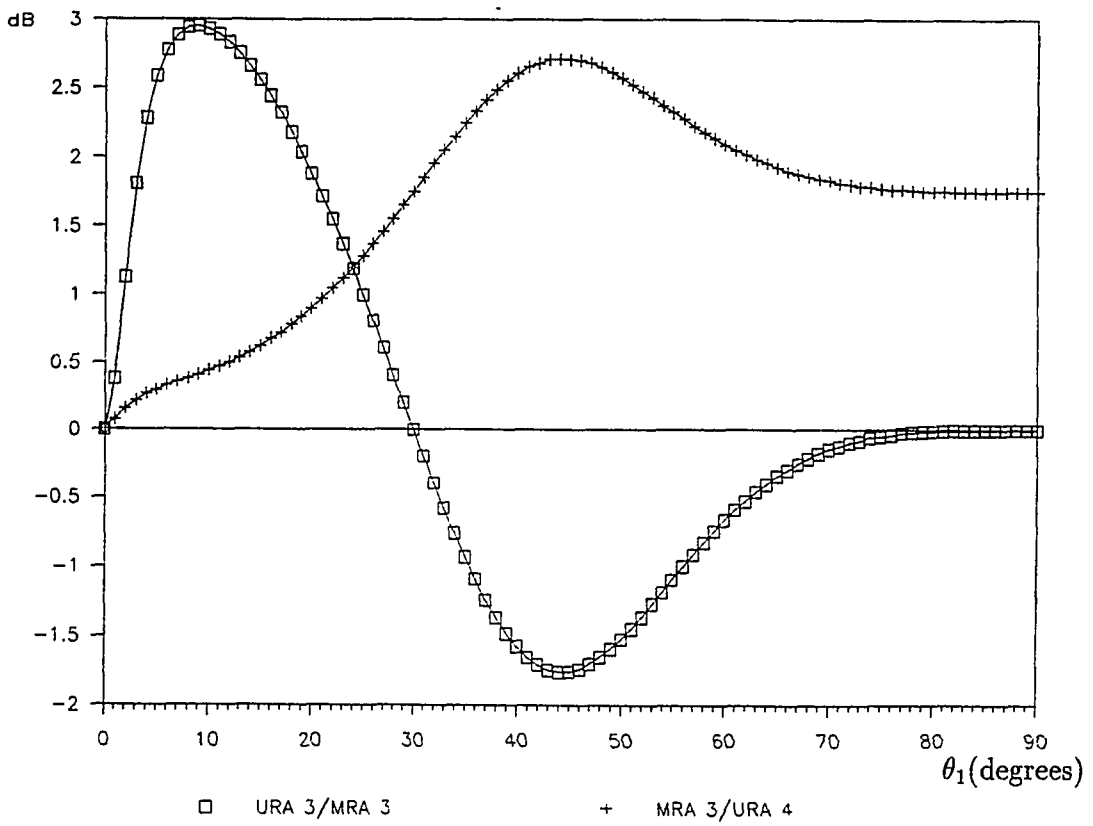

Figure 5 The MNVV ratio as a function of the interferer's direction of the URA-3 to the MRA-3, and of the MRA-3 to the URA-4. Note that the URA-3 and the MRA-3 have the same number of elements while the MRA-3 and the URA-4 have the same aperture. The locations for the MRA-3 is (0, 1, 3). The noise and the interferer power were taken as (σ^2, p_1)=(0.1, 1) for all arrays.

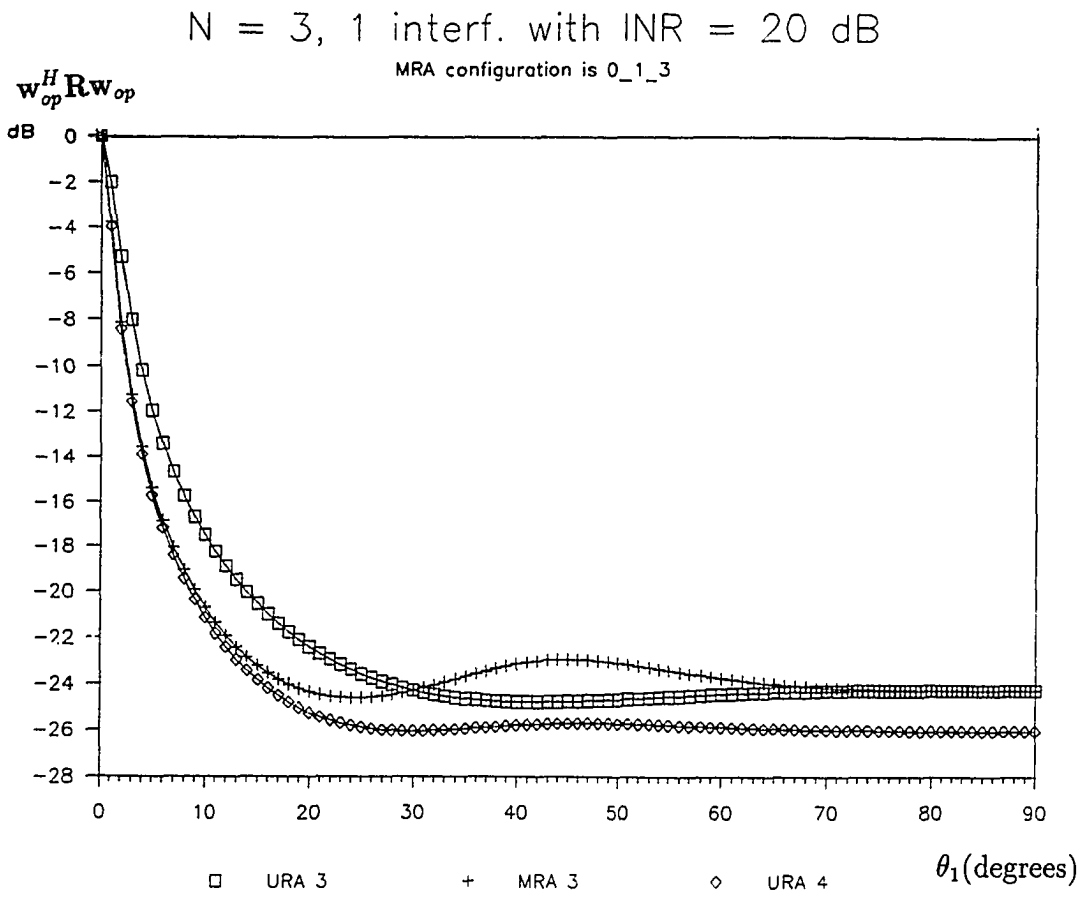

Figure 6 The MNVV comparison between the MRA-3, the URA-3, and the URA-4. Note that the URA-3 and the MRA-3 have the same number of elements while the MRA-4 and the URA-4 have the same aperture. The locations for the MRA-3 is (0, 1, 3). The noise and the interferer power were taken as (σ^2, p_1)=(0.01,1).

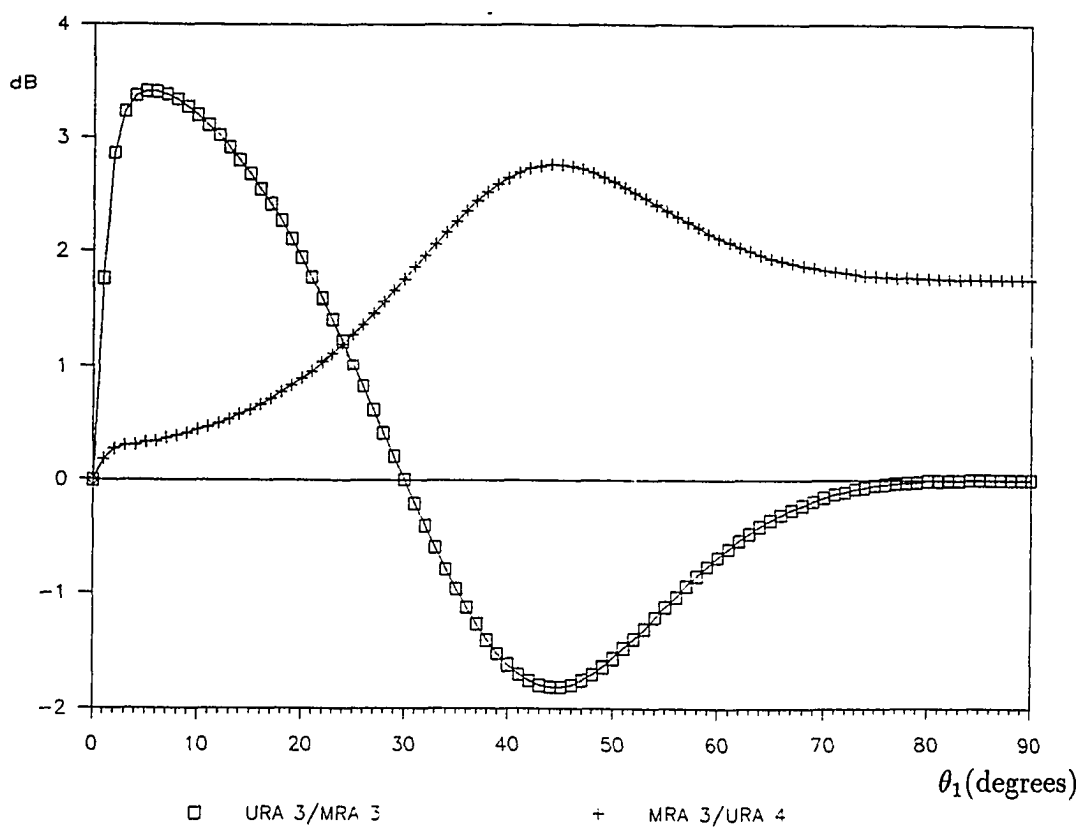

Figure 7 The MNVV ratio as a function of the interferer's direction of the URA-3 to the MRA-3, and of the MRA-3 to the URA-4. Note that the URA-3 and the MRA-3 have the same number of elements while the MRA-3 and the URA-4 have the same aperture. The locations for the MRA-3 elements is (0, 1, 3). The noise and the interferer power were taken as (σ^2, p_1)=(0.01, 1) for all arrays.

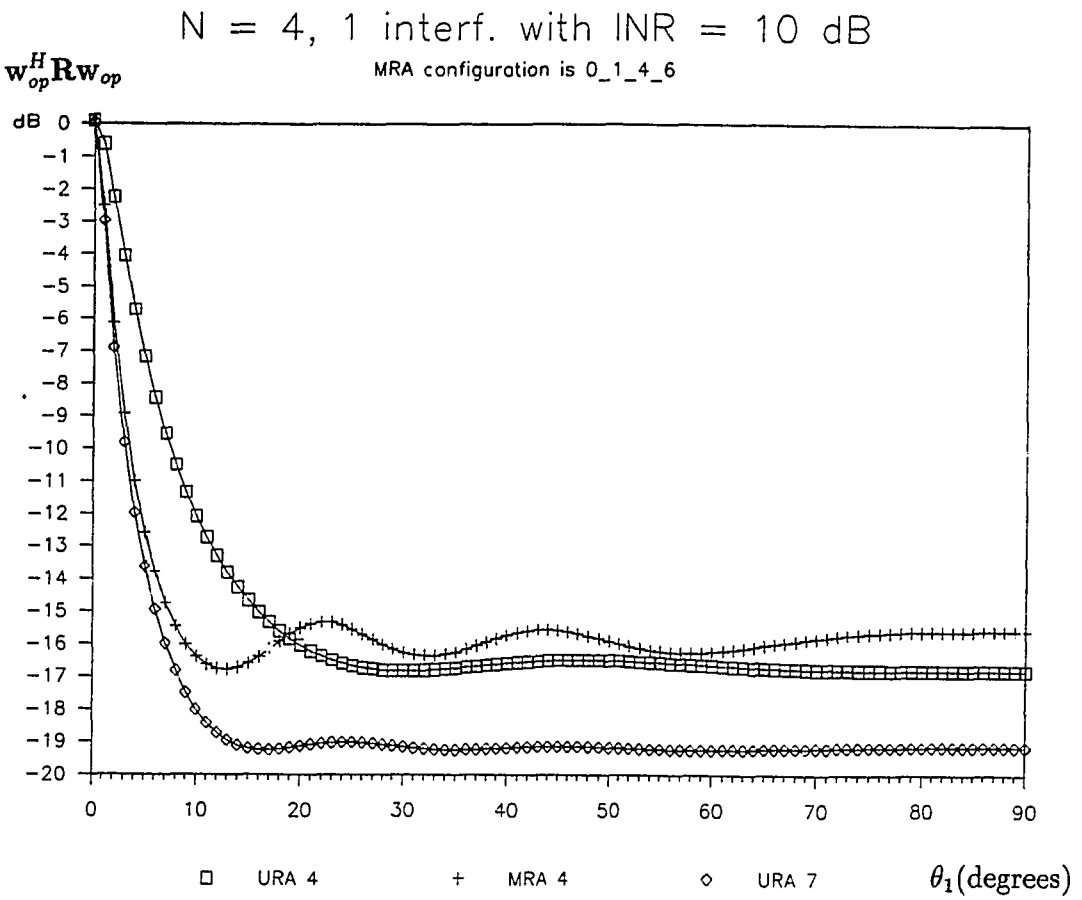

Figure 8 The MNVV comparison between the MRA-4, the URA-4, and the URA-7. Note that the URA-4 and the MRA-4 have the same number of elements while the MRA-4 and the URA-7 have the same aperture. The location for the MRA-4 is (0, 1, 4, 6). The noise and the interferer power were taken as (σ^2, p_1)=(0.1,1).

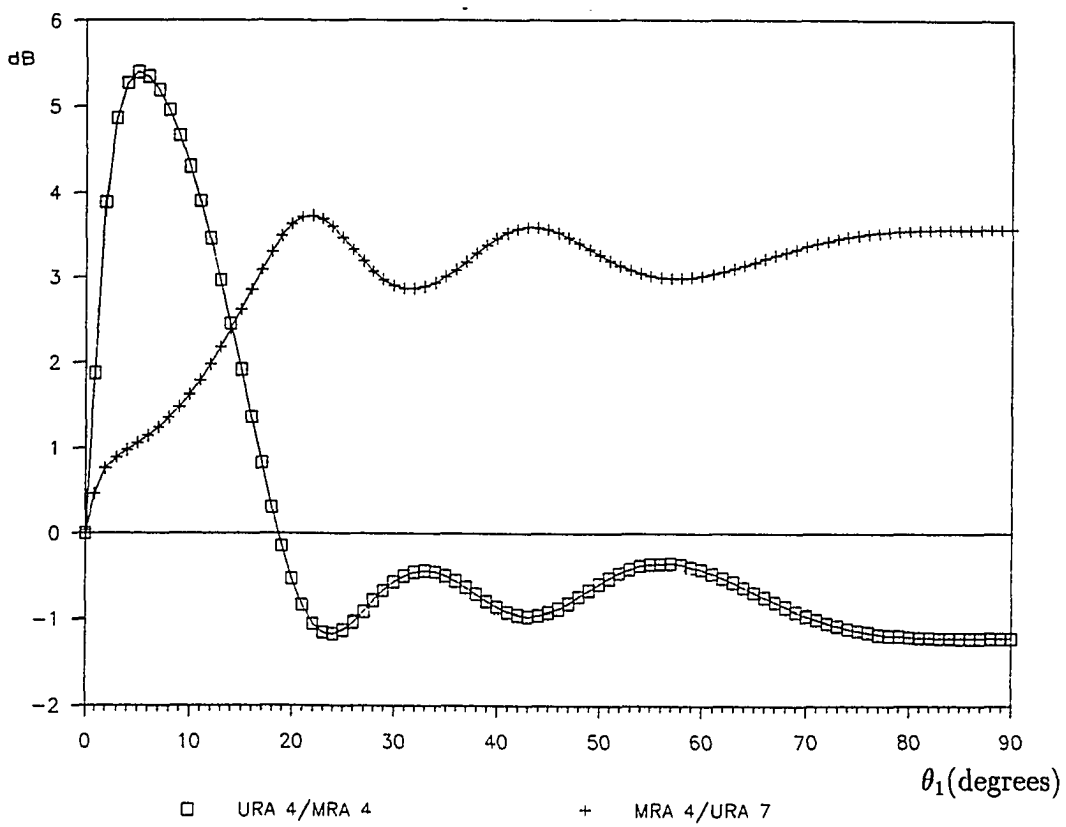

Figure 9 The MNVV ratio as a function of the interferer's direction of the URA-4 to the MRA-4, and of the MRA-4 to the URA-7. Note that the URA-4 and the MRA-4 have the same number of elements while the MRA-4 and the URA-7 have the same aperture. The location for the MRA-4 is (0, 1, 4, 6). The noise and the interferer power were taken as (σ^2, p_1)=(0.1, 1) for all arrays.

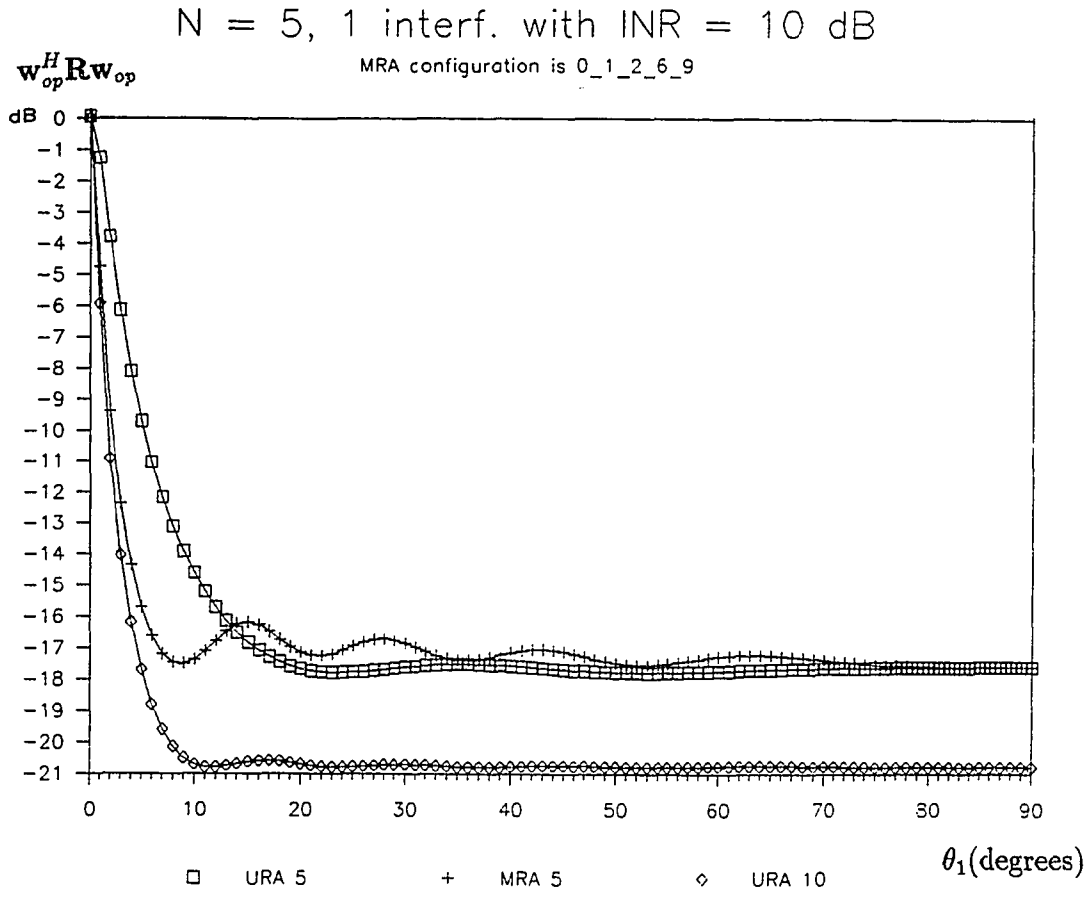

Figure 10 The MNVV comparison between the MRA-5, the URA-5, and the URA-10. Note that the URA-5 and the MRA-5 have the same number of elements while the MRA-5 and the URA-10 have the same aperture. The location for the MRA-5 is (0, 1, 2, 6, 9). The noise and the interferer power were taken as (σ^2, p_1)=(0.1, 1).

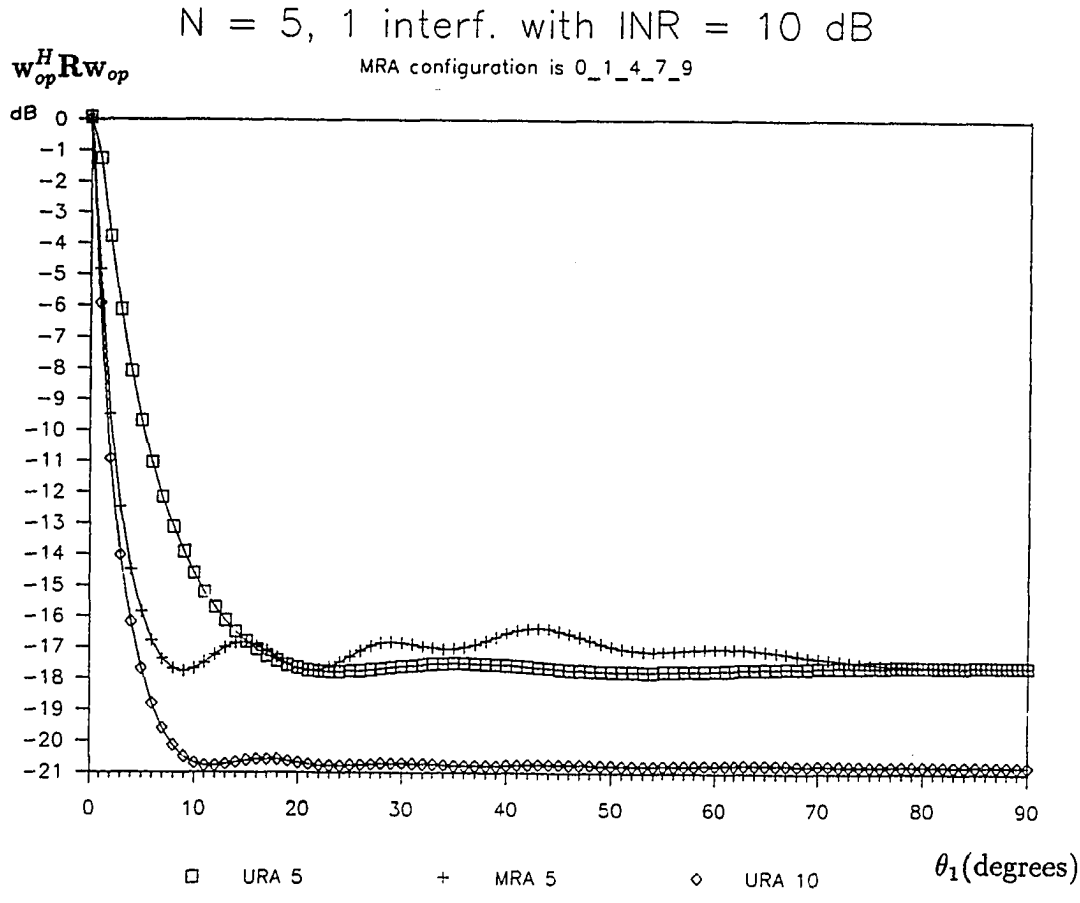

Figure 11 As in Figure 10, The MNVV of the MRA-5, the URA-5 and the URA-10. The location for the MRA-5 is (0, 1, 4, 7, 9).

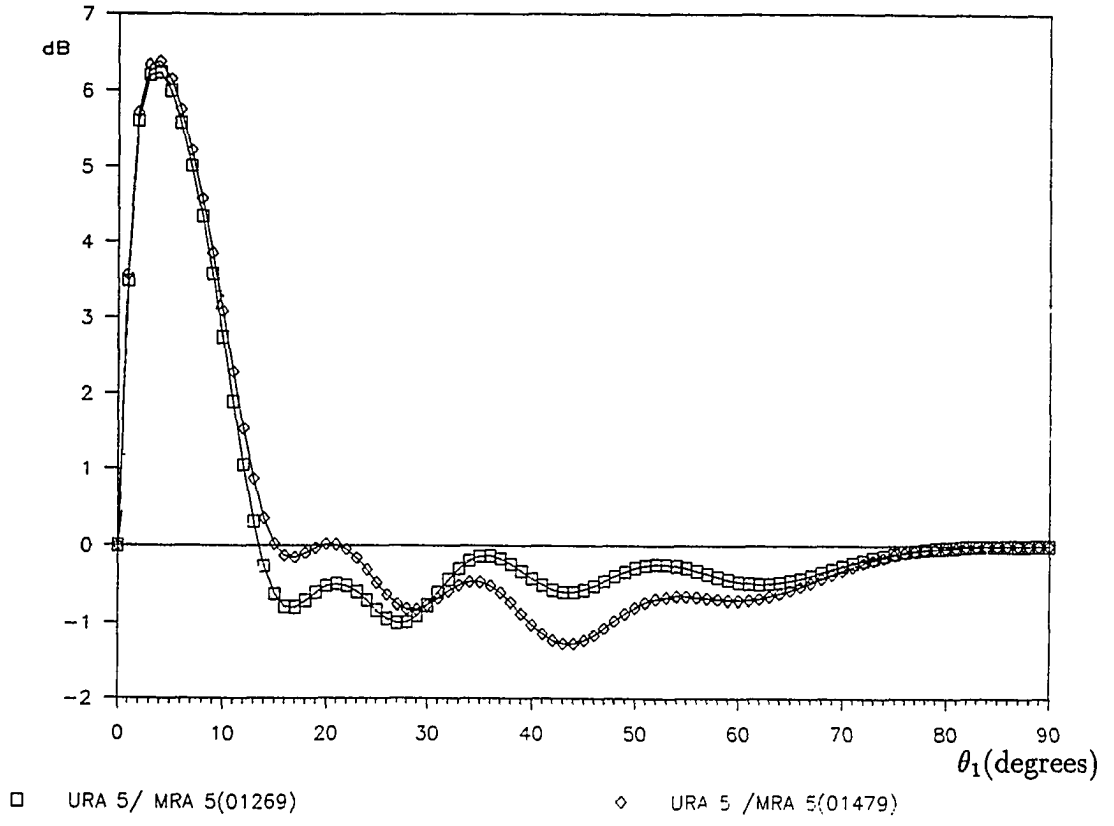

Figure 12 The MNVV ratio as a function of the interferer's direction of the URA-5 to the MRA-5. Two configurations of the MRA-5 were used. The locations for the MRA-5 are (0, 1, 2, 6, 9) and (0, 1, 4, 7, 9). The noise and interference power were taken as (σ^2, p_1)=(0.1, 1) for all arrays.

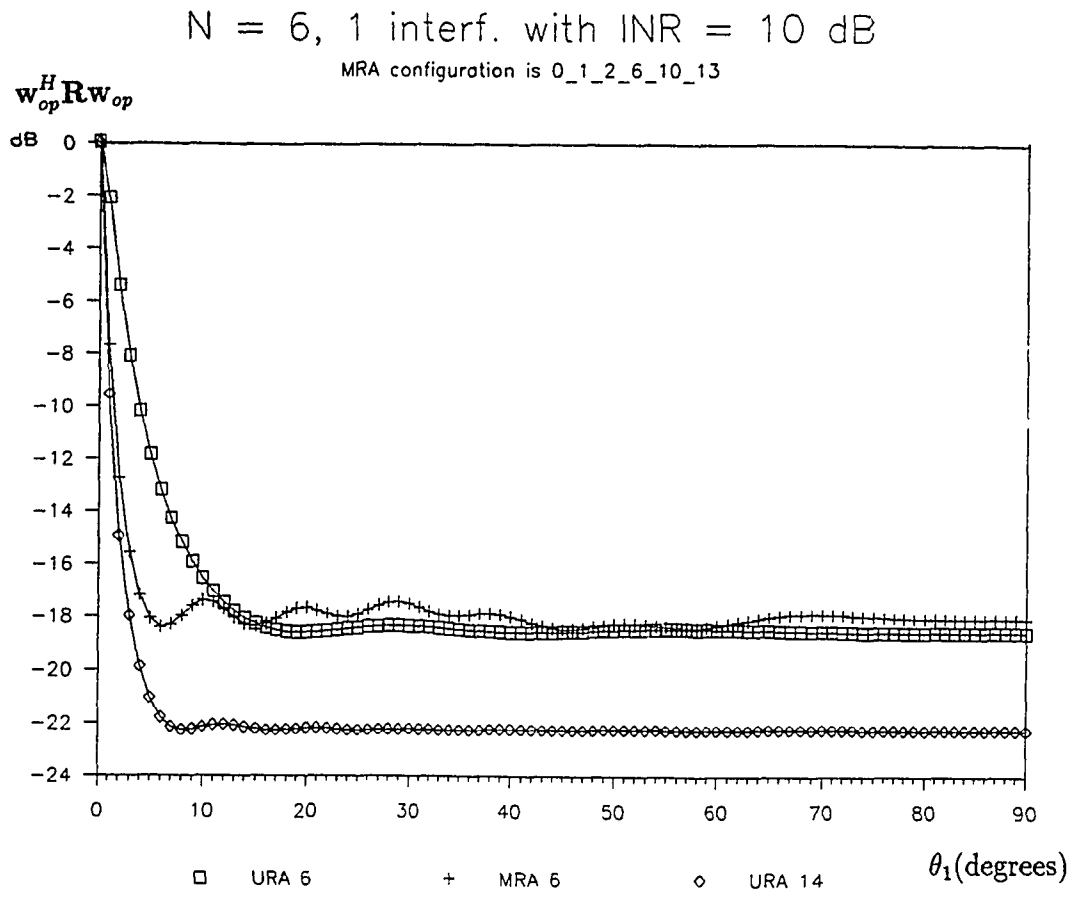

Figure 13 The MNVV comparison between the MRA-6, the URA-6, and the URA-14. Note that the URA-6 and the MRA-6 have the same number of elements while the MRA-6 and the URA-14 have the same aperture. The location for the MRA-6 is (0, 1, 2, 6, 10, 13). The noise and interference power were taken as (σ^2, p_1)=(0.1, 1).

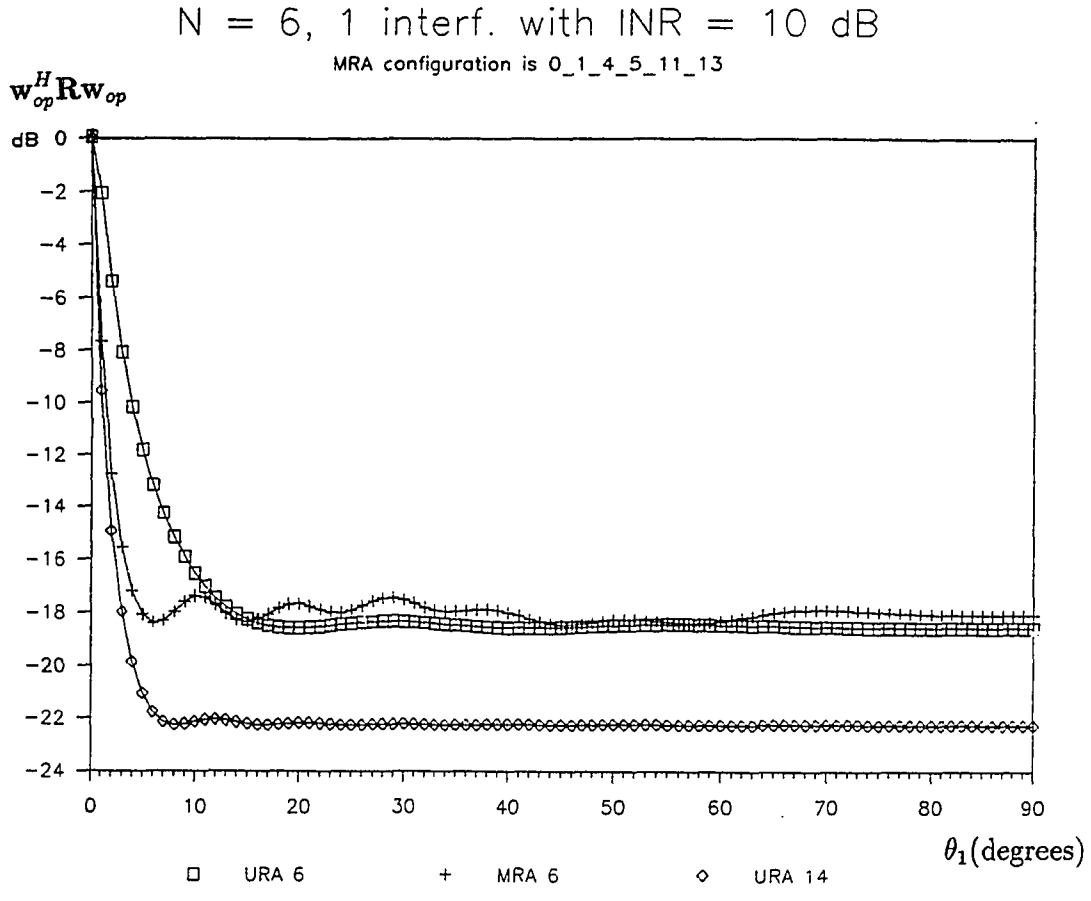

Figure 14 As in Figure 13, The MNVV of the MRA-6 is compared to the URA-6 and the URA-14. The location for the MRA-6 is (0, 1, 4, 5, 11, 13).

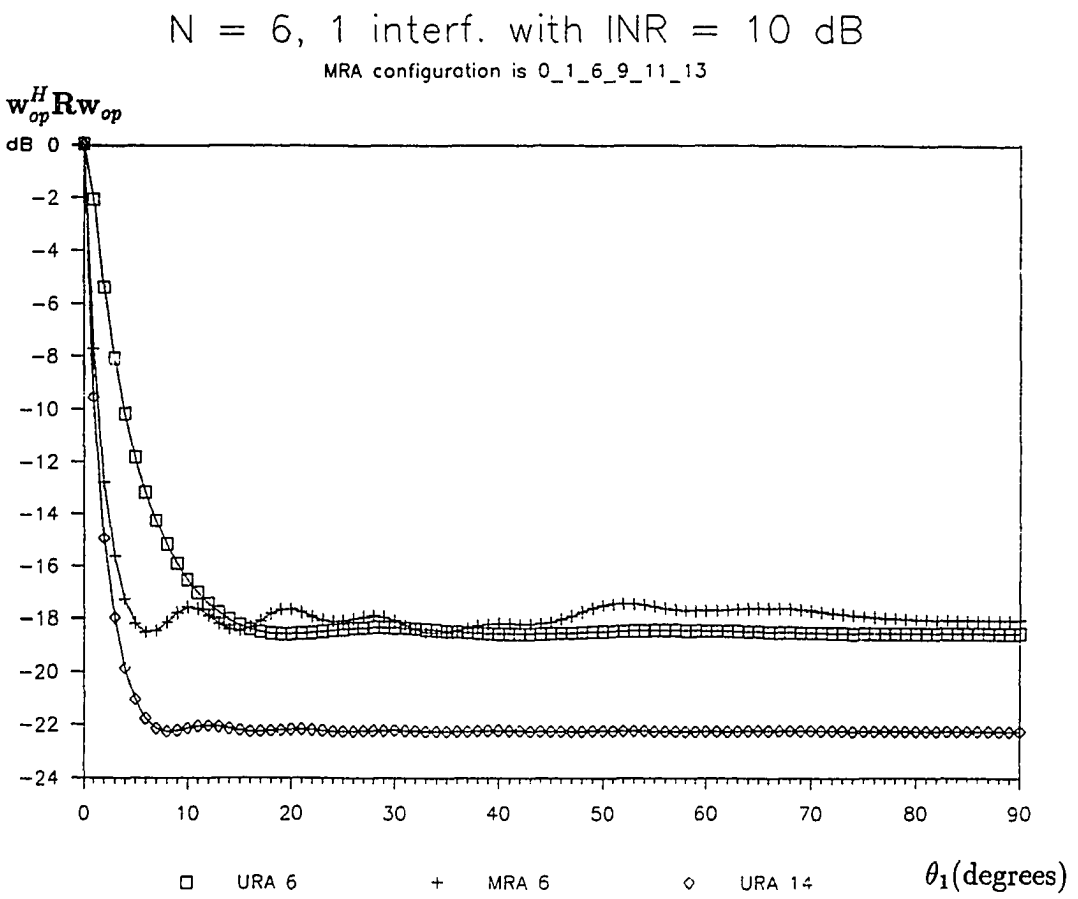

Figure 15 As in Figure 13, The MNVV of the MRA-6 is compared to the URA-6 and the URA-14. The location for the MRA-6 is (0, 1, 6, 9, 11, 13).

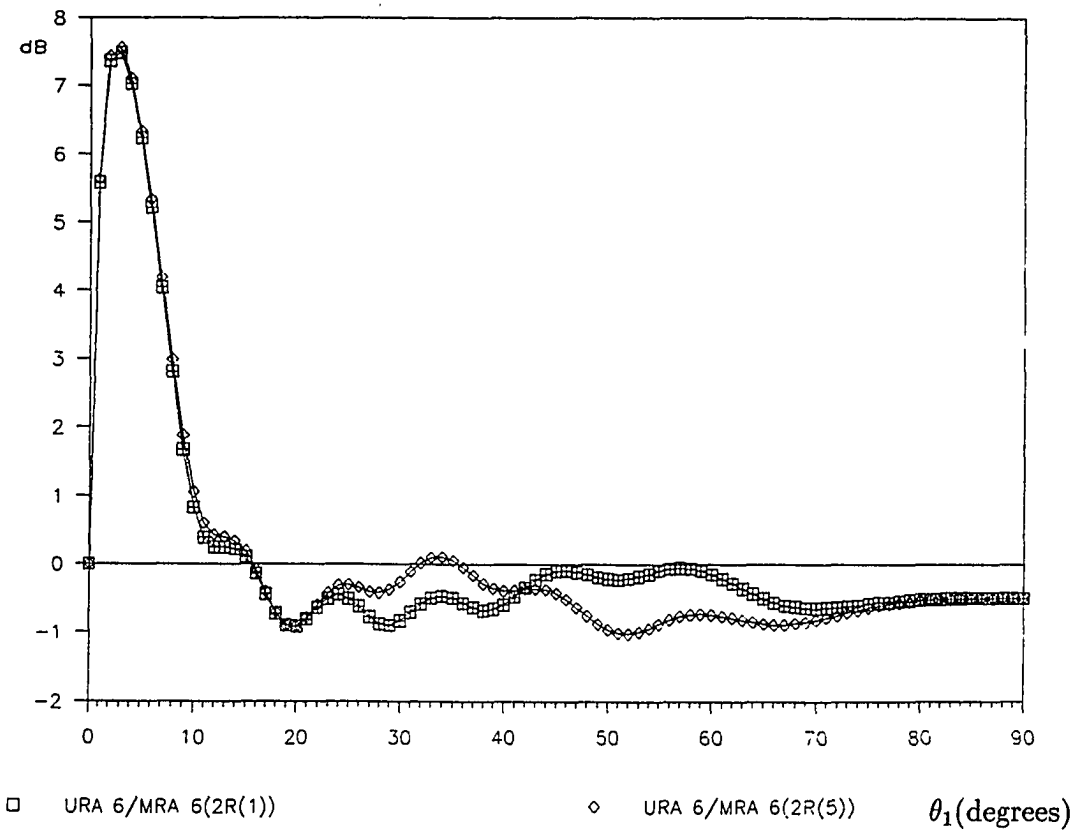

Figure 16 The MNVV ratio as a function of the interferer's direction for the URA-6 to the MRA-6. Two configurations of MRA-6 were used. The location for the MRA-6 is (0, 1, 2, 6, 10, 13) which has two repeated correlation lags at $r(4)$ and $r(1)$. The configuration of (0,1,6,9,11,13) has two repeated correlation lags at $r(2)$ and $r(5)$. The noise and the interferer power were taken as (σ^2, p_1)=(0.1, 1) for all arrays.

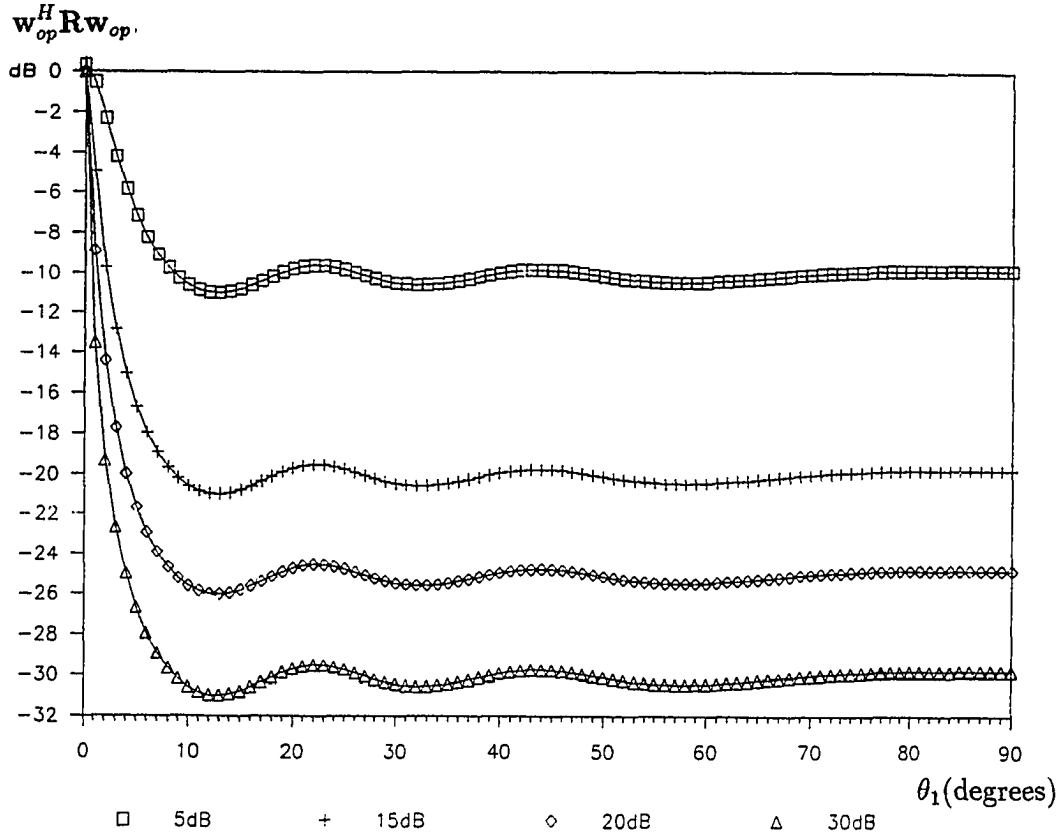

Figure 17 The effect of different interference-to-noise ratio (INR) on the MNVV of the MRA-4. The interferer power was taken as 1.

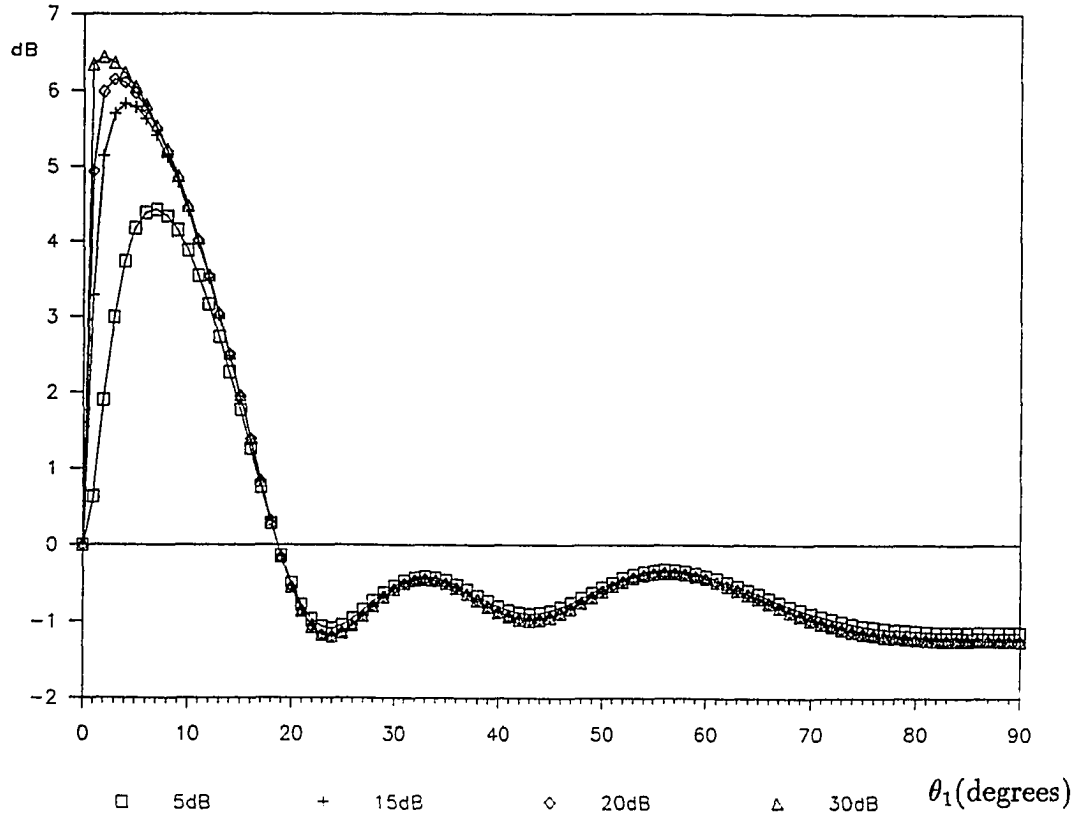

Figure 18 The effect of different interference-to-noise ratio (INR) on the MNVV ratio between the URA-4 and the MRA-4. The interferer power was taken as 1.

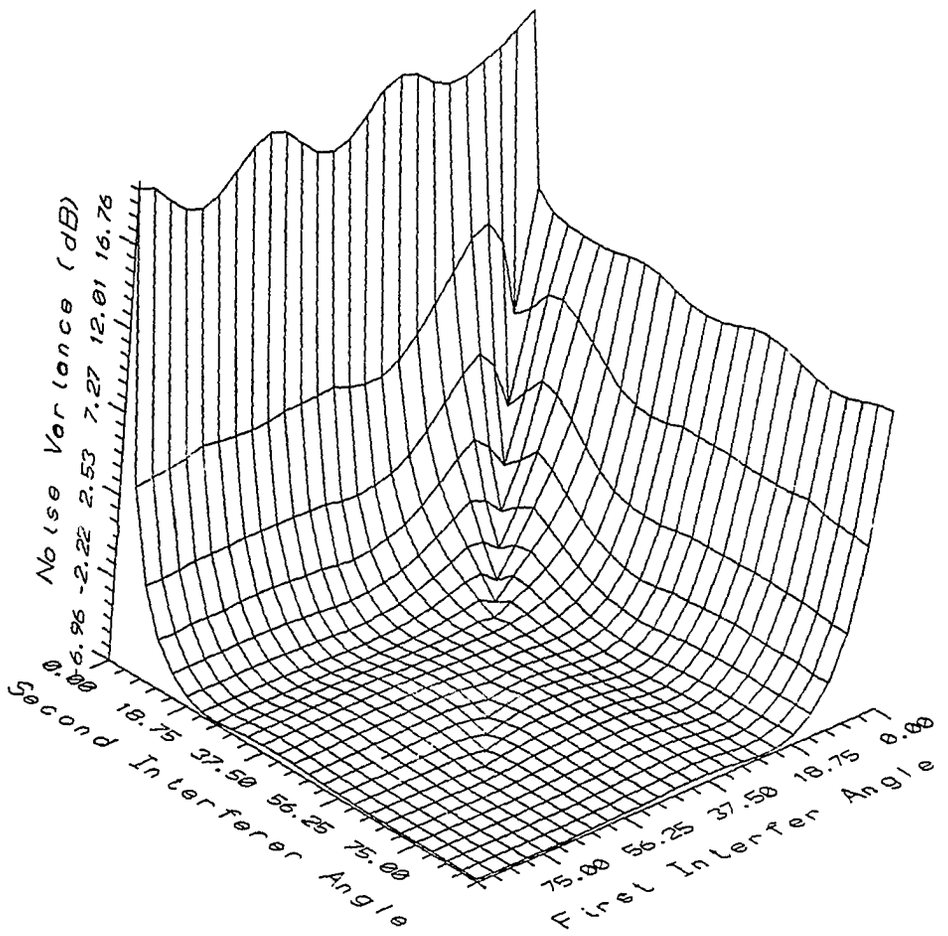

Figure 19 The NMNVV for the URA-5 with two interferers using conventional beamforming method and $(\sigma^2, p_1, p_2) = (1, 100, 10)$.

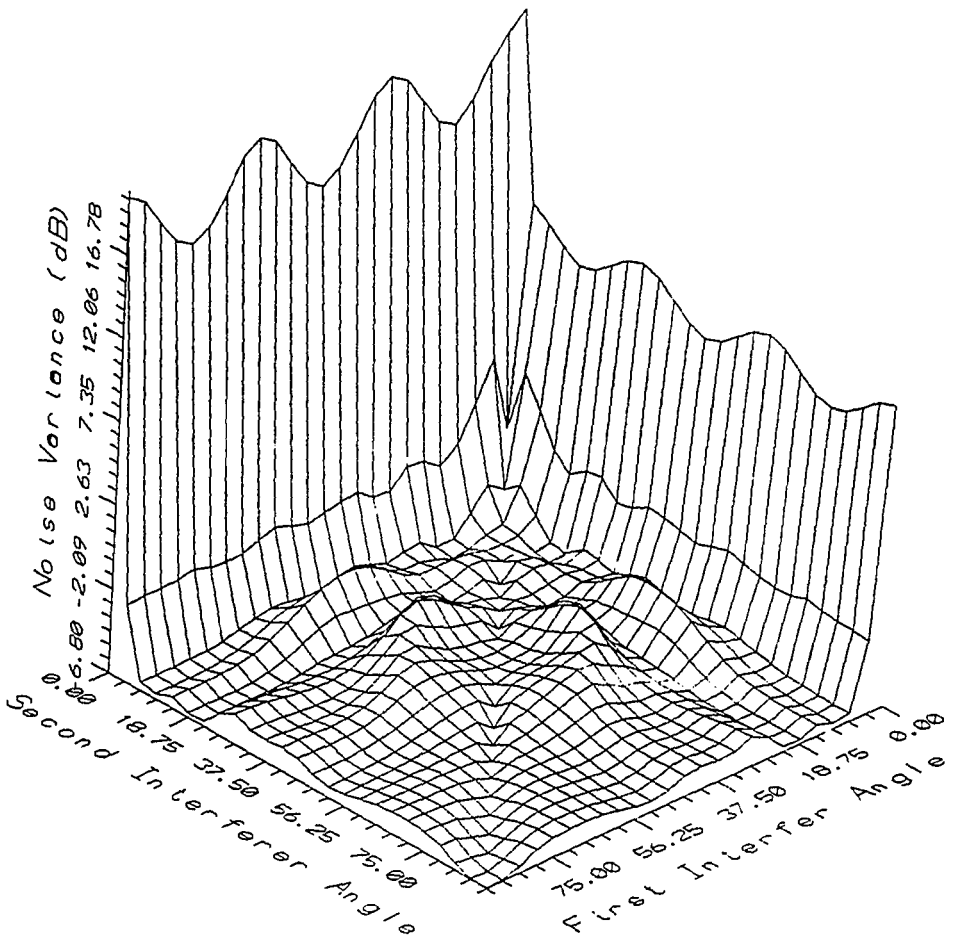

Figure 20 The NMNVV for the MRA-5 with two interferers using conventional beamforming method and (σ^2, p_1, p_2) =(1,100,10).

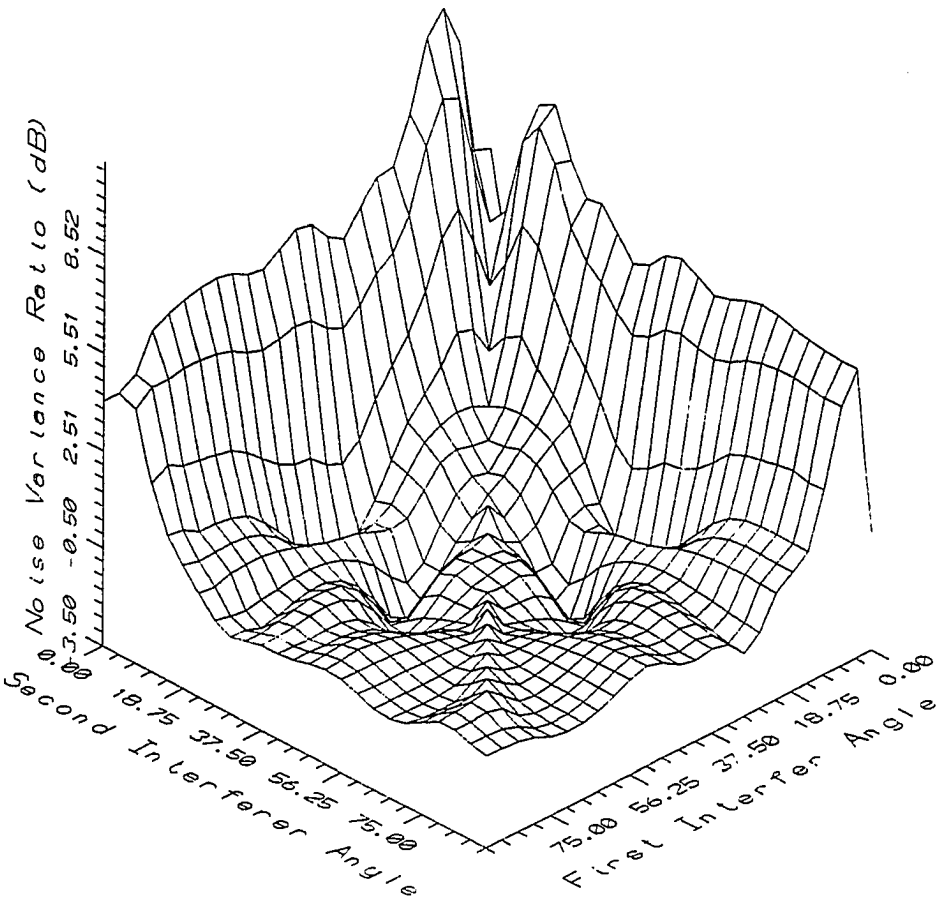

Figure 21 The NMNVV ratio of the URA-5 to the MRA-5 with two interferers using conventional beamforming method and $(\sigma^2, p_1, p_2) = (1, 100, 10)$.

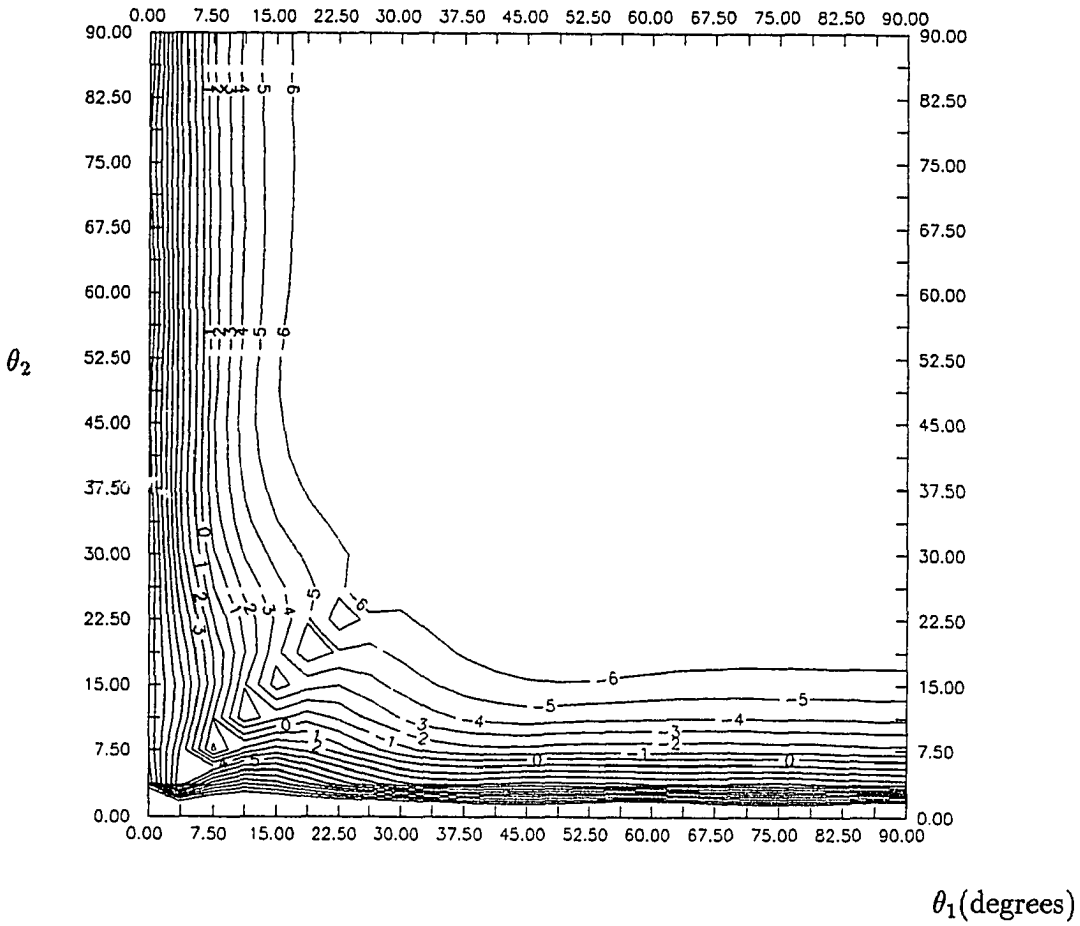

Figure 22 Contour plot (in dB) of the NMNVV for the URA-5 with two interferers using conventional beamforming method and (σ^2, p_1, p_2) =(1, 100, 10). The x axis is the first interferer angle, and the y axis is the second interferer angle.

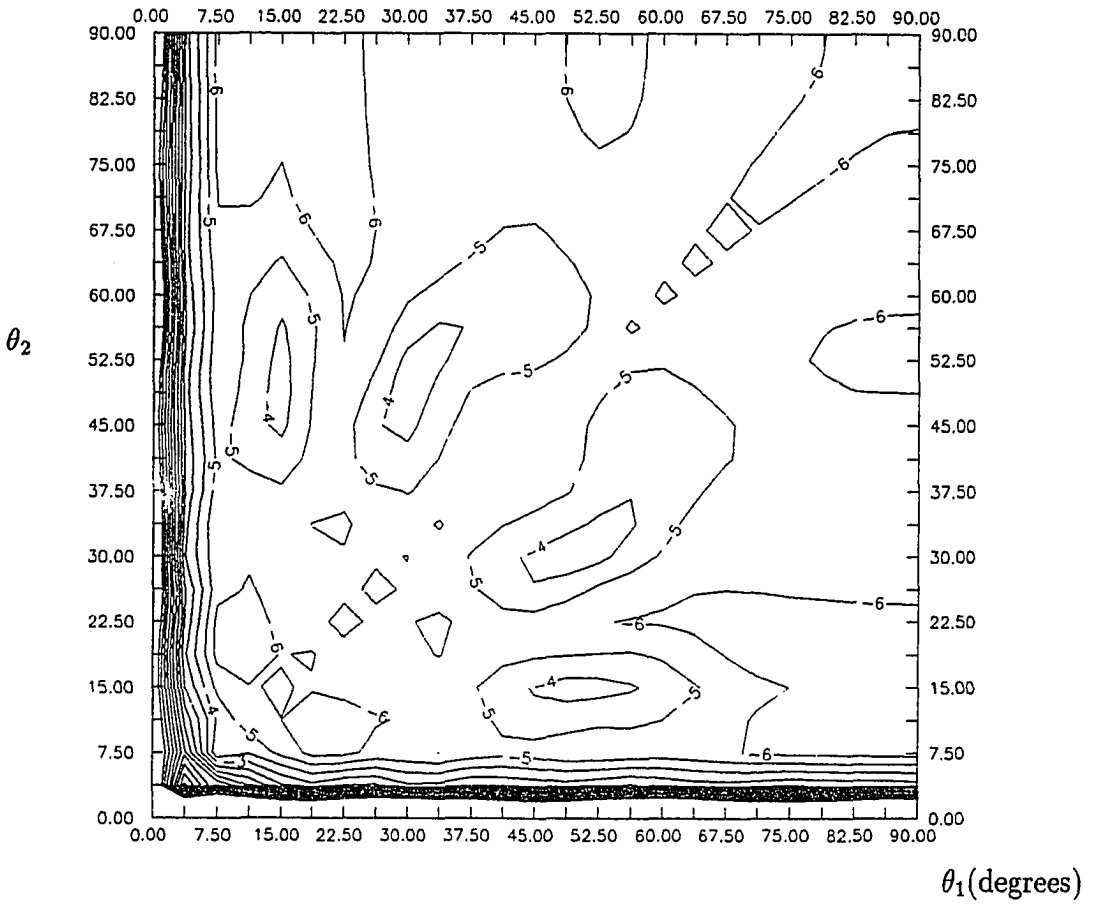

Figure 23 Contour plot (in dB) of the NMNVV for the MRA-5 with two interferers using conventional beamforming method and (σ^2, p_1, p_2) =(1, 100, 10). The x axis is the first interferer angle, and the y axis is the second interferer angle.

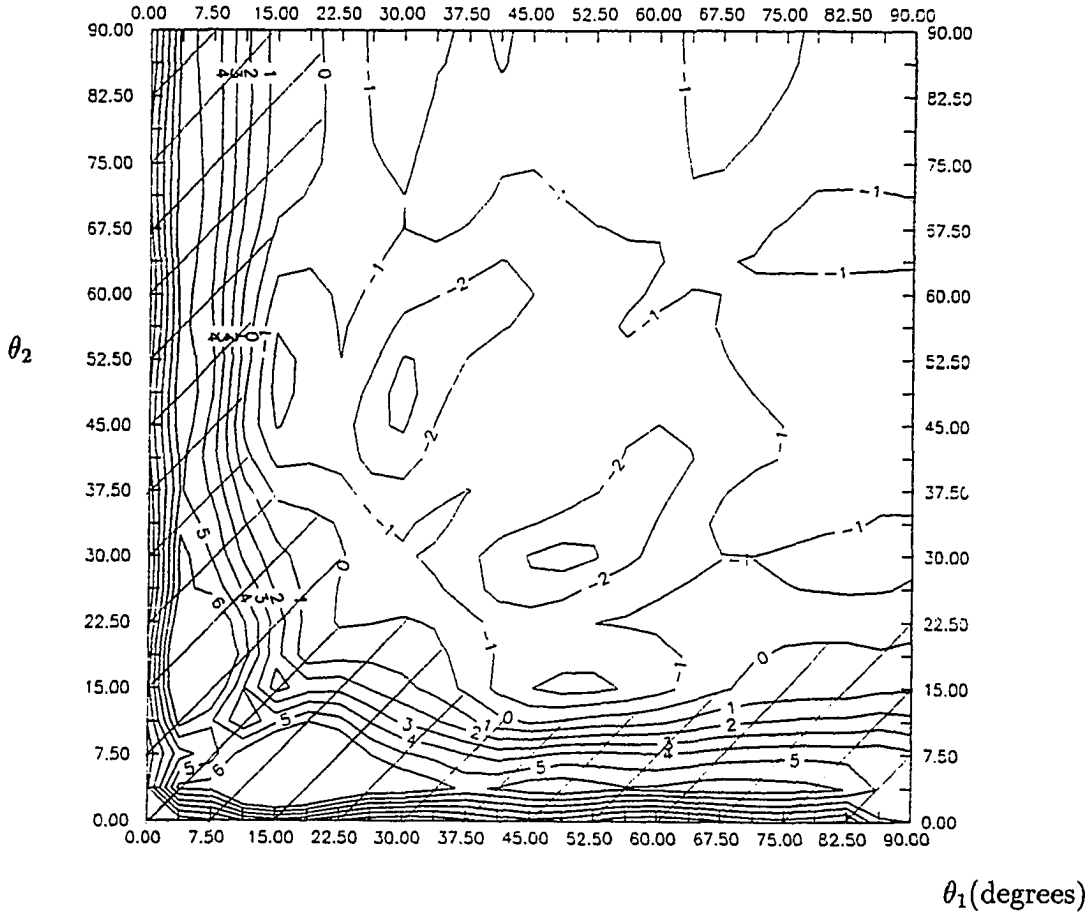

Figure 24 Contour plot (in dB) of the NMNVV ratio of the URA-5 to the MRA-5 with two interferers using conventional beamforming method and (σ^2, p_1, p_2) =(1, 100, 10). The x axis is the first interferer angle, and the y axis is the second interferer angle. The shaded region indicates where the MRA-5 outperforms the URA-5.

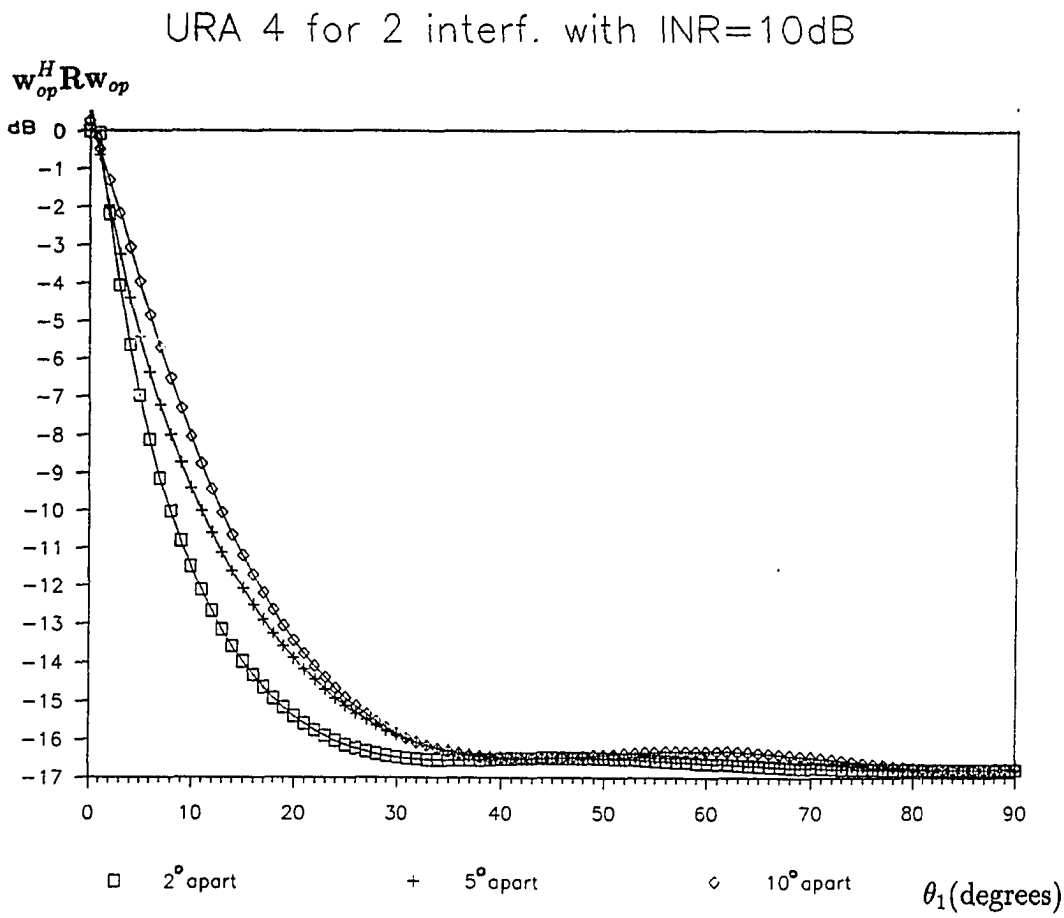

Figure 25 The MNVV for the URA-4 with two interferers. The angle between the interferers is taken to be 2°, 5° and 10° apart to test the sensitivity of the MNVV. The noise and the interferers' power were taken as (σ^2, p_1, p_2) =(0.1, 1, 1). Note that away from the main beam region, the URA is less sensitive to the angle difference between the two interferers.

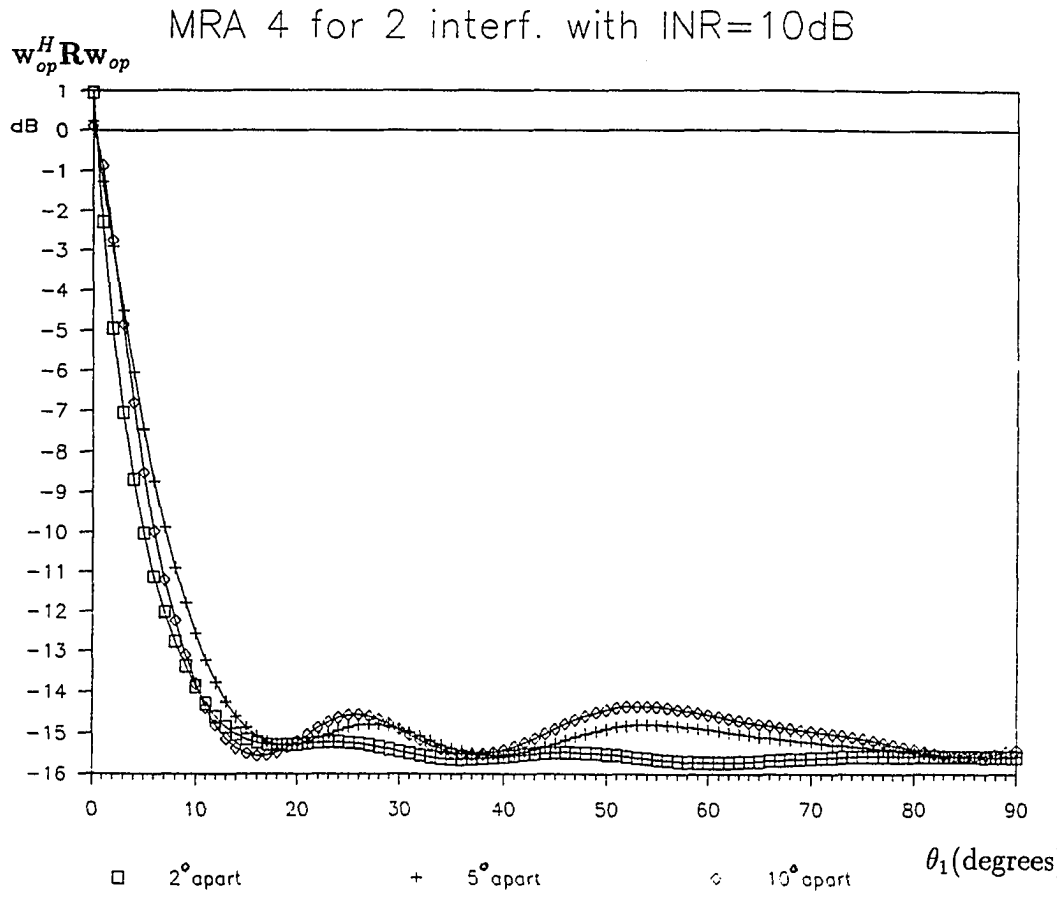

Figure 26 The MNVV for the MRA-4 with two interferers. The angle between the interferers is taken to be 2°, 5° and 10° apart to test the sensitivity of the MNVV. The noise and the interferers' power were taken as (σ^2, p_1, p_2)= (0.1, 1, 1). Note that in the main beam region, the MRA seems to be less sensitive to the angle difference between the two interferers.

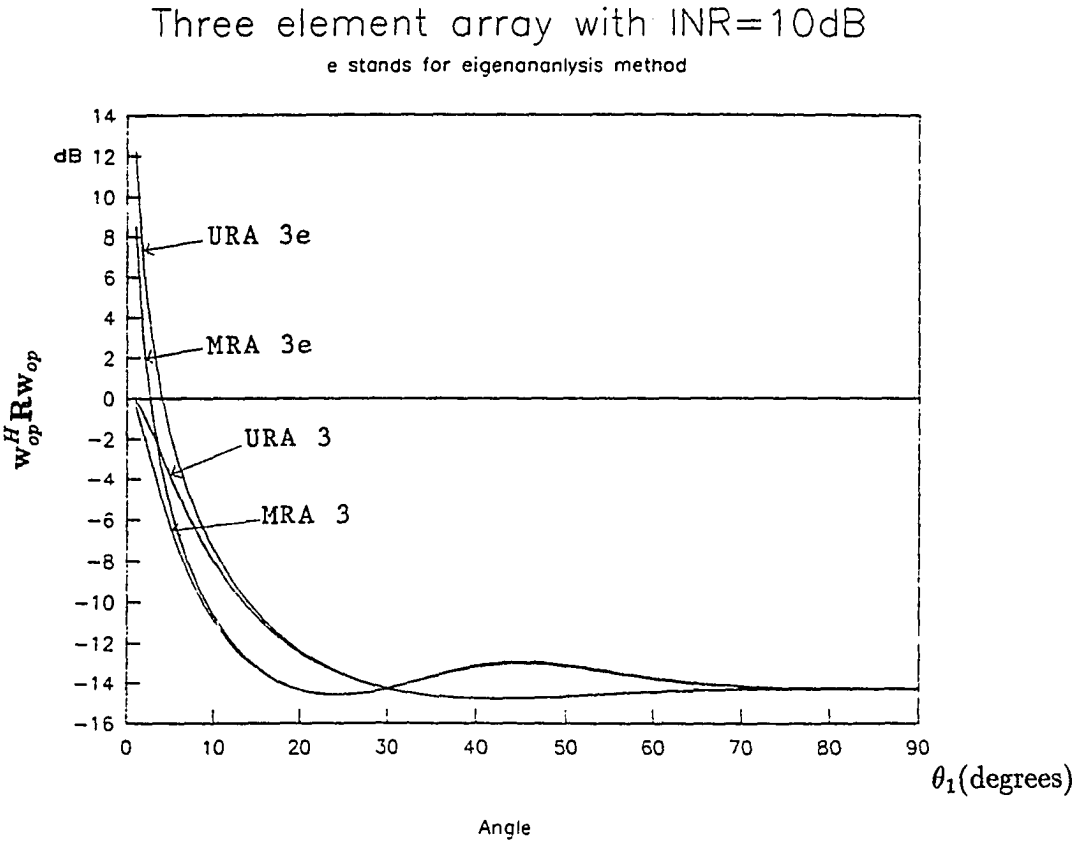

Figure 27 The MNVV comparison for three-element arrays the URA-3 and the MRA-3 using both conventional beamforming and eigencanceling methods. The subscript 'e' stands for eigencanceling method. Here (σ^2, p_1)=(0.1, 1), *i.e.* INR=10dB.

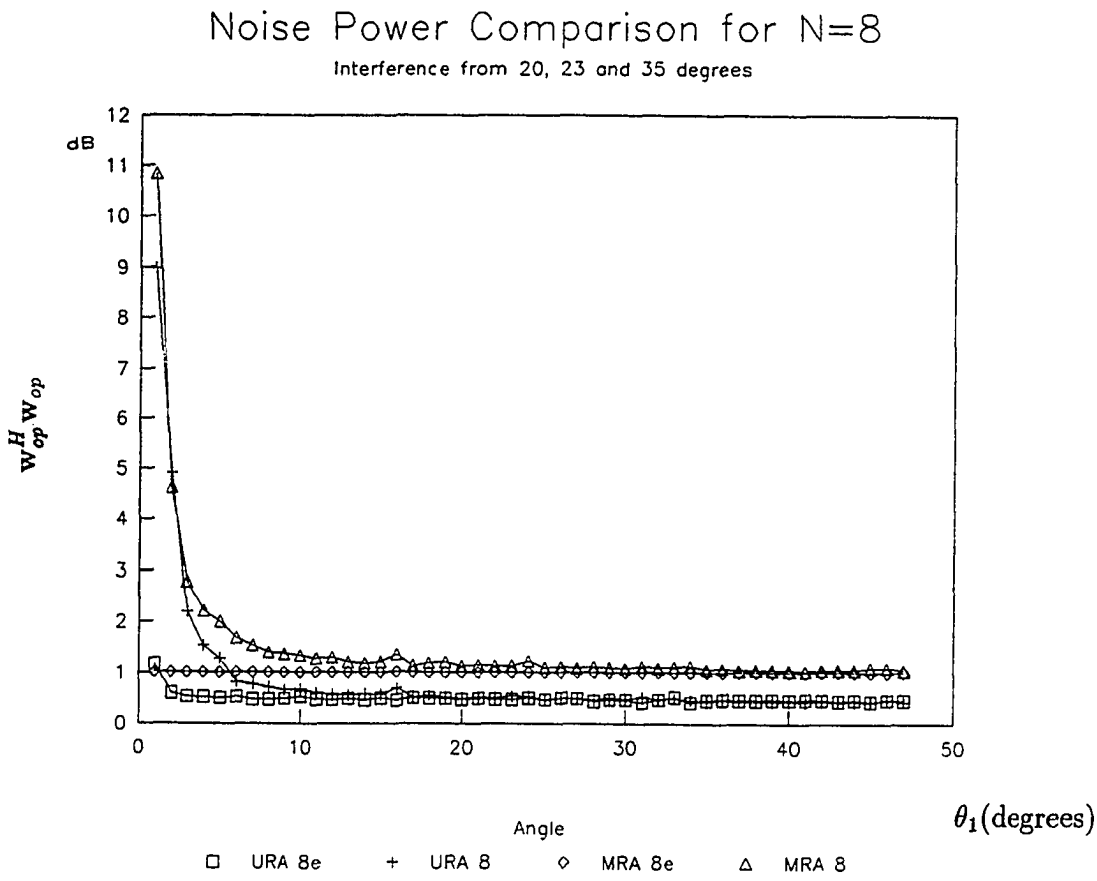

Figure 28 Convergence rate comparison for optimum weight using conventional beamforming and eigencanceling methods. Each point of data represents the 500 run average result. The subscript 'e' stands for eigencanceling method. The-eight element array with three interferers chosen at 20°, 23° and 35°. All the interferers' power were taken to be 1 and the noise power was 0.1.

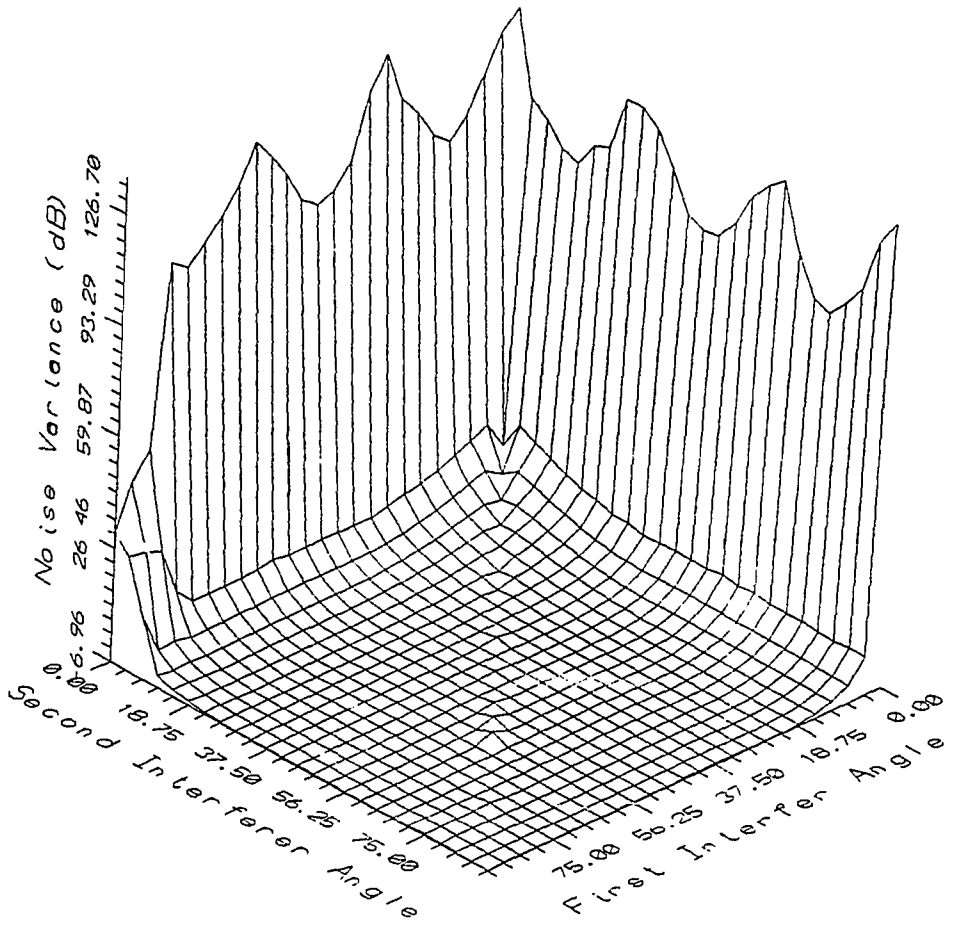

Figure 29 The NMNVV for the URA-5 with two interferers using eigencanceling method and (σ^2, p_1, p_2) =(1,100,10).

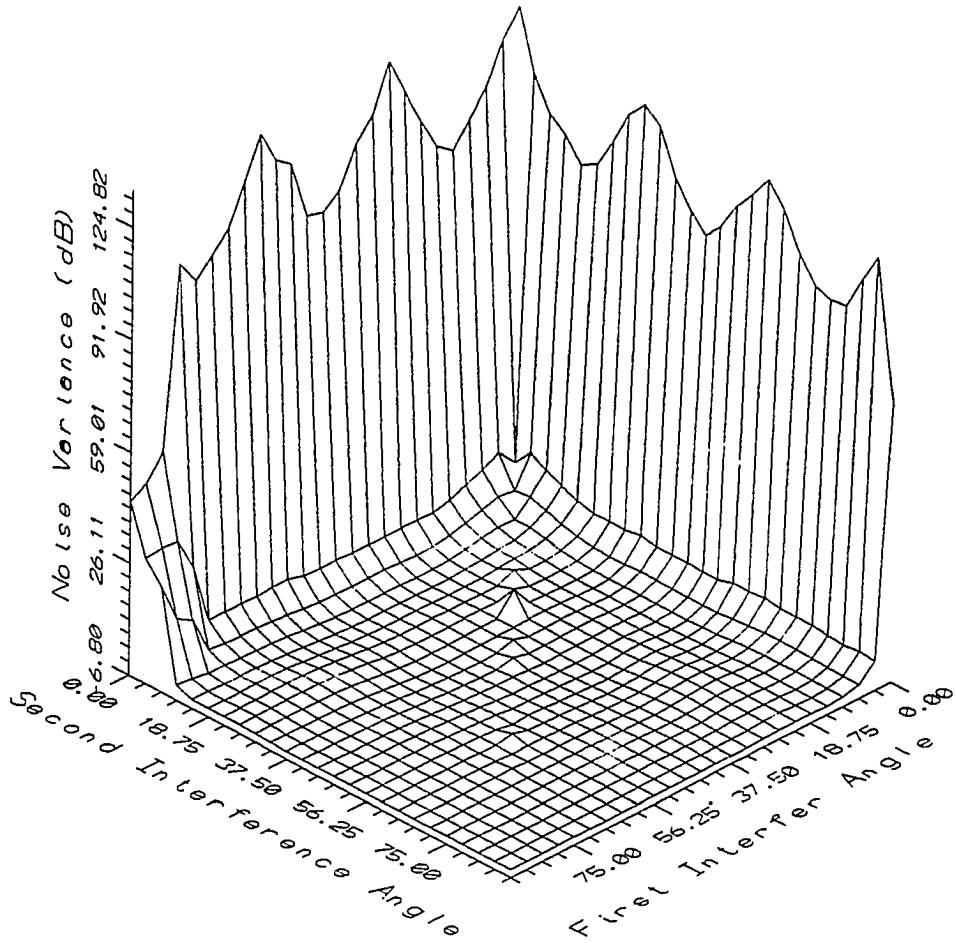

Figure 30 The NMNVV for the MRA-5 with two interferers using eigencanceling method and (σ^2, p_1, p_2) =(1,100,10).

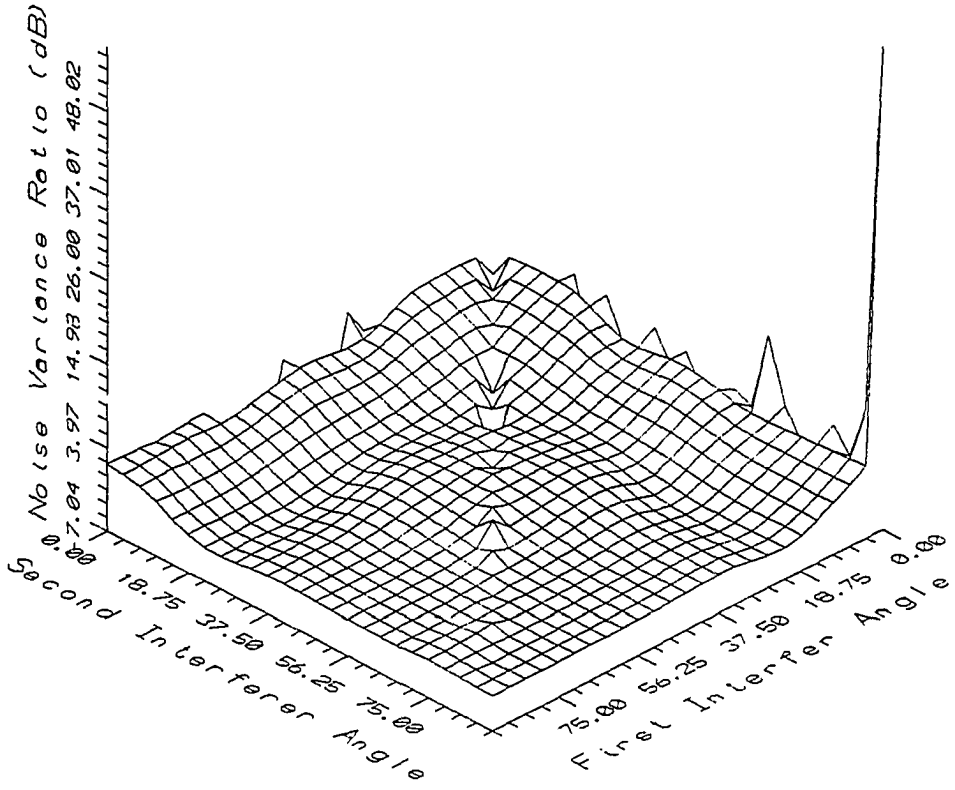

Figure 31 The NMNVV ratio of the URA-5 and the MRA-5 with two interferers using eigencanceling method and (σ^2, p_1, p_2) =(1,100,10).

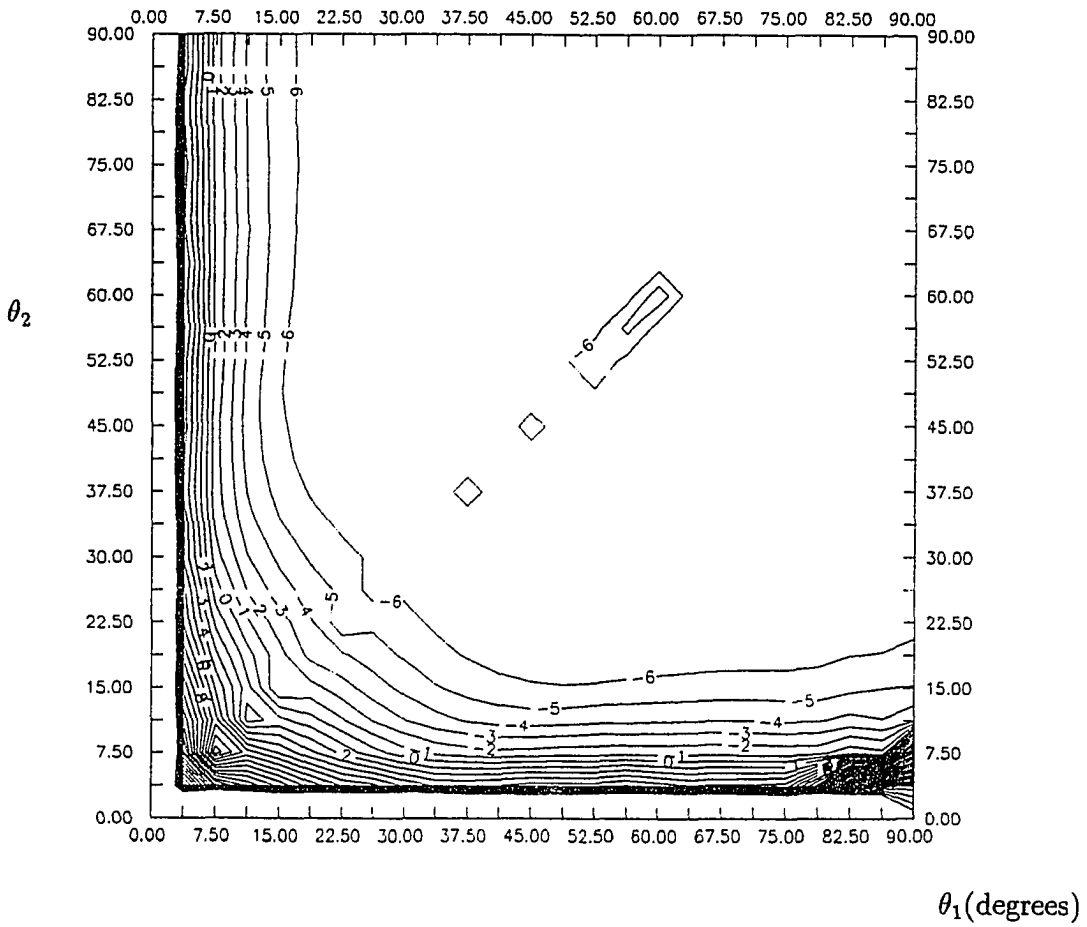

Figure 32 Contour plot of the NMNVV for the URA-5 with two interferers using eigencanceling method and (σ^2, p_1, p_2) =(1,100,10). The x axis is the first interferer angle, and the y axis is the second interferer angle.

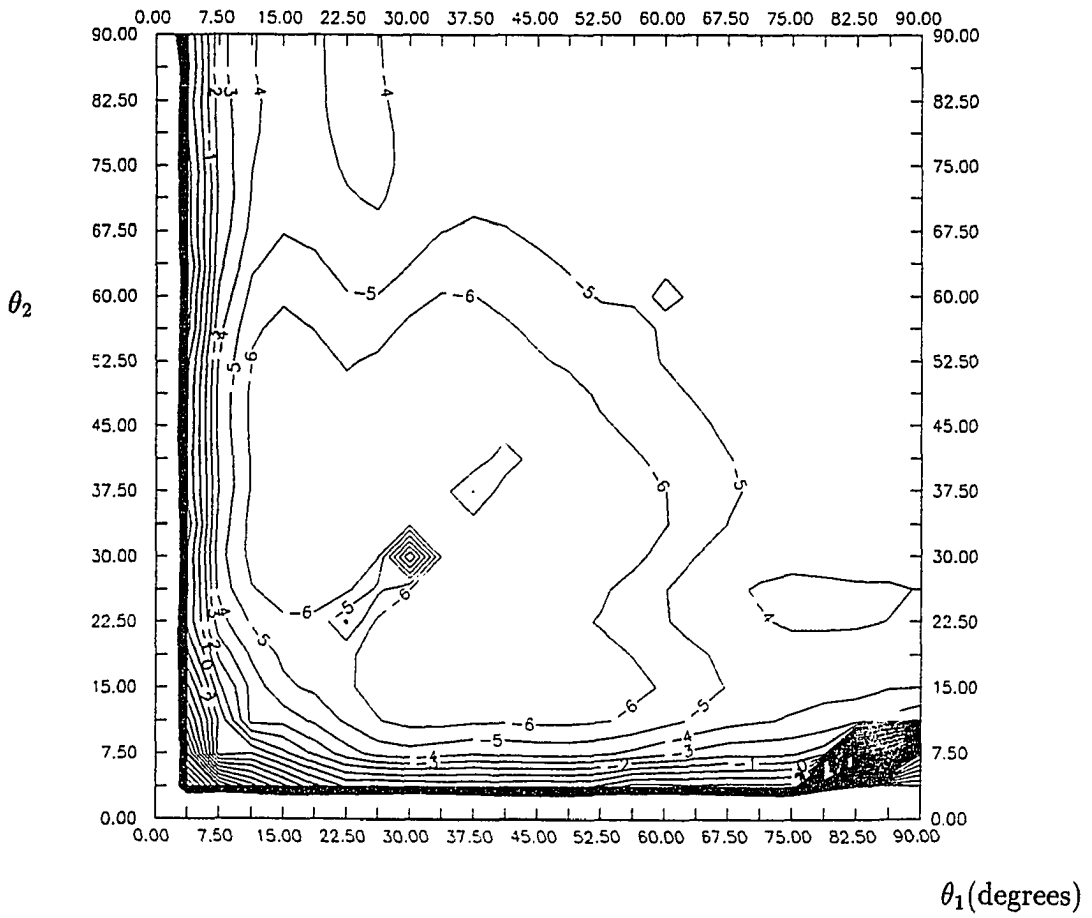

Figure 33 Contour plot of the NMNVV for the MRA-5 with two interferers using eigencanceling method and (σ^2, p_1, p_2) =(1,100,10). The x axis is the first interferer angle, and the y axis is the second interferer angle.

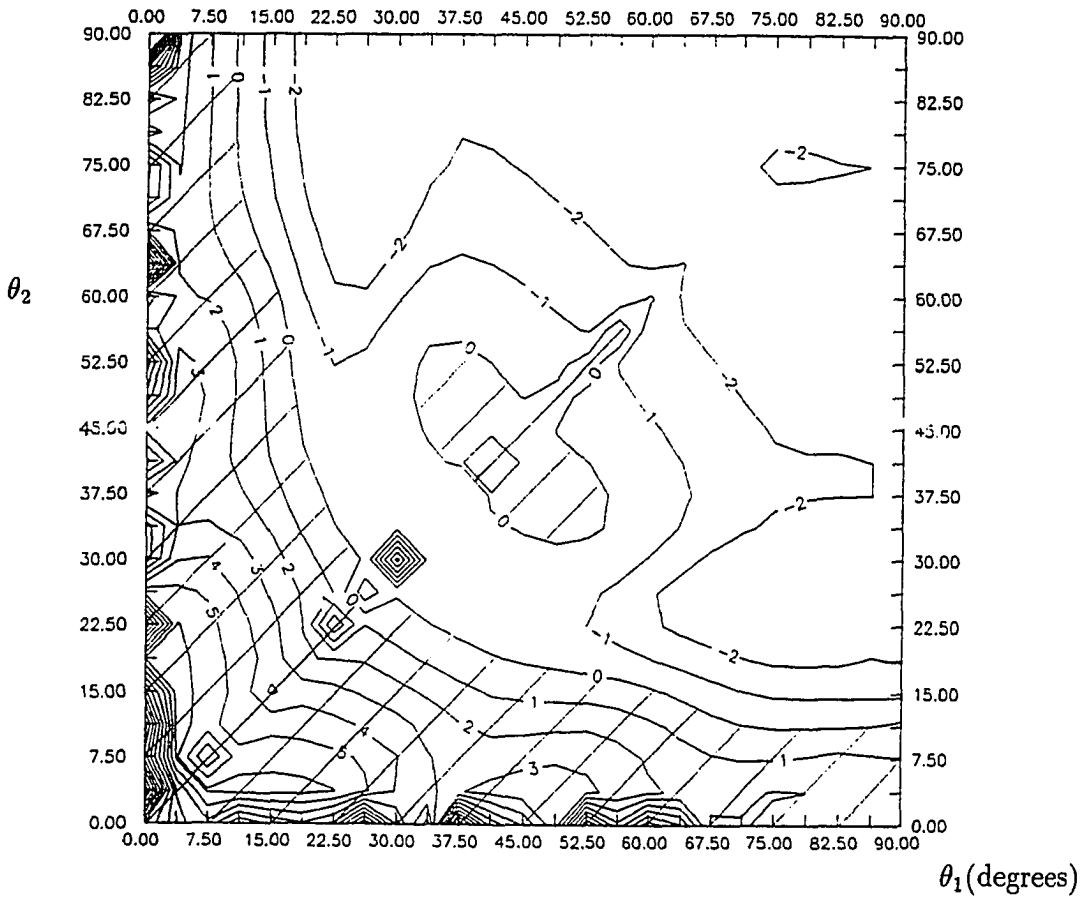

Figure 34 Contour plot of the NMNVV ratio of the URA-5 and the MRA-5 with two interferers using eigencanceling method and (σ^2, p_1, p_2) =(1,100,10). The x axis is the first interferer angle, and the y axis is the second interferer angle. The shaded region indicates where the MRA-5 outperforms the URA-5 with eigencanceling method.

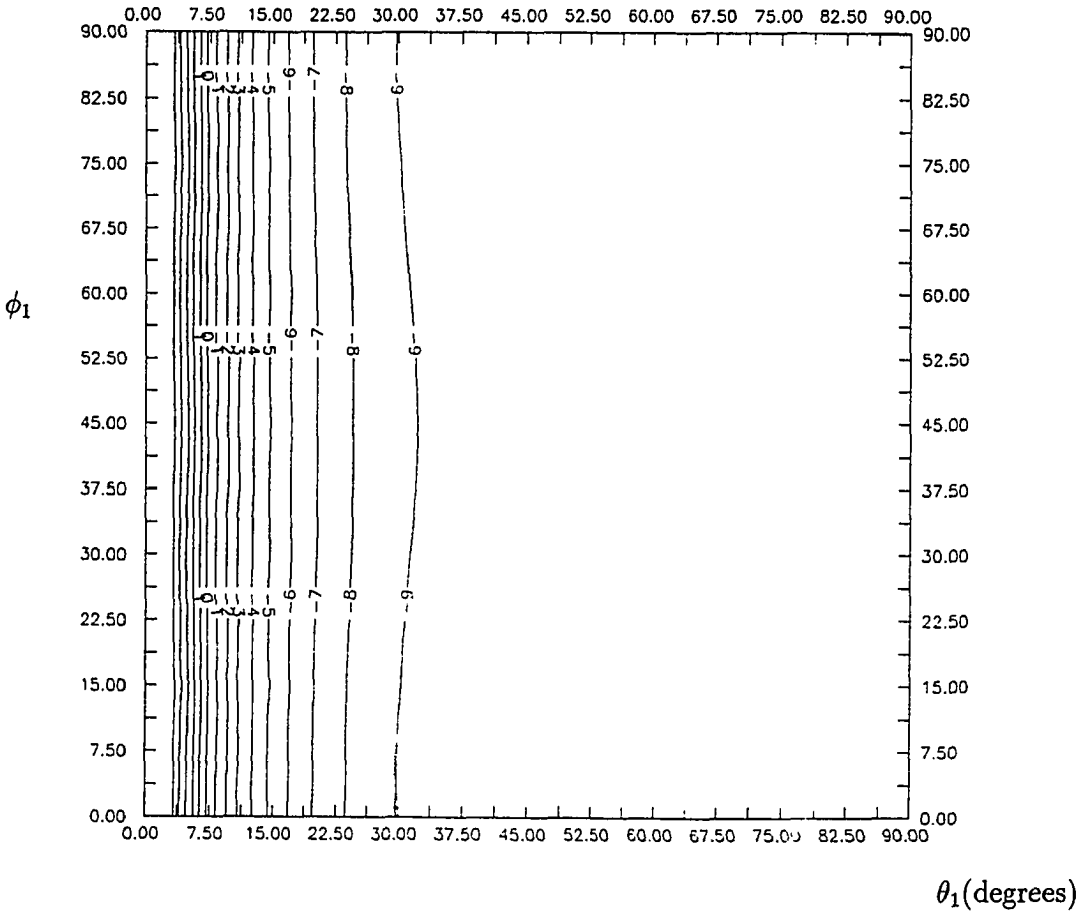

Figure 35 Contour plot of the MNVV for the URA-3 square array with single interferer using the conventional beamforming method and (σ^2, p_1) =(1,10). The x axis is bearing angle θ_1, and the y axis is the elevation angle ϕ_1.

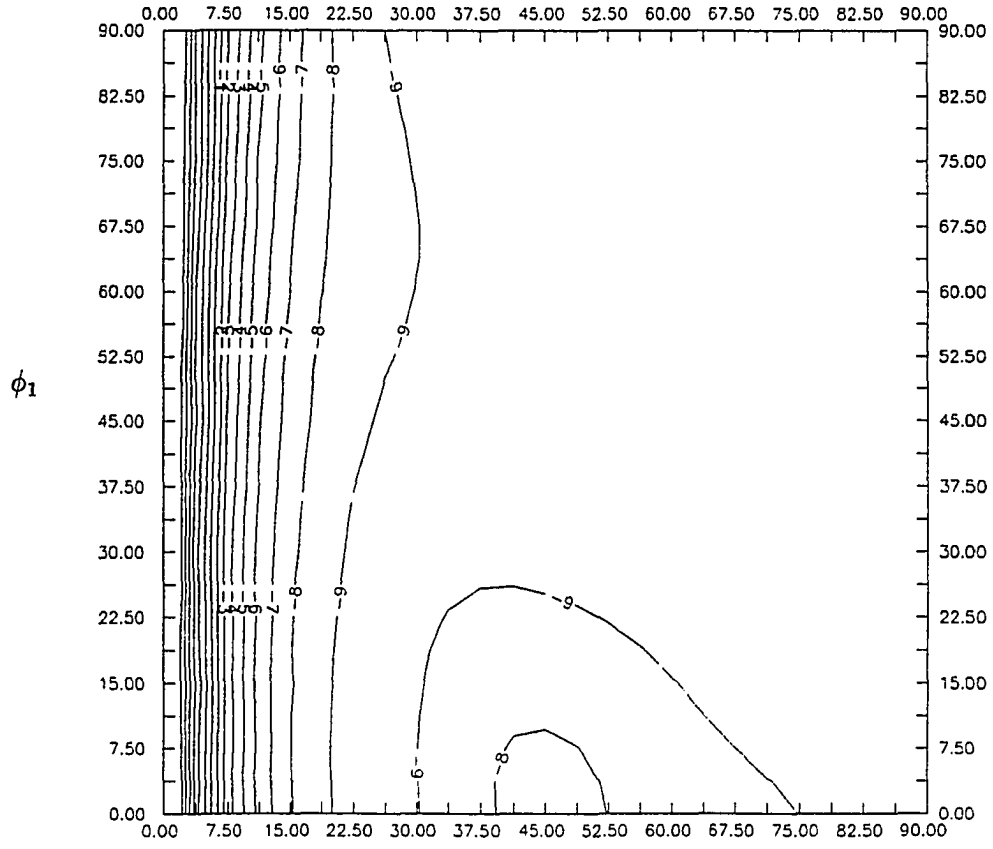

Figure 36 Contour plot of the MNVV for the MRA-3 square array with single interferer using the conventional beamforming method and (σ^2, p_1) =(1,10). The x axis is bearing angle θ_1, and the y axis is the elevation angle ϕ_1.

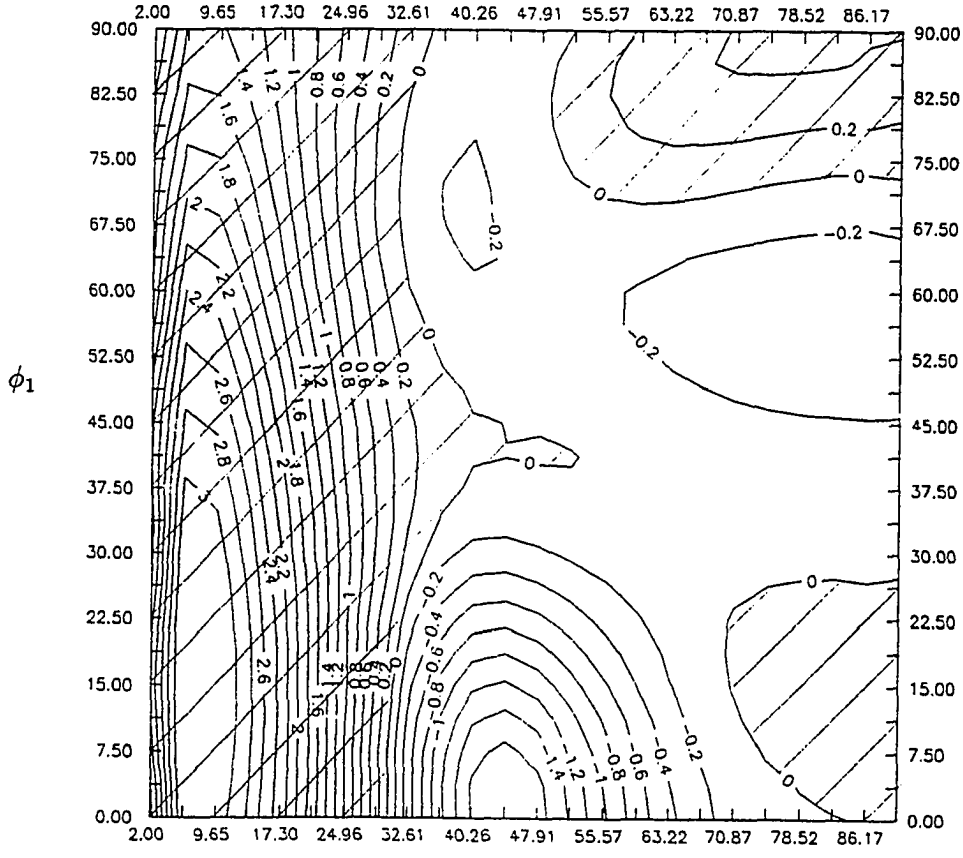

Figure 37 Contour plot of the MNVV ratio for the URA-3 and the MRA-3 square array with single interferer using the conventional beamforming method and (σ^2, p_1)= (1,10). The x axis is bearing angle θ_1, and the y axis is the elevation angle ϕ_1. The zero dB line marks the shaded region for the MRA to outperform the URA.

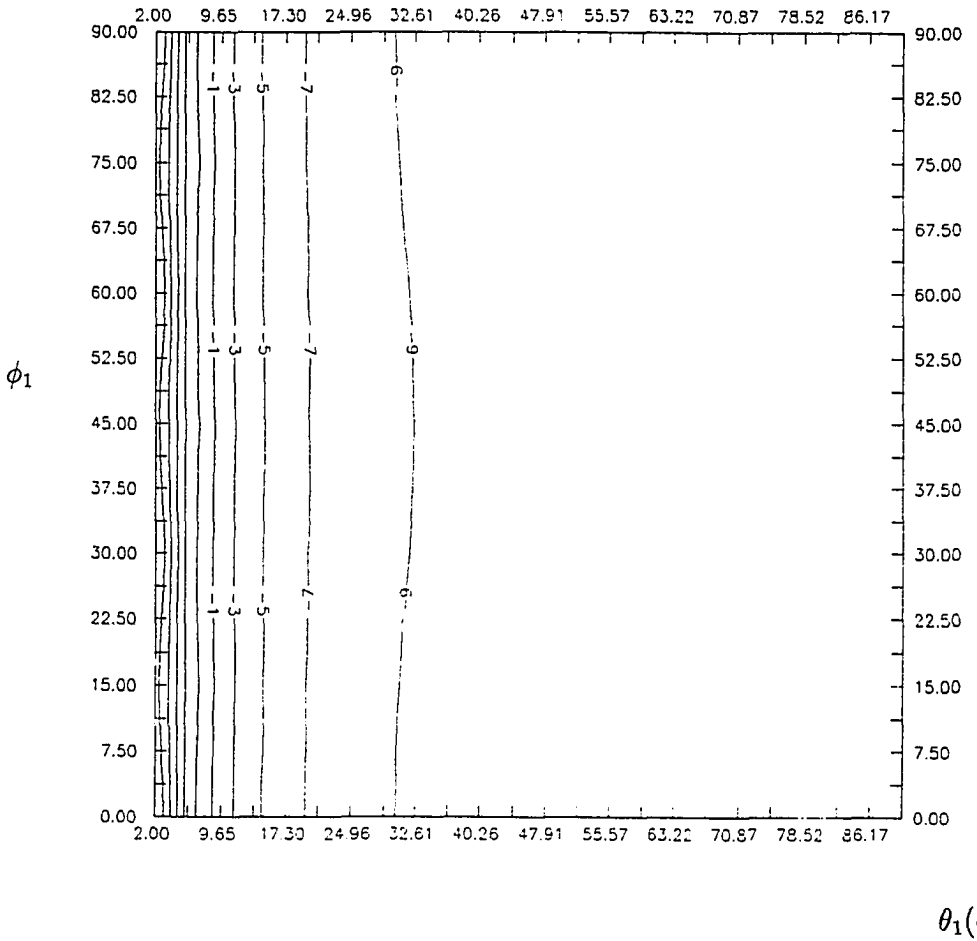

Figure 38 Contour plot of the MNVV for the URA-3 square array with single interferer using eigencanceling method and (σ^2, p_1) =(1,10). The x axis is bearing angle θ_1, and the y axis is the elevation angle ϕ_1.

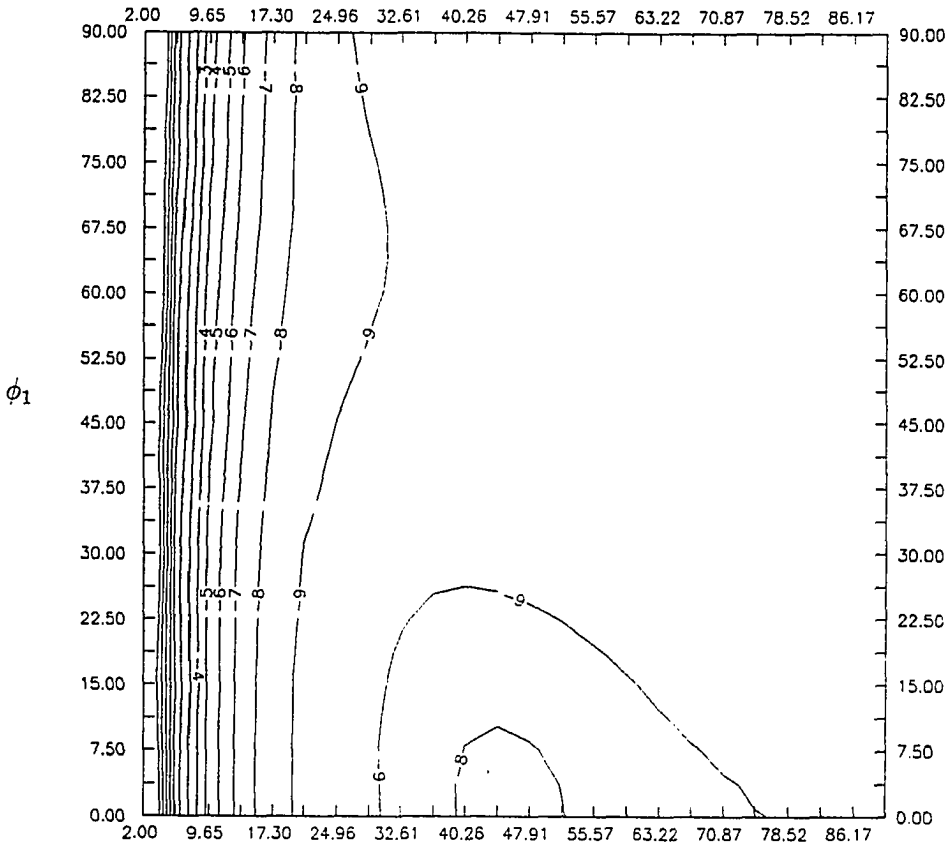

Figure 39 Contour plot of the MNVV for the MRA-3 square array with single interferer using eigencanceling method and (σ^2, p_1) =(1,10). The x axis is bearing angle θ_1, and the y axis is the elevation angle ϕ_1.

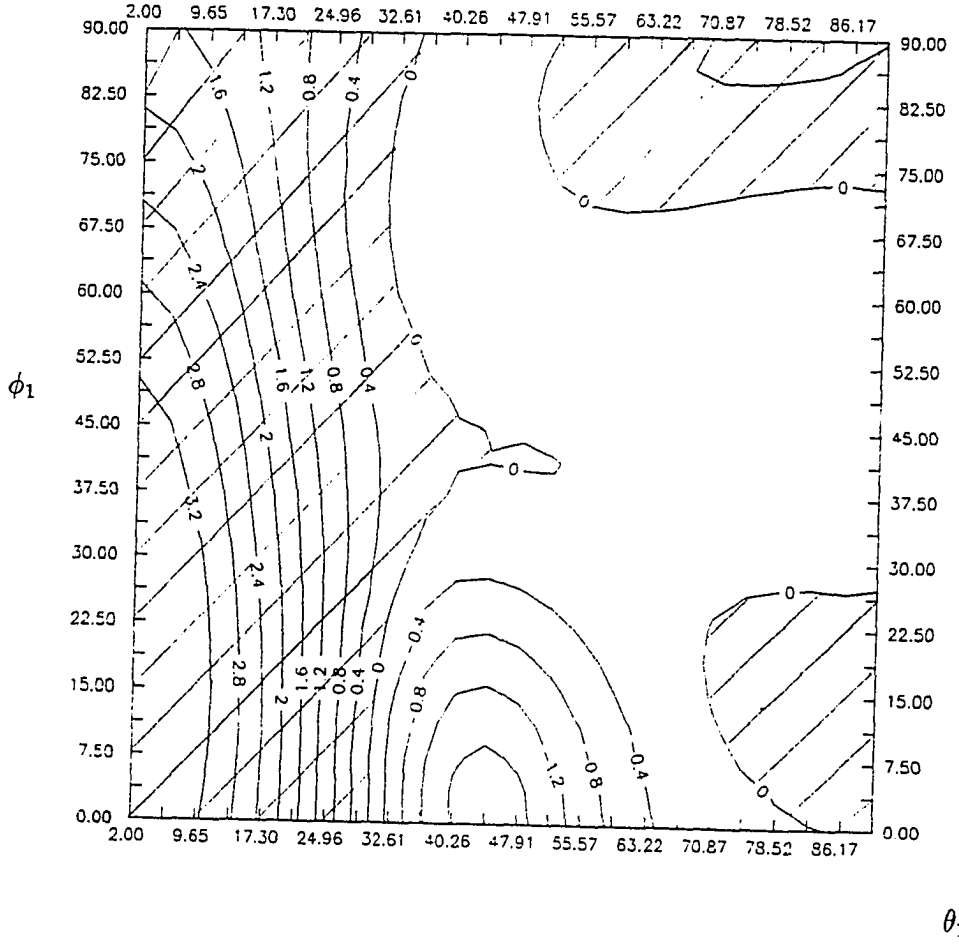

Figure 40 Contour plot of the MNVV ratio for the URA-3 and the MRA-3 square array with single interferer using eigencanceling method and (σ^2, p_1) =(1,10). The x axis is bearing angle θ_1, and the y axis is the elevation angle ϕ_1. If this figure was overlaid on Figure 37, one can see that the zero dB line marks the region for the MRA to outperform the URA are exactly the same.

CHAPTER 6

CONCLUSIONS

The assessment of the Minimum Redundancy Array (MRA) structure for interference cancellation is the goal of this work. Chapter 1 described the special structure of the MRA and listed all the configurations for a given number of array elements (up to 11) to achieve maximum aperture with consecutive correlation lags. Previous applications using MRAs were mainly limited to direction finding. We expanded it to interference cancellation for the linear and planar array cases. The eigencanceling technique was applied to the Uniform Regular Array (URA) structure for interference cancellation before, and the results were quite remarkable — it had total interference cancellation ability, fast convergence rate, and immunity to the interference-to-noise power ratio. The MRA structure for interference cancellation is evaluated using both the conventional beamforming and the eigencanceling methods.

In Chapter 2, the system model was defined with the assumption that the desired signal was previously removed, as in many radar applications, the interferers were narrow-band and uncorrelated. In this case, the Minimum Noise Variance (MNV) criterion was chosen as the performance measure. Directional constraints were imposed on the array pattern to prevent the array from creating nulls in the directions of the desired signals. Due to the structure of the MRAs, the traditionally used augmented autocorrelation matrix for direction finding was considered first. It was found that only the original nonaugmented autocorrelation matrix was necessary for the interference cancellation application. With this discovery, the actual amount of data being processed and the dimension of the autocorrelation matrix that was required for the eigenvector finding and inversion was greatly reduced. The ground work for the formulation of the optimization problem for conventional beamforming

and eigencanceling methods was presented. An efficient recursive formula for the inverse of the autocorrelation matrix was derived to compute the Minimum Noise Variance value (MNVV). The MNVV was obtained when the optimum weight was applied to the process using the MNV criterion. Notice that the number of detectable interferers could be increased by using the augmented autocorrelation matrix for the MRA. However, the number of interferers that can be cancelled is identical to that of the URA with the same number of array elements.

Both the conventional beamforming and eigencanceling methods were applied in Chapter 3 to evaluate the noise variance performance of the MRA structure. The performance was compared to the URA structure with the same number of elements and the URA with the same aperture. Closed-form expressions for the optimal weight vector and noise variance were obtained for both array structures as a function of the number of array elements, the direction of the interferers, and their power-to-noise ratio. The three- and four-element array examples were given to gain a basic understanding of the MRA structure using different interference cancellation techniques. In the last section of Chapter 3, the eigenvalue spread for the dual-interferers case was discussed to explore the effect of the MRA structure when compared to the URA structure with the same number of array elements. The numerical example of the three-element array indicated that spreading the URA elements to the MRA locations does not increase the eigenvalue spread. That is, when the MRA structure was exposed to the same environment as the URA with the same number of array elements, the convergence rate to the optimum weight vector remained about the same. This is a great advantage when compared to the MRA augmented autocorrelation matrix. However, the MRA structure does require twice as many samples to achieve the same result as the URA structure. The case of more than two interferers using the eigencanceling technique is quite difficult in terms of analysis. Nevertheless, a

recursive formula for the inverse of the correlation matrix was described in Chapter 3.

Chapter 4 presented a special approach to analyze the performance of the MRA structure. There exists a matrix to transform the eigenspace of the URA to the eigenspace of the MRA. This transformation matrix was quite valuable when calculating the MNVV for the MRA with the eigencanceling technique. It provided a computational shortcut by enabling us to use the existing URA noise subspace structure to obtain the MNVV of the MRA when using the eigencanceling method. It was also discovered that in order to obtain the MNVVs of both the URA and MRA structures when using the eigencanceling method, one could set the noise-to-interference power to zero in the conventional beamforming method. This again confirmed that the eigencanceling method is independent of the interference-to-noise power ratio.

In Chapter 5 the numerical results of all the formulas derived in Chapter 2 were evaluated and discussed. The MRA structure performed better than the URA structure for interferers very close to the direction of arrival of the desired signal, deep into the main beam region. This was shown both in applying conventional beamforming and eigencanceling techniques. This result was expected since the MRA structure has a much larger aperture when compared to the URA with the same number of array elements. In the main beam region, (close to the direction of arrival of the desired signal), the depth of interference cancellation was almost equal to that obtained from the URA with the same aperture, whose number of elements is much larger. For an interferer impinging on the array in the sidelobe region (away from the direction of the desired signal), the depth of cancellation for the MRA is slightly less than that of the URA with the same number of array elements. But the difference in cancellation depth of the two structures is very small when compared to their

absolute cancellation depths in this sidelobe region.

The numerical results of the dual-interferer cases were also included in Chapter 5 for the conventional beamforming and eigencanceling methods. A performance comparison was done numerically by computer. Three-dimensional plots and their contours also provided better insight about the dual-interferer case. The region for an MRA to perform better than a URA was changed when different cancellation techniques were applied. The numerical results of the square array structure were also included in the last section of Chapter 5. For the single interferer case, the boundary for an MRA to perform better than a URA remains unchanged regardless of the cancellation method used.

Only conventional beamforming and eigencanceling techniques were examined to gain an understanding of the interference cancellation ability of the MRA structure. There are different eigen-based interference cancellation techniques that could be tested on the MRA structure. The transformation matrix between the URA and the MRA eigenspaces for the multiple-interferer case is another problem to look into. The reaction of the MRA to correlated interferers also needs to be addressed. The effect of array element dislocation or element malfunction can be analyzed in terms of performance degradation. An adaptive algorithm may be developed for on-line processing purposes. The potential of the MRA square planar array structure for interference cancellation or is worthy of future investigation. The ability of resolving closely spaced interferers using the MRA structure should be of special interest in the future.

In conclusion, the MRA structure performs better as an interference canceler than the URA for almost all conditions of uncorrelated interference scenarios. Es-

pecially in the main beam region (due to its large aperture), the performance of an MRA follows closely that of a URA with the same aperture. The convergence rate is the same for an MRA and a URA with the same number of array elements using the conventional beamforming. When the eigencanceling technique is applied, the MRA seems to converge even faster than the URA structure experimentally. Another advantage of the MRA structure is that it provides more flexibility in placing the array elements. For a given number of array elements, the MRA structure achieves better interference cancellation than the URA structure.

APPENDIX A

CALCULATIONS RELATED TO THE BEAMFORMING TECHNIQUE

[A-1] Derivation of Equation (2.29)

From Eq. (2.28) we can write

$$\begin{aligned}
\mathbf{R}_i^{-1} &= \mathbf{R}_{i-1}^{-1}\left[\mathbf{I}_N - \frac{p_i\mathbf{d}_i\mathbf{d}_i^H\mathbf{R}_{i-1}^{-1}}{1+p_i\mathbf{d}_i^H\mathbf{R}_{i-1}^{-1}\mathbf{d}_i}\right] \\
&= \mathbf{R}_{i-1}^{-1}\left[\frac{(1+p_i\mathbf{d}_i^H\mathbf{R}_{i-1}^{-1}\mathbf{d}_i)\mathbf{I}_N - p_i\mathbf{d}_i\mathbf{d}_i^H\mathbf{R}_{i-1}^{-1}}{1+p_i\mathbf{d}_i^H\mathbf{R}_{i-1}^{-1}\mathbf{d}_i}\right] \\
&= \mathbf{R}_{i-1}^{-1}\left[\frac{(1+p_i\mathbf{d}_i^H\mathbf{R}_{i-1}^{-1}\mathbf{d}_i)\mathbf{R}_{i-1} - p_i\mathbf{d}_i\mathbf{d}_i^H}{1+p_i\mathbf{d}_i^H\mathbf{R}_{i-1}^{-1}\mathbf{d}_i}\right]\mathbf{R}_{i-1}^{-1} \\
&= \mathbf{R}_{i-1}^{-1}\left[\frac{(2+p_i\mathbf{d}_i^H\mathbf{R}_{i-1}^{-1}\mathbf{d}_i)\mathbf{R}_{i-1} - \mathbf{R}_i}{1+p_i\mathbf{d}_i^H\mathbf{R}_{i-1}^{-1}\mathbf{d}_i}\right]\mathbf{R}_{i-1}^{-1}, \qquad \text{(A.1)}
\end{aligned}$$

where in the last step we used

$$\mathbf{R}_i = \mathbf{R}_{i-1} + p_i\mathbf{d}_i\mathbf{d}_i^H. \qquad \text{(A.2)}$$

[A-2] Derivation of Equation (2.33)

Substituting for $\mathbf{R}_0$ from Eq. (2.31) into Eq. (2.30) we get

$$\begin{aligned}
\mathbf{R}_1^{-1} &= \frac{1}{\sigma^2}\left[\frac{(2+(p_1/\sigma^2)N)\sigma^2\mathbf{I}_N - \mathbf{R}_1}{1+(p_1/\sigma^2)N}\right]\frac{1}{\sigma^2} \\
&= \frac{p_1}{\sigma^4}\left[\frac{(2+N/\gamma_1)\gamma_1\mathbf{I}_N - \mathbf{R}_1/p_1}{1+N/\gamma_1}\right]
\end{aligned}$$

where

$$\frac{p_1}{\sigma^2} = \frac{1}{\gamma_1}. \qquad \text{(A.3)}$$

Therefore,

$$\mathbf{R}_1^{-1} = \frac{(2\gamma_1+N)\mathbf{I}_N - \mathbf{R}_1/p_1}{p_1\gamma_1(\gamma_1+N)}. \qquad \text{(A.4)}$$

[A-3] Derivation of Equation (2.35)

From Eq. (2.33)

$$\mathbf{R}_1^{-1} = \sigma^{-2}\left[\mathbf{I} - \frac{\mathbf{d}_1\mathbf{d}_1^H}{\gamma_1 + N}\right], \tag{A.5}$$

therefore,

$$\begin{aligned}\mathbf{d}_2^H\mathbf{R}_1^{-1}\mathbf{d}_2 &= \frac{\mathbf{d}_2^H}{\sigma^2}\left[\mathbf{I} - \frac{\mathbf{d}_1\mathbf{d}_1^H}{\gamma_1 + N}\right]\mathbf{d}_2 \\ &= \sigma^{-2}\left[N - \frac{|\,\mathbf{d}_2^H\mathbf{d}_1\,|^2}{\gamma_1 + N}\right] \\ &= \sigma^{-2}\left[\frac{N(\gamma_1 + N) - |\,\mathbf{d}_2^H\mathbf{d}_1\,|^2}{\gamma_1 + N}\right].\end{aligned} \tag{A.6}$$

Thus,

$$1 + p_2\mathbf{d}_2^H\mathbf{R}_1^{-1}\mathbf{d}_2 = \frac{(\gamma_1 + N)(\gamma_2 + N) - |\,\mathbf{d}_2^H\mathbf{d}_1\,|^2}{\gamma_2(\gamma_1 + N)} \tag{A.7}$$

where $\gamma_2 = \sigma^2/p_2$.

Also by Eq. (A.5)

$$\mathbf{R}_1^{-1}\mathbf{d}_2 = \sigma^{-2}\left[\mathbf{d}_2 - \frac{(\mathbf{d}_1^H\mathbf{d}_2)\mathbf{d}_1}{\gamma_1 + N}\right] \tag{A.8}$$

$$\begin{aligned}\mathbf{R}_1^{-1}\mathbf{d}_2\mathbf{d}_2^H\mathbf{R}_1^{-1} &= \sigma^{-4}\left[\mathbf{d}_2 - \frac{(\mathbf{d}_1^H\mathbf{d}_2)\mathbf{d}_1}{\gamma_1 + N}\right]\left[\mathbf{d}_2^H - \frac{(\mathbf{d}_2^H\mathbf{d}_1)\mathbf{d}_1^H}{\gamma_1 + N}\right] \\ &= \sigma^{-4}\left[\mathbf{d}_2\mathbf{d}_2^H + \frac{|\,\mathbf{d}_2^H\mathbf{d}_1\,|^2}{(\gamma_1 + N)^2}\mathbf{d}_1\mathbf{d}_1^H - 2Re\left(\frac{\mathbf{d}_1^H\mathbf{d}_2}{\gamma_1 + N}\mathbf{d}_1\mathbf{d}_2^H\right)\right]\end{aligned}$$

$$p_2\mathbf{R}_1^{-1}\mathbf{d}_2\mathbf{d}_2^H\mathbf{R}_1^{-1} = \frac{1}{\gamma_2\sigma^2}\left[\mathbf{d}_2\mathbf{d}_2^H + \frac{|\,\mathbf{d}_2^H\mathbf{d}_1\,|^2}{(\gamma_1 + N)^2}\mathbf{d}_1\mathbf{d}_1^H - 2Re\left\{\frac{\mathbf{d}_1^H\mathbf{d}_2}{\gamma_1 + N}\mathbf{d}_1\mathbf{d}_2^H\right\}\right] \tag{A.9}$$

Combining Eqs. (A.7) and (A.9) we get

$$\frac{p_2\mathbf{R}_1^{-1}\mathbf{d}_2\mathbf{d}_2^H\mathbf{R}_1^{-1}}{1 + p_2\mathbf{R}_1^{-1}\mathbf{d}_2\mathbf{d}_2^H\mathbf{R}_1^{-1}} = \frac{(\gamma_1 + N)\left[\mathbf{d}_2\mathbf{d}_2^H + \frac{|\mathbf{d}_2^H\mathbf{d}_1|^2}{(\gamma_1+N)^2}\mathbf{d}_1\mathbf{d}_1^H - 2Re\left\{\frac{\mathbf{d}_1^H\mathbf{d}_2}{\gamma_1+N}\mathbf{d}_1\mathbf{d}_2^H\right\}\right]}{\sigma^2[(\gamma_2 + N)(\gamma_1 + N) - |\,\mathbf{d}_2^H\mathbf{d}_1\,|^2]}. \tag{A.10}$$

But

$$\mathbf{R}_1^{-1} = \sigma^{-2}\left[\mathbf{I} - \frac{\mathbf{d}_1\mathbf{d}_1^H}{\gamma_1 + N}\right], \tag{A.11}$$

therefore together with Eq. (A.10) we get,

$$\begin{aligned}
\mathbf{R}_1^{-1} &- \frac{p_2\mathbf{R}_1^{-1}\mathbf{d}_2\mathbf{d}_2^H\mathbf{R}_1^{-1}}{1 + p_2\mathbf{R}_1^{-1}\mathbf{d}_2\mathbf{d}_2^H\mathbf{R}_1^{-1}} \\
&= \sigma^{-2}\left[I - \frac{\mathbf{d}_1\mathbf{d}_1^H}{\gamma_1 + N} - \frac{(\gamma_1 + N)\mathbf{d}_2\mathbf{d}_2^H + \frac{|\mathbf{d}_2^H\mathbf{d}_1|^2}{\gamma_1 + N}\mathbf{d}_1\mathbf{d}_1^H - 2Re\left\{(\mathbf{d}_1^H\mathbf{d}_2)\mathbf{d}_1\mathbf{d}_2^H\right\}}{(\gamma_2 + N)(\gamma_1 + N) - |\,\mathbf{d}_2^H\mathbf{d}_1\,|^2}\right] \\
&= \sigma^{-2}\left[I - \frac{(\gamma_1 + N)\mathbf{d}_2\mathbf{d}_2^H + (\gamma_2 + N)\mathbf{d}_1\mathbf{d}_1^H - 2Re\left\{(\mathbf{d}_1^H\mathbf{d}_2)\mathbf{d}_1\mathbf{d}_2^H\right\}}{(\gamma_2 + N)(\gamma_1 + N) - |\,\mathbf{d}_2^H\mathbf{d}_1\,|^2}\right].
\end{aligned} \tag{A.12}$$

[A-4] Finding the Crossover Point of URA-3 and MRA-3

From Eq. (3.35)

$$\cos 3\omega_1 < \cos\omega_1. \tag{A.13}$$

It can easily be shown that this is equivalent to

$$4\cos\omega_1(\cos\omega_1 + 1)(\cos\omega_1 - 1) < 0. \tag{A.14}$$

For $0 < \omega_1 < \pi/2$,

$$\begin{aligned}
\cos\omega_1 &> 0, \\
\cos\omega_1 + 1 &> 0, \\
\cos\omega_1 - 1 &< 0,
\end{aligned}$$

and the condition of Eq. (A.14) is satisfied.

For $\pi/2 < \omega_1 < \pi$,

$$\begin{aligned} \cos\omega_1 &< 0, \\ \cos\omega_1 + 1 &> 0, \\ \cos\omega_1 - 1 &< 0, \end{aligned}$$

and the reverse inequality of Eq. (A.13) is satisfied.

[A-5] The MNVs of the MRA with Single Interferer

By definition,

$$2\sum_{n=1}^{L-1} e_n \cos n\omega_1 = \sum_{n=0}^{L-1} e_n(e^{jn\omega_1} + e^{-jn\omega_1}) - 2. \tag{A.15}$$

But

$$\sum_{n=0}^{L-1} e^{jn\omega_1} = e^{j(L-1)\omega_1/2}\frac{\sin(\frac{2L-1}{2}\omega_1)}{\sin(\omega_1/2)}. \tag{A.16}$$

Therefore if $e_n = 1$ for all $n = 0, 1, \ldots, L-1$, then

$$\begin{aligned} 2\sum_{n=1}^{L-1} \cos n\omega_1 &= \left[e^{j(\frac{L-1}{2}\omega_1)}\frac{\sin(L\omega_1/2)}{\sin(\omega_1/2)} + c.c.\right] - 2 \\ &= 2\frac{\sin(L\omega_1/2)}{\sin(\omega_1/2)}\cos(\frac{L-1}{2}\omega_1) - 2. \end{aligned}$$

Now, using some trigonometric identities yields,

$$2\sum_{n=1}^{L-1} \cos n\omega_1 = \frac{\sin(\frac{2L-1}{2}\omega_1)}{\sin(\omega_1/2)} - 1. \tag{A.17}$$

[A-6] Derivation of Eqution (3.26)

From Eq. (2.40)

$$\begin{aligned} |\rho|^2 &= \frac{|\mathbf{d}_1^H\mathbf{d}_2|^2}{N^2} \\ &= \frac{\mathbf{d}_1^H\mathbf{d}_2\mathbf{d}_2^H\mathbf{d}_1}{N^2} \\ &= \frac{\text{trace}\left[\mathbf{d}_1\mathbf{d}_1^H\mathbf{d}_2\mathbf{d}_2^H\right]}{N^2}. \end{aligned}$$

Let A be the matrix $\mathbf{d}_1\mathbf{d}_1^H$ with the ones along the main diagonal replaced by zero, similarly B for $\mathbf{d}_2\mathbf{d}_2^H$. Define A_L and B_L to be the lower triangle of A and B, respectively, while A_u and B_u to be the corresponding upper triangle. Therefore

$$\begin{aligned}\text{trace}\,[\mathbf{d}_1\mathbf{d}_1^H\mathbf{d}_2\mathbf{d}_2^H] &= \text{trace}\,[(A_u + A_L + \boldsymbol{\Sigma})(B_u + B_L + \boldsymbol{\Sigma})] \\ &= \text{trace}\,[A_uB_L] + \text{trace}\,[A_LB_u] + \text{trace}\,\boldsymbol{\Sigma}^2\end{aligned}$$

where $\boldsymbol{\Sigma}$ is diagonal of ones. Since $\mathbf{d}_1\mathbf{d}_1^H$ and $\mathbf{d}_2\mathbf{d}_2^H$ are Hermitian, $A_u = A_L^H$ and $B_u = B_L^H$. Also trace$[A_uB_u]$ =trace$[A_LB_L]$=0. Hence,

$$\begin{aligned}\text{trace}\,[\mathbf{d}_1\mathbf{d}_1^H\mathbf{d}_2\mathbf{d}_2^H] &= \text{trace}\,[A_uB_u^H] + \text{trace}\,[A_u^HB_u] + N \\ &= \text{trace}\,[A_uB_u^H] + \text{trace}\,[B_uA_u^H] + N \\ &= \text{trace}\,[A_uB_u^H] + \text{complex conjugate} + N.\end{aligned}$$

Therefore,

$$|\,\rho\,|^2 = \frac{1}{N^2}\left(N + 2\sum_{n=1}^{L-1} e_n \cos n(\omega_1 - \omega_2)\right). \tag{A.18}$$

[A-7] Derivation for Equation (3.28)

By definition,

$$\rho\|\mathbf{d}_1\mathbf{d}_2^H\| = \rho(\mathbf{1}^T\mathbf{d}_1)(\mathbf{d}_2^H\mathbf{1}). \tag{A.19}$$

From Eqs. (3.24) and (3.15)

$$\begin{aligned}\rho &= \frac{1}{N}e^{j\frac{N-1}{2}(\omega_1-\omega_2)}\frac{\sin(N(\omega_1-\omega_2)/2)}{\sin((\omega_1-\omega_2)/2)}, \\ \mathbf{1}^T\mathbf{d}_1 &= e^{-j\frac{N-1}{2}\omega_1}\frac{\sin(N\omega_1/2)}{\sin(\omega_1/2)}, \\ \mathbf{d}_2^H\mathbf{1} &= e^{j\frac{N-1}{2}\omega_2}\frac{\sin(N\omega_2/2)}{\sin(\omega_2/2)}.\end{aligned}$$

Therefore,

$$\rho\|\mathbf{d}_1\mathbf{d}_2^H\| = \frac{1}{N}\frac{\sin(N\omega_1/2)}{\sin(\omega_1/2)}\frac{\sin(N\omega_2/2)}{\sin(\omega_2/2)}\frac{\sin(N(\omega_1-\omega_2)/2)}{\sin(\omega_1-\omega_2)/2}. \tag{A.20}$$

APPENDIX B

CALCULATIONS RELATED TO EIGENCANCELING TECHNIQUE

[B-1] Determination of the Eigenvalues of U

Let us first determine the determinant of the matrix $\Delta_{N-1}(\lambda) = \mid \mathbf{U} - \lambda\mathbf{I} \mid$.

$\Delta_{N-1}(\lambda) =$

$$\begin{bmatrix} 2-\lambda & -e^{ji_1\omega_1} & 0 & \dots & 0 & 0 \\ -e^{-ji_1\omega_1} & 2-\lambda & -e^{j(i_2-i_1)\omega_1} & \dots & 0 & 0 \\ 0 & -e^{-j(i_2-i_1)\omega_1} & 2-\lambda & \dots & 0 & 0 \\ 0 & 0 & -e^{-j(i_3-i_2)\omega_1} & \dots & 0 & 0 \\ \vdots & \vdots & \vdots & \vdots & \vdots & \vdots \\ 0 & 0 & 0 & \dots & -e^{j(i_{N-3}-i_{N-4})\omega_1} & 0 \\ 0 & 0 & 0 & \dots & 2-\lambda & -e^{j(i_{N-2}-i_{N-3})\omega_1} \\ 0 & 0 & 0 & \dots & -e^{-j(i_{N-2}-i_{N-3})\omega_1} & 2-\lambda \end{bmatrix}$$

Expanding this determinant we obtain the following recursion relation:

$$\Delta_n(\lambda) = (2-\lambda)\Delta_{n-1}(\lambda) - \Delta_{n-2}(\lambda), \quad n = 1, 2, \dots, N-1 \tag{B.1}$$

with initial conditions $\Delta_0 = 1, \Delta_1 = 2-\lambda$. Let

$$\lambda - 2 = -2\cos x, \tag{B.2}$$

$$\Delta_n(-2\cos x + 2) = 2\Delta_{n-1}(-2\cos x + 2)\cos x - \Delta_{n-2}(-2\cos x + 2).$$

The equation $\rho^2 = 2\rho\cos x - 1$ has the roots $e^{\pm jx}$ so that

$$\Delta_n(-2\cos x + 2) = Ae^{jnx} + Be^{-jnx} \tag{B.3}$$

where the constants A and B determined from n=0 and n=1 can be shown to equal

$$A = e^{jx}/(e^{jx} - e^{-jx}) \qquad B = -e^{-jx}/(e^{jx} - e^{-jx}).$$

Substituting in equation (B.3) we get,

$$\triangle_n(-2\cos x + 2) = \frac{\sin(n+1)x}{\sin x} = 0, \tag{B.4}$$

the roots are found to be

$$x = \frac{\pi k}{n+1} \quad \text{for} \quad k = 1, 2, ..., n. \tag{B.5}$$

Therefore, the resulting eigenvalues of the matrix **U** can be determined from Eqs. (B.2) and (B.3) with n=N-1,

$$\lambda_k = 2(1 - \cos\frac{\pi k}{N}) = 4\sin^2(\frac{\pi k}{2N}), \quad k = 1, 2, \ldots, N-1 \tag{B.6}$$

This result can also be cited in [48]

[B-2] Determination of the Eigenvectors of U

Let $\mathbf{x}^{(k)}$ be the k-th eigenvector of **U** corresponding to the k-th eigenvalue λ_k. That is

$$\mathbf{U}\mathbf{x}^{(k)} = \lambda_k \mathbf{x}^{(k)}, \quad k = 1, 2, \ldots, N-1 \tag{B.7}$$

where $\mathbf{x}^{(k)} = [\, x_1^{(k)}, x_2^{(k)}, \ldots, x_{N-1}^{(k)} \,]^T$.

Omitting the index k for simplicity, Eq. (B.7) can be expanded as follows:

$$z_1 x_2 = (2 - \lambda)x_1$$

$$
\begin{aligned}
z_2 x_3 &= (2-\lambda)x_2 - z_1^* x_1 \\
&\vdots \quad \vdots \quad \vdots \\
z_n x_{n+1} &= (2-\lambda)x_n - z_{n-1}^* x_{n-1}, \quad n = 1, 2, \ldots, N-1
\end{aligned} \tag{B.8}
$$

where $z_n = e^{j(i_n - i_{n-1})\omega}$, $i_0 = 0$. Clearly from the first equation $x_0 = 0$ and from the last equation $x_N = 0$. Let,

$$x_n = e^{-j i_{n-1}\omega} a_n \tag{B.9}$$

then the Eq. (A.8) can be written in the form

$$a_n^{(k)} = (2 - \lambda_k)a_{n-1} - a_{n-2}. \tag{B.10}$$

For n= 2, 3, ..., N-1 with boundary conditions, a_0=0 and a_N=0. The solution of Eq. (A.10) has the form of Eq. (B.3):

$$
\begin{aligned}
a_n^{(k)}(-2\cos v_k + 2) &= A^{(k)} e^{jnv_k} + B^{(k)} e^{jnv_k} \\
\text{where } 2 - \lambda_k &= 2\cos v_k.
\end{aligned}
$$

For n=0

$$
\begin{aligned}
a_0^{(k)} &= A^{(k)} + B^{(k)} = 0 \\
\Rightarrow B^{(k)} &= -A^{(k)} \\
a_n^{(k)} &= A^{(k)}(e^{jnv_k} - e^{-jnv_k}).
\end{aligned}
$$

For n=N

$$a_N^{(k)} = A(e^{jNv_k} - e^{-jNv_k}) = 0$$

we must require $Nv_k = l\pi \Rightarrow v_k = \pi l/N$, where l is any integer. We can normalize our vectors by requiring their first component is one,*i.e.*,

$$\begin{aligned} a_1^{(k)} &= A^{(k)}(e^{jnv_k} - e^{-jnv_k}) = 1, \\ \Rightarrow A^{(k)} &= \frac{1}{e^{jnv_k} - e^{-jnv_k}}. \end{aligned}$$

Therefore

$$a_n^{(k)} = \frac{\sin nv_k}{\sin v_k} \quad \text{with } n = \frac{\pi l}{N} \tag{B.11}$$

or by substituting the integer k for l in the different vectors we finally obtain

$$a_n^{(k)} = \frac{\sin(n\pi k/N)}{\sin(\pi k/N)}, \quad n = 1, 2, \ldots, N-1 \quad k = 1, 2, \ldots, N-1. \tag{B.12}$$

Substituting in Eq. (A.9) we find the n-th component of the k-th eigenvector to be

$$x_n^{(k)} = e^{-ji_{n-1}\omega_1} \frac{\sin(n\pi k/N)}{\sin(\pi k/N)}, \quad n = 1, 2, \ldots, N-1 \quad k = 1, 2, \ldots, N-1. \tag{B.13}$$

The magnitude of these vectors is given by

$$| \mathbf{x}^{(k)} | = \frac{\sqrt{\sum_{n=1}^{N-1} \sin^2(\pi nk/N)}}{\sin(\pi k/N)}.$$

After normalization by the magnitude we obtain

$$u_n^{(k)} = e^{-ji_{n-1}\omega_1} \frac{\sin(n\pi k/N)}{\sqrt{\sum_{n=1}^{N-1} \sin^2(\pi nk/N)}}. \tag{B.14}$$

[B-3] Determination of $\mathbf{u}^{(n)^H}\mathbf{a}$

From Eqs. (3.55) and (3.57) together with Eq. (3.61) we get

$$\mathbf{a}^T = [(-1+e^{ji_1\omega_1}),(-1+e^{j(i_2-i_1)\omega_1}),\ldots,(-1+e^{j(i_{N-1}-i_{N-2})\omega_1})]$$

and with Eq. (3.64)

$$\begin{aligned}\mathbf{u}^{(n)^H}\mathbf{a} &= \sum_{k=1}^{N-1}(-1+e^{j(i_k-i_{k-1})\omega_1})e^{ji_{k-1}}\frac{\sin(n\pi k/N)}{\sqrt{\sum_{n=1}^{N-1}\sin^2(\pi nk/N)}} \\ &= \sum_{k=1}^{N-1}(e^{ji_k\omega_1}-e^{ji_{k-1}\omega_1})\frac{\sin(n\pi k/N)}{\sqrt{\sum_{n=1}^{N-1}\sin^2(\pi nk/N)}}. \qquad \text{(B.15)}\end{aligned}$$

[B-4] Derivation for Equation (3.67)

From Eq. (3.65) we can write

$$\sum_{n=1}^{N-1}P_n\left[\sum_{l=1}^{N-1}Q_{nl}(e^{ji_l\omega_1}-e^{ji_{l-1}\omega_1})\right]\left[\sum_{k=1}^{N-1}Q_{nk}(e^{ji_k\omega_1}-e^{ji_{k-1}\omega_1})\right]$$

$$\begin{aligned}= \sum_{n=1}^{N-1}P_n \;\{\; &\sum_{l=1}^{N-1}Q_{nl}(e^{ji_l\omega_1}-e^{ji_{l-1}\omega_1}) \\ &[\;\sum_{k=1}^{l-1}Q_{nk}(e^{ji_k\omega_1}-e^{ji_{k-1}\omega_1}) \\ &+\sum_{k=l+1}^{N-1}Q_{nk}(e^{ji_k\omega_1}-e^{ji_{k-1}\omega_1}) \\ &+ Q_{nl}(e^{ji_l\omega_1}-e^{ji_{l-1}\omega_1})]\}.\end{aligned}$$

But

$$\begin{aligned}&\sum_{l=1}^{N-1}\sum_{k=1}^{l-1}Q_{nl}Q_{nk}(e^{ji_l\omega_1}-e^{ji_{l-1}\omega_1})(e^{ji_k\omega_1}-e^{ji_{k-1}\omega_1}) \\ &\quad=\sum_{k=1}^{N-1}\sum_{l=k+1}^{N-1}Q_{nl}Q_{nk}(e^{ji_l\omega_1}-e^{ji_{l-1}\omega_1})(e^{ji_k\omega_1}-e^{ji_{k-1}\omega_1}).\end{aligned}$$

By exchanging indices k and l, we get

$$\sum_{l=1}^{N-1}\sum_{k=l+1}^{N-1} Q_{nk}Q_{nl}(e^{ji_k\omega_1} - e^{ji_{k-1}\omega_1})(e^{ji_l\omega_1} - e^{ji_{l-1}\omega_1}).$$

Notice that this is the complex conjugate of the second term. Hence equation (3.56) is equivalent to

$$\begin{aligned}\sum_{n=1}^{N-1} P_n \quad \{ \quad & \sum_{l=1}^{N-1}\sum_{k=l+1}^{N-1} [Q_{nl}Q_{nk}(e^{ji_l\omega_1} - e^{ji_{l-1}\omega_1})(e^{ji_k\omega_1} - e^{ji_{k-1}\omega_1}) \\ + \quad & \text{complex conjugate}] + Q_{nl}Q_{nl} \mid e^{ji_l\omega_1} - e^{ji_{l-1}\omega_1} \mid^2\}. \qquad \text{(B.16)}\end{aligned}$$

[B-5] Determination of a_n

From Eqs. (3.80) and (3.85)

$$a_n = -p_n^* + q_n^* p_{n+1} = \frac{\xi}{\Delta_{n+1}\Delta_n^*},$$

where from Eq. (3.76) we get

$$\begin{aligned}\Delta_{n+1}\Delta_n^* = \quad & [z_1(i_{n+2})z_2(i_{n+3}) - z_1(i_{n+3})z_2(i_{n+2})] \\ \times \quad & [z_1^*(i_{n+1})z_2^*(i_{n+2}) - z_1^*(i_{n+2})z_2^*(i_{n+1})],\end{aligned}$$

Using the fact that $z_1(i_n) = e^{j\omega_1 i_n}$ and $z_2(i_n) = e^{j\omega_2 i_n}$, this can be arranged in the form;

$$\Delta_{n+1}\Delta_n^* = -[z_1(i_{n+3}-i_{n+2}) - z_2(i_{n+3}-i_{n+2})][z_1(i_{n+2}-i_{n+1}) - z_2(i_{n+2}-i_{n+1})]. \quad \text{(B.17)}$$

Also by using Eqs. (3.75) and (3.74)

$$\begin{aligned}\xi = \quad - \quad & \{[z_1(i_{n+2})z_2(i_{n+3}) - z_1(i_{n+3})z_2(i_{n+2})] \\ \times \quad & [z_1^*(i_n)z_2^*(i_{n+2}) - z_2^*(i_n)z_1^*(i_{n+2})]\} \\ + \quad & \{[-z_1^*(i_n)z_2^*(i_{n+1}) + z_2^*(i_n)z_1^*(i_{n+1})] \\ \times \quad & [z_1(i_{n+1})z_2(i_{n+3}) - z_2(i_{n+1})z_1(i_{n+3})]\}\end{aligned}$$

$$
\begin{aligned}
= \; - \; & z_1(i_{n+2})z_2(i_{n+3})z_1^*(i_n)z_2^*(i_{n+2}) + z_1(i_{n+2})z_2(i_{n+3})z_2^*(i_n)z_1^*(i_{n+2}) \\
+ \; & z_1(i_{n+3})z_2(i_{n+2})z_1^*(i_n)z_2^*(i_{n+2}) - z_1(i_{n+3})z_2(i_{n+2})z_2^*(i_n)z_1^*(i_{n+2}) \\
- \; & z_1^*(i_n)z_2^*(i_{n+1})z_1(i_{n+1})z_2(i_{n+3}) + z_1^*(i_n)z_2^*(i_{n+1})z_2(i_{n+1})z_1(i_{n+3}) \\
+ \; & z_2^*(i_n)z_1^*(i_{n+1})z_1(i_{n+1})z_2(i_{n+3}) - z_2^*(i_n)z_1^*(i_{n+1})z_2(i_{n+1})z_1(i_{n+3}).
\end{aligned}
$$

Again due to the definition of $z_1(i_n)$ and $z_2(i_n)$ we can change the second, third, sixth and seventh terms above and get

$$
\begin{aligned}
\xi = \; - \; & z_1(i_{n+2})z_2(i_{n+3})z_1^*(i_n)z_2^*(i_{n+2}) + z_2(i_{n+1})z_2(i_{n+3})z_2^*(i_n)z_2^*(i_{n+1}) \\
+ \; & z_1(i_{n+3})z_1(i_{n+1})z_1^*(i_n)z_1^*(i_{n+1}) - z_1(i_{n+3})z_2(i_{n+2})z_2^*(i_n)z_1^*(i_{n+2}) \\
- \; & z_1^*(i_n)z_2^*(i_{n+1})z_1(i_{n+1})z_2(i_{n+3}) + z_1^*(i_n)z_1(i_{n+2})z_1^*(i_{n+2})z_1(i_{n+3}) \\
+ \; & z_2^*(i_n)z_2^*(i_{n+2})z_2(i_{n+2})z_2(i_{n+3}) - z_2^*(i_n)z_1^*(i_{n+1})z_2(i_{n+1})z_1(i_{n+3}).
\end{aligned}
$$

Combining the second, third, fifth and eighth terms together, with the rest of the terms, we get

$$
\begin{aligned}
\xi = \; & \{[z_1(i_{n+1} - i_n) - z_2(i_{n+1} - i_n)] \\
\times \; & [z_1(i_{n+3} - i_{n+1}) - z_2(i_{n+3} - i_{n+1})]\} \\
+ \; & \{[z_1(i_{n+3} - i_{n+2}) - z_2(i_{n+3} - i_{n+2})] \\
\times \; & [z_1(i_{n+2} - i_n) - z_2(i_{n+2} - i_n)]\}. \qquad \text{(B.18)}
\end{aligned}
$$

Finally we get from Eqs. (B.17) and (B.18)

$$
\begin{aligned}
a_n = \; - \; & \{\frac{[z_1(i_{n+1} - i_n) - z_2(i_{n+1} - i_n)]}{[z_1(i_{n+3} - i_{n+2}) - z_2(i_{n+3} - i_{n+2})]} \\
\times \; & \frac{[z_1(i_{n+3} - i_{n+1}) - z_2(i_{n+3} - i_{n+1})]}{[z_1(i_{n+2} - i_{n+1}) - z_2(i_{n+2} - i_{n+1})]}\} \\
- \; & \frac{z_1(i_{n+2} - i_n) - z_2(i_{n+2} - i_n)}{z_1(i_{n+2} - i_{n+1}) - z_2(i_{n+2} - i_{n+1})}. \qquad \text{(B.19)}
\end{aligned}
$$

For the special case of a URA $i_n = n$, using $z_i(n) = e^{jn\omega_i}$, we have

$$
\begin{aligned}
a_n &= -2\frac{z_1(2) - z_2(2)}{z_1(1) - z_2(1)} \\
&= -2[z_1(1) + z_2(1)] \qquad \text{(B.20)}
\end{aligned}
$$

[B-6] Determination of b_n

From Eqs. (3.81), (3.75) and (3.76) we have

$$\begin{aligned} b_n &= -\frac{-z_1^*(i_n)z_2^*(i_{n+1}) + z_1^*(i_{n+1})z_2^*(i_n)}{z_1^*(i_{n+1})z_2^*(i_{n+2}) - z_1^*(i_{n+2})z_2^*(i_{n+1})} \\ &= -\frac{z_1^*(i_{n+1})z_2^*(i_{n+1})}{z_2^*(i_{n+2})z_1^*(i_{n+2})} \cdot \frac{-z_1^*(i_n)z_1(i_{n+1}) + z_2(i_{n+1})z_2^*(i_n)}{z_1^*(i_{n+1})z_1(i_{n+2}) - z_2^*(i_{n+1})z_2(i_{n+2})} \\ &= -z_1(i_{n+2} - i_{n+1})z_2(i_{n+2} - i_{n+1})\frac{z_2(i_{n+1} - i_n) - z_1(i_{n+1} - i_n)}{z_1(i_{n+2} - i_{n+1}) - z_2(i_{n+2} - i_{n+1})} \end{aligned} \quad \text{(B.21)}$$

[B-7] Calculating $P_{l,k}$ for MRA 3 with Single Interfer

$$\begin{aligned} P_{1,1} &= \frac{1}{4\sum_{n=1}^{2}\sin^2(n\pi/3)}\sum_{n=1}^{2}\frac{\sin^2(n\pi/3)}{\sin^2(n\pi/6)} \\ &= \frac{2}{4\sum_{n=1}^{2}\sin^2(n\pi/3)}\sum_{n=1}^{2}\frac{1-\cos^2(n\pi/3)}{1-\cos^2(n\pi/3)} \\ &= \frac{1}{2}\cdot\frac{\sum_{n=1}^{2}1+\cos(n\pi/3)}{\sum_{n=1}^{2}1-\cos(n\pi/3)} \\ &= \frac{1}{2}\cdot\frac{2+\cos(\pi/3)+\cos(2\pi/3)}{2-\cos^2(\pi/3)-\cos^2(2\pi/3)} \\ &= \frac{1}{2}\cdot\frac{2}{2-1/2} = \frac{2}{3} \end{aligned} \quad \text{(B.22)}$$

$$\begin{aligned} P_{2,2} &= \frac{1}{4\sum_{n=1}^{2}\sin^2(2n\pi/3)}\sum_{n=1}^{2}\frac{\sin^2(2n\pi/3)}{\sin^2(n\pi/6)} \\ &= \frac{1}{4\sum_{n=1}^{2}[1-\cos^2(2n\pi/3)]}\sum_{n=1}^{2}\frac{1-\cos^2(2n\pi/3)}{1-\cos^2(n\pi/6)} \\ &= \frac{1}{4(2-1/4-1/4)}\left(\frac{1-\cos^2(2\pi/3)}{1-\cos^2(\pi/6)}+\frac{1-\cos^2(4\pi/3)}{1-\cos^2(2\pi/6)}\right) \end{aligned}$$

$$
\begin{aligned}
&= \frac{1}{4\cdot 1.5}\left(\frac{1-1/4}{1-3/4}+\frac{1-1/4}{1-1/4}\right) \\
&= \frac{1}{1.5}=\frac{2}{3} \qquad\qquad (B.23)\\
P_{1,2} &= \frac{1}{4\sqrt{\sum_{n=1}^{2}\sin^2(n\pi/3)}\sqrt{\sum_{n=1}^{2}\sin^2(2n\pi/3)}}\sum_{n=1}^{2}\frac{\sin(n\pi/3)\sin(2n\pi/3)}{\sin^2(n\pi/6)} \\
&= \frac{1}{4(3/4+3/4)}\left(\frac{\sqrt{3}/2\cdot\sqrt{3}/2}{1/4}+\frac{\sqrt{3}/2\cdot\sqrt{3}/2}{3/4}\right)=\frac{2}{3}
\end{aligned}
$$

[B-8] Derivation of $2Re\{p_nq_n^* - p_n - q_n\}$

From Eqs. (3.74–3.76),

$$
\begin{aligned}
p_n &= \frac{e^{ji_{n+2}\omega_2}e^{ji_n\omega_1}-e^{ji_n\omega_2}e^{ji_{n+2}\omega_1}}{\triangle_n} \\
q_n &= \frac{e^{ji_n\omega_2}e^{ji_{n+1}\omega_1}-e^{ji_{n+1}\omega_2}e^{ji_n\omega_1}}{\triangle_n}
\end{aligned}
$$

where

$$\triangle_n = e^{ji_{n+2}\omega_2}e^{ji_{n+1}\omega_1}-e^{ji_{n+1}\omega_2}e^{ji_{n+2}\omega_1}.$$

Now

$$
\begin{aligned}
|\,p_n\,|^2 &= \frac{1-\cos(\triangle\omega(i_{n+2}-i_n))}{1-\cos(\triangle\omega(i_{n+2}-i_{n+1}))}, \\
|\,q_n\,|^2 &= \frac{1-\cos(\triangle\omega(i_{n+1}-i_n))}{1-\cos(\triangle\omega(i_{n+2}-i_{n+1}))},
\end{aligned}
$$

$$
\begin{aligned}
1+|\,p_n\,|^2+|\,q_n\,|^2 = {} & \{3-\cos[\triangle\omega(i_{n+2}-i_{n+1})]-\cos[\triangle\omega(i_{n+2}-i_n)] \\
& -\cos[\triangle\omega(i_{n+1}-i_n)]\} \\
& /\ \{1-\cos[\triangle\omega(i_{n+2}-i_{n+1})]\}. \qquad (B.24)
\end{aligned}
$$

Also

$$
\begin{aligned}
Re\{p_nq_n^*\} = {} & \{\cos[(i_{n+2}-i_n)\omega_2-(i_{n+1}-i_n)\omega_1] \\
& +\cos[(i_{n+2}-i_n)\omega_1-(i_{n+1}-i_n)\omega_2]
\end{aligned}
$$

$$
\begin{aligned}
&- \cos[(i_{n+2}-i_{n+1})\omega_2] - \cos[(i_{n+2}-i_{n+1})\omega_1]\} \\
&/ \{2[1-\cos(\Delta\omega(i_{n+2}-i_{n+1}))]\},
\end{aligned}
$$

$$
\begin{aligned}
Re\{p_n\} = \{&\cos[(i_{n+1}-i_n)\omega_1] + \cos[(i_{n+1}-i_n)\omega_2] \\
&- \cos[(i_{n+2}-i_n)\omega_1 - (i_{n+2}-i_{n+1})\omega_2] \\
&- \cos[(i_{n+2}-i_n)\omega_2 - (i_{n+2}-i_{n+1})\omega_1]\} \\
&/ \{2[1-\cos(\Delta\omega(i_{n+2}-i_{n+1})]\}
\end{aligned}
$$

and

$$
\begin{aligned}
Re\{q_n\} = \{&\cos[(i_{n+2}-i_n)\omega_2] + \cos[(i_{n+2}-i_n)\omega_1] \\
&- \cos[(i_{n+2}-i_{n+1})\omega_2 + (i_{n+1}-i_n)\omega_1] \\
&- \cos[(i_{n+2}-i_{n+1})\omega_1 + (i_{n+1}-i_n)\omega_2]\} \\
&/ \{2[1-\cos(\Delta\omega(i_{n+2}-i_{n+1}))]\},
\end{aligned}
$$

$$
\begin{aligned}
2Re\{p_n q_n^* - p_n - q_n\} = \{&\cos[(i_{n+2}-i_n)\omega_2 - (i_{n+1}-i_n)\omega_1] \\
&+ \cos[(i_{n+2}-i_n)\omega_1 - (i_{n+1}-i_n)\omega_2] \\
&+ \cos[(i_{n+2}-i_n)\omega_1 - (i_{n+2}-i_{n+1})\omega_2] \\
&+ \cos[(i_{n+2}-i_n)\omega_2 - (i_{n+2}-i_{n+1})\omega_1] \\
&+ \cos[(i_{n+2}-i_{n+1})\omega_2 + (i_{n+1}-i_n)\omega_1] \\
&+ \cos[(i_{n+2}-i_{n+1})\omega_1 + (i_{n+1}-i_n)\omega_2] \\
&- \cos[(i_{n+1}-i_n)\omega_1] - \cos[(i_{n+1}-i_n)\omega_2] \\
&- \cos[(i_{n+2}-i_{n+1})\omega_1] - \cos[(i_{n+2}-i_{n+1})\omega_2] \\
&- \cos[(i_{n+2}-i_n)\omega_1] - \cos[(i_{n+2}-i_n)\omega_2)]\} \\
&/ \{1-\cos[\Delta\omega(i_{n+2}-i_{n+1})]\}. \qquad \text{(B.25)}
\end{aligned}
$$

[B-9] Calculating $P_{l,k}$ for MRA-4 with Single Interferer

From Eqs. (3.68) and (3.66), we have

$$P_{l,k} = \sum_{n=1}^{3} \frac{1}{4\sin^2(n\pi/8)} \cdot \frac{\sin(\pi nl/4)}{\sqrt{\sum_{n=1}^{3} \sin^2(\pi nl/4)}} \cdot \frac{\sin(\pi nk/4)}{\sqrt{\sum_{n=1}^{3} \sin^2(\pi nk/4)}}.$$

Therefore,

$$\begin{aligned}
P_{1,1} &= \frac{1}{4\sum_{n=1}^{3} \sin^2(n\pi/4)} \sum_{n=1}^{3} \frac{\sin^2(n\pi/4)}{\sin^2(n\pi/8)} \\
&= \frac{2}{4\sum_{n=1}^{3} \sin^2(n\pi/4)} \sum_{n=1}^{3} \frac{1-\cos^2(n\pi/4)}{1-\cos^2(n\pi/4)} \\
&= \frac{1}{2} \cdot \frac{\sum_{n=1}^{3} 1+\cos(n\pi/4)}{\sum_{n=1}^{3} 1-\cos(n\pi/4)} \\
&= \frac{1}{2} \cdot \frac{3+\cos(\pi/4)+\cos(\pi/2)+\cos(3\pi/4)}{3-\cos^2(\pi/4)-\cos^2(\pi/2)-\cos^2(3\pi/4)} \\
&= \frac{1}{2} \cdot \frac{3}{2} = \frac{3}{4}
\end{aligned} \tag{B.26}$$

$$\begin{aligned}
P_{2,2} &= \frac{1}{4\sum_{n=1}^{3} \sin^2(n\pi/2)} \sum_{n=1}^{3} \frac{\sin^2(n\pi/2)}{\sin^2(n\pi/8)} \\
&= \frac{2}{4\times 2}\left(\frac{\sin^2(\pi/2)}{1-\cos(\pi/4)} + \frac{\sin^2\pi}{1-\cos(\pi/2)} + \frac{\sin^2(3\pi/2)}{1-\cos(3\pi/4)}\right) \\
&= \frac{1}{4}\left(\frac{2}{2-\sqrt{2}} + 0 + \frac{2}{2+\sqrt{2}}\right) = 1
\end{aligned} \tag{B.27}$$

$$P_{3,3} = \frac{1}{4\sum_{n=1}^{3} \sin^2(3n\pi/4)} \sum_{n=1}^{3} \frac{\sin^2(3n\pi/4)}{\sin^2(n\pi/8)}$$

$$
\begin{aligned}
&= \frac{2}{4(1/2+1+1/2)} \sum_{n=1}^{3} \frac{\sin^2(3n\pi/4)}{1-\cos(n\pi/4)} \\
&= \frac{1}{4}\left(\frac{1}{2-\sqrt{2}} + \frac{1}{1} + \frac{1}{2+\sqrt{2}}\right) \\
&= 3/4
\end{aligned} \tag{B.28}
$$

$$
\begin{aligned}
P_{1,2} &= \frac{2}{4\sqrt{\sum_{n=1}^{3} \sin^2(n\pi/4)}\sqrt{\sum_{n=1}^{3} \sin^2(3n\pi/4)}} \sum_{n=1}^{3} \frac{\sin(n\pi/4)\sin(n\pi/2)}{1-\cos(n\pi/4)} \\
&= \frac{1}{4}\left(\frac{\sqrt{2}/2 \cdot 1}{1-\sqrt{2}/2} + \frac{1 \cdot 0}{1} + \frac{\sqrt{2}/2 \cdot (-1)}{1+\sqrt{2}/2}\right) \\
&= \frac{\sqrt{2}}{4}\left(\frac{1}{2-\sqrt{2}} - \frac{1}{2+\sqrt{2}}\right) \\
&= 1/2
\end{aligned} \tag{B.29}
$$

$$
\begin{aligned}
P_{1,3} &= \frac{2}{4\sqrt{\sum_{n=1}^{3} \sin^2(n\pi/4)}\sqrt{\sum_{n=1}^{3} \sin^2(3n\pi/4)}} \sum_{n=1}^{3} \frac{\sin(n\pi/4)\sin(3n\pi/4)}{1-\cos(n\pi/4)} \\
&= \frac{1}{4}\left(\frac{(1/\sqrt{2})(1/\sqrt{2})}{1-\sqrt{2}/2} + \frac{1 \cdot (-1)}{1} + \frac{(1/\sqrt{2})(1/\sqrt{2})}{1+\sqrt{2}/2}\right) \\
&= \frac{1}{4}\left(\frac{1}{2-\sqrt{2}} - 1 + \frac{1}{2+\sqrt{2}}\right) \\
&= 1/4
\end{aligned} \tag{B.30}
$$

$$
\begin{aligned}
P_{2,3} &= \frac{2}{4\sqrt{\sum_{n=1}^{3} \sin^2(2n\pi/4)}\sqrt{\sum_{n=1}^{3} \sin^2(3n\pi/4)}} \sum_{n=1}^{3} \frac{\sin(n\pi/2)\sin(3n\pi/4)}{1-\cos(n\pi/4)} \\
&= \frac{1}{4}\left(\frac{1 \cdot 1/\sqrt{2}}{1-\sqrt{2}/2} + \frac{0 \cdot (-1)}{1} + \frac{(-1 \cdot (1/\sqrt{2})}{1+\sqrt{2}/2}\right) \\
&= \frac{\sqrt{2}}{4}\left(\frac{1}{2-\sqrt{2}} - \frac{1}{2+\sqrt{2}}\right) \\
&= 1/2
\end{aligned} \tag{B.31}
$$

APPENDIX C

EIGENVALUES AND EIGENVECTORS OF SINGLE- AND DUAL-INTERFERER CASES

[C-1] The Single-Interferer Case

Eigenvalue

Consider a matrix with the form of

$$\mathbf{R} = p_1 \mathbf{d}_1 \mathbf{d}_1^H + \sigma^2 \mathbf{I}_N$$

where p_1 and σ are positive real numbers and $\mathbf{d}_1$ is an N $\times$ 1 matrix. The largest eigenvalue of the matrix $\mathbf{R}$ is $\sigma^2 + p_1 N$ and the rest of the N-1 eigenvalues are equal to σ^2.

Proof: In order to find the eigenvalues of the matrix $\mathbf{R}$, the following equation must be satisfied:

$$\det(\lambda \mathbf{I} - \mathbf{R}) = 0. \tag{C.1}$$

Therefore,

$$\begin{aligned}
\det(\lambda \mathbf{I} - p_1 \mathbf{d}_1 \mathbf{d}_1^H - \sigma^2 \mathbf{I}_N) &= \det\left[(\lambda - \sigma^2)\mathbf{I}_N - \mathbf{d}_1 \mathbf{d}_1^H\right] && \text{(C.2)} \\
&= (\lambda - \sigma^2)^N \det\left[\mathbf{I} - \frac{p_1 \mathbf{d}_1 \mathbf{d}_1^H}{\lambda - \sigma^2}\right] && \text{(C.3)} \\
&= (\lambda - \sigma^2)^N \left[1 - \text{trace}\left(\frac{p_1 \mathbf{d}_1 \mathbf{d}_1^H}{\lambda - \sigma^2}\right)\right] && \text{(C.4)} \\
&= (\lambda - \sigma^2)^N \left[1 - \frac{p_1 \|\mathbf{d}_1\|^2}{\lambda - \sigma^2}\right] && \text{(C.5)} \\
&= (\lambda - \sigma^2)^N - (\lambda - \sigma^2)^{N-1} \|\mathbf{d}_1\|^2 && \text{(C.6)} \\
&= (\lambda - \sigma^2)^{N-1} \left(\lambda - (\sigma^2 + p_1 \|\mathbf{d}_1\|^2)\right) && \text{(C.7)} \\
&= 0. && \text{(C.8)} \\
\Rightarrow \lambda_1 &= \sigma^2 + p_1 \|\mathbf{d}_1\|^2 && \text{(C.9)} \\
\lambda_2 &= \lambda_3 = \ldots = \lambda_N = \sigma^2 && \text{(C.10)}
\end{aligned}$$

where $\|\mathbf{d}_1\|^2$ is the Euclidean length of the vector $\mathbf{d}_1$. From the fact that the interference vector $\mathbf{d}_1$ has length N, $\|\mathbf{d}_1\|^2 = N$.

Eigenvector of R Corresponding to the Largest Eigenvalue

$\mathbf{d}_1$ is the eigenvector of $\mathbf{R}$ with corresponding eigenvalue of $\sigma^2 + p_1\|\mathbf{d}_1\|^2$.

Proof :

$$\mathbf{R}\mathbf{d}_1 = (p_1\mathbf{d}_1\mathbf{d}_1^H + \sigma^2\mathbf{I})\mathbf{d}_1 \tag{C.11}$$

$$= \mathbf{d}_1\|\mathbf{d}_1\|^2 + \sigma^2\mathbf{d}_1 \tag{C.12}$$

$$= (\|\mathbf{d}_1\| + \sigma^2)\mathbf{d}_1 \tag{C.13}$$

$\Longrightarrow$ $\mathbf{d}_1$ is the eigenvector of $\mathbf{R}$ corresponding to the eigenvalue $\sigma^2 + p_1\|\mathbf{d}_1\|^2$.

[C-2] The Dual-Interferer Case

Eigenvalues

Use the relation [47]

$$\det[\mathbf{I}_n - \mathbf{AB}] = \det[\mathbf{I}_m - \mathbf{BA}] \tag{C.14}$$

where $\mathbf{I}_n$ is an $n \times n$ identity matrix and $\mathbf{A}$ is an $n \times m$ matrix, while $\mathbf{B}$ is a $m \times n$ matrix.

The autocorrelation matrix of the dual interferers case is

$$\mathbf{R} = p_1\mathbf{d}_1\mathbf{d}_1^H + p_2\mathbf{d}_2\mathbf{d}_2^H + \sigma^2\mathbf{I}_N. \tag{C.15}$$

Let $\mathbf{A}=\left[\sqrt{p_1}\mathbf{d}_1, \sqrt{p_2}\mathbf{d}_2\right]_{N\times 2}$ and $\mathbf{B}= \mathbf{A}^H$ and $\mathbf{d}_1$ is a $N \times 1$ vector. The eigenvalues of $\mathbf{R}$ can be obtained through the following calculation:

$$\mathbf{R} = \sigma^2\mathbf{I}_N + \mathbf{A}\mathbf{A}^H \tag{C.16}$$

$$\det(\lambda \mathbf{I}_N - \mathbf{R}) = \det\left[(\lambda - \sigma^2)\mathbf{I}_N - \mathbf{A}\mathbf{A}^H\right] \tag{C.17}$$

$$= (\lambda - \sigma^2)^N \det\left[\mathbf{I}_2 - \frac{\mathbf{A}^H\mathbf{A}}{\lambda - \sigma^2}\right] \tag{C.18}$$

$$= (\lambda - \sigma^2)^N \begin{vmatrix} 1 - \frac{p_1\|\mathbf{d}_1\|^2}{\lambda-\sigma^2} & -\frac{\sqrt{p_1 p_2}\mathbf{d}_1^H\mathbf{d}_2}{\lambda-\sigma^2} \\ \sqrt{p_1\|\mathbf{d}_1\|^2}\lambda - \sigma^2 & 1 - \frac{p_1\|\mathbf{d}_2\|^2}{\lambda-\sigma^2} \end{vmatrix} \tag{C.19}$$

$$= (\lambda - \sigma^2)^N \left[\left(1 - \frac{p_1\|\mathbf{d}_1\|^2}{\lambda - \sigma^2}\right)\left(1 - \frac{p_2\|\mathbf{d}_2\|^2}{\lambda - \sigma^2}\right) - \frac{\sqrt{p_1 p_2} \mid \mathbf{d}_1^H\mathbf{d}_2 \mid^2}{(\lambda - \sigma^2)^2}\right]$$

$$= (\lambda - \sigma^2)[(\lambda - \sigma^2)^2 - (\lambda - \sigma^2)(p_1\|\mathbf{d}_1\|^2 + \|\mathbf{d}_2\|^2)$$
$$+(p_1 p_2\|\mathbf{d}_1\|^2 \cdot \|\mathbf{d}_2\|^2 - \mid \mathbf{d}_1^H\mathbf{d}_2 \mid^2)] \tag{C.20}$$

$$= 0 \tag{C.21}$$

$$\Longrightarrow \quad \lambda_{1,2} = \sigma^2 + \frac{(p_1\|\mathbf{d}_1\|^2 + p_2\|\mathbf{d}_2\|^2 \pm \sqrt{(\|p_1\|\mathbf{d}_1\|^2 - p_2\|\mathbf{d}_2\|^2)^2 + 4p_1 p_2 \mid \mathbf{d}_1^H\mathbf{d}_2 \mid^2}}{2} \tag{C.22}$$

and $\lambda_3 = \lambda_4 = \ldots = \lambda_N = \sigma^2$

Eigenvectors of R Corresponding to the Two Largest Eigenvalues

The eigenvectors corresponding the largest eigenvalue of $\mathbf{R}$ should lie in the span of vectors $\mathbf{d}_1$ and $\mathbf{d}_2$. We seek scalar a and b be some scalar so that $a\mathbf{d}_1 + b\mathbf{d}_2$ is the eigenvector which corresponding to the largest eigenvalue of $\mathbf{R}$. Then the following equation must be satisfied:

$$\mathbf{R}(a\mathbf{d}_1 + b\mathbf{d}_2) = \lambda_1(a\mathbf{d}_1 + b\mathbf{d}_2) \tag{C.23}$$

$$= \left(a\|\mathbf{d}_1^2 + b\mathbf{d}_1^H\mathbf{d}_2 + a\sigma^2\right)\mathbf{d}_1 + \left(b\|\mathbf{d}_2\|^2 + a\mathbf{d}_2^H\mathbf{d}_1 + b\sigma^2\right)\mathbf{d}_2$$

$$= = \lambda_1 a\mathbf{d}_1 + \lambda_1 b\mathbf{d}_2. \tag{C.24}$$

Equating the coefficient of $\mathbf{d}_1$ and $\mathbf{d}_2$, we have the following equations:

$$\Rightarrow \begin{cases} a\|\mathbf{d}_1\|^2 + b\mathbf{d}_1^H\mathbf{d}_2 + a\sigma^2 = \lambda a \\ b\|\mathbf{d}_2\|^2 + a\mathbf{d}_2^H\mathbf{d}_1 + b\sigma^2 = \lambda b. \end{cases}$$

It can be rearranged in the form of:

$$\Rightarrow \begin{cases} a\left(\|\mathbf{d}_1^2 + \sigma^2 - \lambda_1\right) + b\mathbf{d}_1^H\mathbf{d}_2 = 0 \\ a\mathbf{d}_2^H\mathbf{d}_1 + b\left(\|\mathbf{d}_2\|^2 + \sigma^2 - \lambda_1\right) = 0. \end{cases}$$

Solving the above equations, we have

$$a = -\frac{\mathbf{d}_1^H\mathbf{d}_2}{\|\mathbf{d}_1\|^2 + \sigma^2 - \lambda_1}b \quad \text{or} \quad a = -\frac{\left(\|\mathbf{d}_2\|^2 + \sigma^2 - \lambda_1\right)}{\mathbf{d}_2^H\mathbf{d}_1}b \tag{C.25}$$

λ_2 and its corresponding eigenvector can be found in the similar way. Since the number a is only a scaling factor, we can set it to 1. The corresponding eigenvectors of the largest eigenvalues will be $\mathbf{d}_1 + b\mathbf{d}_2$ where

$$b = \frac{\mathbf{d}_2^H\mathbf{d}_1}{\lambda - \sigma^2 - \|\mathbf{d}_2\|^2}$$

or

$$b = \frac{2\mathbf{d}_2^H\mathbf{d}_1}{\left(\|\mathbf{d}_1\|^2 - \|\mathbf{d}_2\|^2\right) \pm \sqrt{\left(p_1\|\mathbf{d}_1\|^2 - p_2\|\mathbf{d}_2\|^2\right)^2 + 4p_1p_2 \mid \mathbf{d}_1^H\mathbf{d}_2 \mid^2}}. \tag{C.26}$$

Note that the above derivation can be applied to any matrix with the form of $\mathbf{R} = p_1\mathbf{d}_1\mathbf{d}_1^H + p_2\mathbf{d}_2\mathbf{d}_2^H + \sigma^2\mathbf{I}_N$ where p_1, p_2 and σ^2 are positive numbers and $\mathbf{d}_1$ and $\mathbf{d}_2$ are vectors of equal dimension.

APPENDIX D

MATRIX INVERSE FOR SINGLE-INTERFERER USING EIGENCANCELING TECHNIQUE

From Eq. (4.8), the minimum noise variance for single interference using eigenanalysis method is:

$$\begin{aligned} J_{min} &= \frac{\sigma^2}{\mathbf{A}^H\mathbf{U}^{-1}\mathbf{A}} \\ &= \frac{\sigma^2}{(e^{-j\omega_1}-1)(e^{j\omega_1}-1)\|\mathbf{U}^{-1}\|_b} \end{aligned} \tag{D.1}$$

where $\|\cdot\|_b$ demotes for the sum of all the matrix elements. From equation (4.9) the $\mathbf{U}$ has the following form:

$$\begin{aligned} \mathbf{U} &= \mathbf{E}_\nu^H\mathbf{E}_\nu \\ &= \begin{bmatrix} 2 & -e^{j\omega_1} & 0 & \dots & 0 \\ -e^{-j\omega_1} & 2 & -e^{j\omega} & \dots & 0 \\ 0 & -e^{-j\omega_1} & 2 & \dots & 0 \\ \vdots & \vdots & \vdots & \vdots & \vdots \\ 0 & 0 & \dots & -e^{-j\omega_1} & 2 \end{bmatrix}_{(N-1)\times(N-1)} . \end{aligned} \tag{D.2}$$

Using the block inversion formula [47]:

$$\begin{bmatrix} \mathbf{A} & \mathbf{D} \\ \mathbf{C} & \mathbf{B} \end{bmatrix}^{-1} = \begin{bmatrix} \mathbf{A}^{-1}+\mathbf{E}\triangle^{-1}\mathbf{F} & -\mathbf{E}\triangle^{-1} \\ -\triangle^{-1}\mathbf{F} & \triangle^{-1} \end{bmatrix}, \tag{D.3}$$

where

$$\triangle = \mathbf{B}-\mathbf{C}\mathbf{A}^{-1}\mathbf{D}, \tag{D.4}$$

$$\mathbf{E} = \mathbf{A}^{-1}\mathbf{D}, \tag{D.5}$$

$$\mathbf{F} = \mathbf{C}\mathbf{A}^{-1} \tag{D.6}$$

only the $\|\mathbf{U}^{-1}\|_b$ was interested here,

$$\left\| \begin{bmatrix} \mathbf{A} & \mathbf{D} \\ \mathbf{C} & \mathbf{B} \end{bmatrix}^{-1} \right\|_b = \|\mathbf{A}^{-1}\|_b+\|\mathbf{E}\triangle^{-1}\mathbf{F}\|_b+\|-\triangle^{-1}\mathbf{F}\|_b+\|-\mathbf{E}\triangle^{-1}\|_b+\|\triangle^{-1}\|_b. \tag{D.7}$$

Let

$$\mathbf{A} = \begin{bmatrix} 2 & -e^{j\omega_1} & 0 & \dots & 0 \\ -e^{-j\omega_1} & 2 & -e^{j\omega} & \dots & 0 \\ 0 & -e^{-j\omega_1} & 2 & \dots & 0 \\ \vdots & \vdots & \vdots & \vdots & \vdots \\ 0 & 0 & \dots & -e^{-j\omega_1} & 2 \end{bmatrix}_{(N-2)\times(N-2)},$$

$$\begin{aligned} \mathbf{B} &= [2]_{1\times 1}, \\ \mathbf{C} &= \left[0, 0, \dots, 0, -e^{-j\omega_1}\right]_{1\times(N-2)}, \\ \mathbf{D} &= \mathbf{C}^H = \left[0, 0, \dots, 0, -e^{j\omega_1}\right]^T_{1\times(N-2)}, \\ \text{and } \Delta &= (\mathbf{B} - \mathbf{C}\mathbf{A}^{-1}\mathbf{D})_{1\times 1}. \end{aligned}$$

Since Δ is a scalar, so is $\|\Delta^{-1}\|_b$, and

$$\|\mathbf{U}\|_b^{-1} = \|\mathbf{A}^{-1}\|_b + \Delta^{-1}(\|\mathbf{E}\mathbf{F}\|_b + \|-\mathbf{F}\|_b + \|-\mathbf{E}\|_b + 1). \tag{D.8}$$

Observing the form of matrix $\mathbf{A}$, we see that it's in the exact form of $\mathbf{U}$ with order of $(N-2)\times(N-2)$ instead of $(N-1)\times(N-1)$. A recursive formula can be derived using induction to find $\|\mathbf{U}^{-1}\|$.

Define

$$\mathbf{A}_n = \mathbf{U}_{n-1} \tag{D.9}$$

$$\mathbf{U}_n = \begin{bmatrix} \mathbf{U}_{n-1} & \mathbf{D}_n \\ \mathbf{C}_n & \mathbf{B}_n \end{bmatrix} \tag{D.10}$$

$$\Delta_n = \mathbf{B} - \mathbf{C}\mathbf{A}^{-1}\mathbf{D} \tag{D.11}$$

$$= 2 - \Delta_{n-1}^{-1} \quad \text{with} \quad \Delta_1 = 2 \tag{D.12}$$

$$\Delta_n = 2 - \frac{n-1}{n} \tag{D.13}$$

$$\Rightarrow \Delta_n^{-1} = \frac{2n}{n+1} \tag{D.14}$$

Then

$$\mathbf{U}_n^{-1} = \begin{bmatrix} \mathbf{U}_{n-1}^{-1} + \mathbf{E}_n\Delta_n^{-1}\mathbf{F}_n & -\mathbf{E}_n\Delta_n^{-1} \\ -\Delta_n^{-1}\mathbf{F}_n & \Delta_n^{-1} \end{bmatrix} \quad \text{for} \quad n \geq 3 \tag{D.15}$$

where

$$\mathbf{E}_n = \mathbf{U}_{n-1}^{-1}\mathbf{D}_n = -e^{j\omega_1} * [\text{last column of } \mathbf{U}_{n-1}^{-1}] \tag{D.16}$$

$$\mathbf{F}_n = \mathbf{C}_n\mathbf{U}_{n-1}^{-1} = e^{-j\omega_1} * [\text{last row of } \mathbf{U}_{n-1}^{-1}] \tag{D.17}$$

$$\mathbf{E}_n\Delta_n^{-1}\mathbf{F}_n = (2 - \frac{n}{n+1})^{-1} * [\text{last column of } \mathbf{U}_{n-1}^{-1}] * [\text{last row of } \mathbf{U}_{n-1}^{-1}]$$

Examples

$$\mathbf{U}_1 = [2]$$

$$\Rightarrow \mathbf{U}_1^{-1} = \left[\frac{1}{2}\right]$$

$$\mathbf{U}_2 = \begin{bmatrix} 2 & -e^{j\omega_1} \\ -e^{-j\omega_1} & 2 \end{bmatrix}$$

$$\Rightarrow \mathbf{U}_2^{-1} = \frac{1}{3}\begin{bmatrix} 2 & e^{j\omega_1} \\ e^{-j\omega_1} & 2 \end{bmatrix}$$

$$\mathbf{U}_3 = \begin{bmatrix} 2 & -e^{j\omega_1} & 0 \\ -e^{-j\omega_1} & 2 & -e^{j\omega_1} \\ 0 & -e^{-j\omega_1} & 2 \end{bmatrix}$$

$$\text{with} \quad \Delta_3^{-1} = (2 - \frac{2}{3})^{-1} = \frac{3}{4}$$

$$\mathbf{U}_3^{-1} = \frac{1}{4}\begin{bmatrix} 3 & 2e^{j\omega_1} & e^{2j\omega_1} \\ 2e^{-j\omega_1} & 4 & 2e^{j\omega_1} \\ e^{-2j\omega_1} & 2e^{-j\omega_1} & 3 \end{bmatrix}$$

By induction, the general form for $\mathbf{U}_{n-1}^{-1}$ becomes:

$$\mathbf{U}_n^{-1} = \frac{1}{n+1}\begin{bmatrix} n & (n-1)e^{j\omega_1} & (n-2)e^{2j\omega_1} & \dots & 2e^{(n-2)j\omega_1} & e^{(n-1)j\omega_1} \\ (n-1)e^{-j\omega_1} & 2(n-1) & 2(n-2)e^{j\omega_1} & \dots & 4e^{(n-3)j\omega_1} & 2e^{(n-2)j\omega_1} \\ (n-2)e^{-2j\omega_1} & 2(n-2)e^{-j\omega_1} & 2(n-1) & \dots & \dots & 3e^{(n-3)j\omega_1} \\ \vdots & \vdots & \vdots & \vdots & \vdots & \vdots \\ 2e^{-(n-2)j\omega_1} & 4e^{-(n-3)j\omega_1} & 6e^{-(n-4)j\omega_1} & \dots & 2(n-1) & (n-1)e^{j\omega_1} \\ e^{-(n-1)j\omega_1} & 2e^{-(n-2)j\omega_1} & 3e^{-(n-3)j\omega_1} & \dots & (n-1)e^{-j\omega_1} & n \end{bmatrix} \tag{D.18}$$

and,

$$\|\mathbf{U}_n^{-1}\|_b = \frac{1}{n+1}\sum_{l=0}^{n-1}[2(n-l)+2(n-1-l)(n-2-l)]\cos(l\omega_1). \tag{D.19}$$

For URA with single interferer case, the dimension of the U matrix is $(N-1)\times(N-1)$.

The MNVV then become

$$J_{min} = \frac{N\sigma^2}{2(1-\cos\omega_1)\sum_{k=0}^{N-2}[2(N-1-k)+2(N-2-k)(N-3-k))]\cos(k\omega_1)}. \tag{D.20}$$

In the following, Eq. (D.20) will be simplified to

$$J_{min} = \frac{N\sigma^2}{N(N-1)-2\sum_{n=1}^{N-1}(N-n)\cos(n\omega_1)}. \tag{D.21}$$

Notice the only difference between Eqs. (D.20) and (D.21) is in the denominator. Let

$$\begin{aligned} f_1(N) &= 2(1-\cos\omega_1)\sum_{k=0}^{N-2}[2(N-1-k)+2(N-2-k)(N-3-k))]\cos k\omega_1 \\ f_2(N) &= N(N-1)-2\sum_{n=1}^{N-1}(N-n)\cos(n\omega_1), \end{aligned}$$

For N=3,

$$\begin{aligned} f_2(3) &= 3\cdot 2-2\sum_{n=1}^{2}(3-n)\cos(n\omega_1) = 6-2(2\cos\omega_1+\cos 2\omega_1) \\ &= 6-4\cos\omega_1-2\cos 2\omega_1 \\ f_1(3) &= 2(1-\cos\omega_1)\sum_{k=0}^{1}2(2-k)\cos k\omega_1 \\ &= 2(1-\cos\omega_1)(4+2\cos\omega_1) = 2(4-2\cos\omega_1-2\cos^2\omega_1 \\ &= 8-4\cos\omega_1-2(1+\cos 2\omega_1) = 6-4\cos\omega_1-2\cos 2\omega_1 \\ &= f_2(3). \end{aligned}$$

Assume for a given N, $f_1(N) = f_2(N)$,

$$f_2(N+1) = (N+1)N-2\sum_{n=1}^{N}(N+1-n)\cos n\omega_1$$

$$
\begin{aligned}
&= N(N-1) + 2N - 2\sum_{n=1}^{N}[(N-n)\cos n\omega_1 + \cos n\omega_1] \\
&= N(N-1) - \left[2\sum_{n=1}^{N-1}(N-n)\cos(n\omega_1)\right] + 2N - 2\sum_{n=1}^{N}\cos n\omega_1 \\
&= f_2(N) + 2g_2(N) \qquad \text{(D.22)}
\end{aligned}
$$

$$
\begin{aligned}
f_1(N+1) &= 2(1-\cos\omega_1)\sum_{k=0}^{N-1}[2(N-k) + 2(N-1-k)(N-2-k)]\cos k\omega_1 \\
&= 2(1-\cos\omega_1)\{\sum_{k=0}^{N-1}[2(N-1-k) + 2(N-2-k)(N-3-k))]\cos k\omega_1 \\
&\quad + \sum_{k=0}^{N-1}[2 + 4(N-2-k)]\cos k\omega_1\} \\
&= f_1(N) + 2(1-\cos\omega_1)\left[4\cos(N-1)\omega_1 + \sum_{k=0}^{N-1}2(2N-3-2k)\cos k\omega_1\right] \\
&= f_1(N) + 2g_1(N). \qquad \text{(D.23)}
\end{aligned}
$$

For $f_1(N+1) = f_2(N+1)$, provided that $f_1(N) = f_2(N)$, from Eqs. (D.22) and (D.23), only $g_1(N) = g_2(N)$ is needed.

$$
\begin{aligned}
g_2(N) &= N - \sum_{n=1}^{N}\cos n\omega_1 \\
g_1(N) &= (1-\cos\omega_1)\left[4\cos(N-1)\omega_1 + \sum_{k=0}^{N-1}2(2N-3-2k)\cos k\omega_1\right] \\
&= 4\cos(N-1)\omega_1 + \sum_{k=0}^{N-1}2(2N-3-2k)\cos k\omega_1 - 4\cos(N-1)\omega_1\cos\omega_1 \\
&\quad - \sum_{k=0}^{N-1}2(2N-3-2k)\cos k\omega_1\cos\omega_1 \\
&= \left[4\cos(N-1)\omega_1 + \sum_{k=0}^{N-1}2(2N-3-2k)\cos k\omega_1\right] \\
&\quad + \left[-2\cos N\omega_1 - 2\cos(N-2)\omega_1 - \sum_{k=0}^{N-1}(2N-3-2k)\cos(k-1)\omega_1\right] \\
&\quad - \sum_{k=0}^{N-1}(2N-3-2k)\cos(k+1)\omega_1 \\
&= N - \sum_{n=1}^{N}\cos n\omega_1 = g_2(N)
\end{aligned}
$$

By induction,the above derivation concluded that Eq. (4.12) and Eq. (4.27) are equivalent.

REFERENCES

1. R. Compton, *Introduction to Adaptive Arrays*, John Wiley and Son, New York, 1980.

2. A. Haimovich and Y. Bar-Ness, "Interference Cancellation by Eigenanalysis Methods," The 1988 DSP Workshop, Sep., 1988.

3. A. Haimovich and Y. Bar-Ness, "Adaptive Antenna Array using Eigenvector Methods," IEEE Int. Conf. on Antenna and Propagation, 1988.

4. S. U. Pillai, Y. Bar-Ness and F. Haber, "A New Approach to Array Geometry for the Improved Spatial Spectrum Estimation," IEEE Proc. Vol. 73, No. 10 pp. 1522-1524, Oct. 1985.

5. J. Leech, "On the Representation of 1,2,...,N by Differences," J. London Math. Soc., Vol. 31, pp. 160-169, 1956.

6. L. Rédei and A. Rényi, "On the Representation of 1,2, ...,N by Differences," Mat. Sbornik (Recueil Math.), Vol. 66 (NS 24), pp. 385-389 (Russian), 1949.

7. A. Brauer, " A Problem of Additive Number Theory and its Application in Electrical Engineering," J. Elisha Mitchell Sci. Soc., Vol. 61, pp. 55-66, 1945.

8. P. Erdös and I. S. Gál, "On the Representation of 1,2, ..., N by Differences," Nederl. Akad. Wetensch. Proc., Vol. 51, pp. 1155-1158, 1948; Indagationes Math., Vol. 10, pp. 379-382, 1948.

9. D. Pearson, S. U. Pillai and Y. Lee, " An Algorithm for Near- Optimal Placement of Sensor Elements," in ONR Annual Report, Polytechnic University, June 1988.

10. B. H. Kwon, "New High Resolution Techniques and their Performance Analysis for Angle-of-Arrival Estimation," Ph.D. Dissertation, Polytechnic Univ. Brooklyn, NY, 1989.

11. Y. Lee, S. U. Pillai and D. C. Youla, "Direction Finding from First Order Statistics," in ONR Annual Report, Polytechnic Univ., Dec. 1987.

12. C. R. Greene and R. C. Wood, "Sparse Array Performance," J. Acoust. Soc. Am. Vol. 63, No. 6, June 1978.

13. A. T. Moffet, "Minimum Redundancy Linear Array," IEEE Trans. AP. Vol-16, No. 2, March, 1968.

14. A. Paulraj, R. Roy, and T. Kailath, " Estimation of Signal Parameters via Rotational Invariance Techniques - ESPRIT," in Proc. 19th Asilomar Conf., Pacific Grove, CA, Nov. 1985.

15. R. Roy, A. Paulraj, and T. Kailath, " ESPRIT - a Subspace Rotation Approach to Estimation of Parameters of Cisoids in Noise," IEEE Trans. Acoust., Speech and Signal Processing, Vol. ASSP-34, pp. 1340-1342, Oct. 1986.

16. R. H. Roy, "ESPIRT : Estimation of Signal Parameter via Rotational Invariance Technique," Ph. D. Dissertation, Stanford Univ., Stanford, CA, 1987.

17. S. U. Pillai and B. H. Kwon, " GEESE (GEneralized Eigenvalues utilizing Signal subspace Eigenvectors) - A New Technique for Direction Finding," Proc. 22nd Annual Asilomar Conf. on Signal, Systems and Computers, Pacific Grove, CA, Oct.31 - Nov. 2, 1988.

18. J. E. Hudson, *Adaptive Array Principles*, IEEE London & New York, Peter Peregnhus Ltd. Stevenage, UK and New York 1981.

19. D. H. Johnson and S. R. DeGraaf, " Improving the Resolution of Bearing in Passive Sonar Arrays by Eigenvalue Analysis," IEEE Trans. on Acoust. Speech and Sig. Proc., Vol. ASSP-30, pp. 638-647, Aug. 1982.

20. R. L. Johnson, G. E. Miner, "Comparison of Superresolution Algorithms for Radio Direction Finding," IEEE Trans. on Aero. and Elec. Sys., Vol. AES-22, pp. 432-441, July 1986.

21. T. K. Citron and T. Kailath, " Eigenvector Methods and Beamforming, " Proc. IEEE Inter. Conf. on Accoust., Speech and Sig. Proc., 1984.

22. A. Haimovich and Y. Bar-Ness, "An Eigenanalysis Interference Canceler," IEEE Trans. ASSP, Vol. 39, No. 1, pp. 76-84, Jan. 1991.

23. H. P. Bucker, "High Resolution Cross-Sensor Beamforning for a Billboard Array," J. Accoust. Soc. Am. Vol. 65, No. 1, Jan. 1979.

24. H. P. Bucker, "Adaptive Cross-Sensor Beam Forming with Planar Arrays," J. Acoust. Soc. Am. Vol. 62, No. 5, Nov. 1977.

25. G. H. Golub and C. F. Van Loan, *Matrix Computation*, Baltimore, MD: The John Hopkins University Press, 1983.

26. R. A. Monzingo and T. W. Miller, *Introduction to Adaptive Arrays*, J. Wiley, 1980.

27. H. Cox, "Resolving Power and Sensitivity to Mismatch of Optimum Array Processors," JASA, Vol. 54, pp. 771-785, 1973.

28. J. W. R. G. Griffitts, P. L. Stocklin and C. Van Schoonereld (Eds.) ,"Signal Processing," Proc. of the NATO Advanced study Inst. on sig. proc. and underwater acoust., Loughborough, UK, 1972. (Academic Press, 1973).

29. C. L. Zahm, "Effects of Errors in the Direction of Incidence on the Performance of an Adaptive Array," Proc. IEEE Vol. 60, pp. 1008-1009, 1972.

30. R. N. Adams, L. L. Horowitz and K. D. Senne, "Adaptive Main-Beam Nulling for Narrow-Beam Antenna Array," IEEE Trans. AES-16, pp. 509-516, 1980.

31. J. T. Mayhan, "Adaptive Nulling with Multiple Beam Antennas," IEEE Trans. AAP-26, pp/. 267-273, 1978.

32. D. K. Cheng and F. T. Tseng, "Optimum Spatial Processing in a Noisy Environment for Arbitrary Antenna Arrays Subject to Random Errors," IEEE Trans. AP-16 pp. 164-171, 1968.

33. C. Drane Jr. and J. McI'lvenna, "Gain Maximisation and Controlled Null Placement Simultaneously Achieved in Aerial Array Pattern," Radio and Electro. Eng. Vol. 39, pp. 49-57, 1970.

34. J. B. Lewis and P. M. Schultheiss, " Optimum and Conventional Detection using a Linear Array," JASA Vol. 49, pp. 1083-1091, 1971.

35. T. N. E. Greville, "Some Application of the Pseudoinverse of a Matrix," SIAM Rev. Vol. 2 pp. 15-22, 1960.

36. W.-L. Chen and Y. Bar-Ness, "Minimum Redundancy Array Structure for Interference Cancellation," Inter. IEEE AP-S symposium, pp. 121-124, May, 1991.

37. E. A. Wolff, *Antenna Analysis*, John Wiley & Sons, Inc. , 1966.

38. M. T. Ma, *Theory and Application of Antenna Arrays*, John Wiley & Sons, Inc., 1974.

39. E. Panayirci, Y. Bar-Ness and W.-L. Chen,"Conventional Interference Cancellation for Minimum Redundancy Array Structure," ICASSP proc. pp. IV-541 - IV-544, March, 1992.

40. Y. Bar-Ness, E. Panayirci and W.-L. Chen, "Eigenanalysis of Interference Cancellation with Minimum Redundancy Array Structure," IEEE SSAP workshop proceeding , pp. 50-53, Oct. 1992.

41. Y. Bar-Ness, E. Panayirci, A. Haimovich and W.-L. Chen, " Interference Cancellation by Superresolution Method," Progress Report on Research Contract No. N66001-87-D-0136,Naval Ocean System Center, San Diego State Univ., San Diego, CA , March 1991.

42. Y. Bar-Ness, E. Panayirci and W.-L. Chen, "Conventional and Eigenanalysis Interference Cancellation with Minimum Redundancy Array Structure," Final Report, Research Contract No. N660011- 87-D-0136, Naval Ocean System Center, San Diego State Univ., San Diego, CA , Feb. 1993.

43. S. Barnett, *Matrices in Control Theory*, Van Nostrand Reinhold, New York, 1972.

44. P.C.K. Kwok and P. S. Brandon, " Eigenvalues of the Noise Covariance Matrix of a Linear Array in the Presence of Two Directional Interferences," Electronics Letters, No. 15, pp. 50-51, 1959.

45. R. D. Morgan, "Partially Adaptive Array Techniques," IEEE Trans. on Antenna and Propagation, Vol. AP-26, No. 6, Nov. 1976.

46. S. U. Pillai and F. Haber, "Spectrum Estimator Utilizing an Augmented Covariance Matrix," IEEE Trans. on Acous., Speech and Sig. Proc. Vol. ASSP-35, No. 11, Nov. 1982.

47. T. Kailath, *Linear Systems*, Prentice-Hall, Inc. 1980.

48. G. D. Smith, *Numerical Solution of Partial Defferential Equations: Finite Difference Methods*, 3rd Ed. Clarendon Press, Oxford, 1985.